School of Design and the Built Environment

Statistical and Probabilistic Risk Assessment for an Induced Gas Explosion on an Offshore Platform

KiYeob Kang

This thesis is presented for the Degree of

Doctor of Philosophy

of

Curtin University

August 2019

Declaration

To the best of my knowledge and belief this thesis contains no material previously published by any other person except where due acknowledgment has been made.

This thesis contains no material which has been accepted for the award of any other degree or diploma in any university.

Signature:

Date: 12.08.2019

Supervisor: **Prof. Xiangyu Wang**

Co-Supervisor: **Dr. Changzhi Wu**

Abstract

In offshore oil and gas industries, Explosion Risk Assessment (ERA) rest on probabilistic risk assessment is widely used to obtain the numerical information of accidental loads in the primary design process. The objective of this evaluation is to predict the extent of explosion damage and to check potential issues before they occur. A gas explosions in an offshore structures can be catastrophic because of the presence of risky and combustible hydrocarbon materials, so all required safety systems must be maintained to ensure the integrity of a target structure within certain level of explosion impact. It is necessary to grasp the relationship between the level of explosion pressure and structural physical deformation to mitigate the critical damage from the explosion impact and reduce the acceptance level for explosion hazards as much as possible during the design process. In the case of explosions, live testing using a real structure is not possible due to the many safety concerns and excessive cost. Therefore numerical computational simulation is often undertaken using a 3D model. This computational method is able to extensively investigate the variety of potential explosion situations. Computational Fluid Dynamics (CFD) analysis is also an important part of an ERA to estimate potential explosion consequences in a risk area. By applying this method, various explosion pressure wave data can be obtained for established explosion scenario. Although substantial efforts have been made to advance the ERA process, scope remains for further research on detailed analysis of the explosion pressure wave time history and the assessment of risk to structural integrity.

To suggest a method for gas explosion risk assessment, this study investigated the features of the explosion pressure wave, identified the structural damage due to explosion loading, and provided a risk evaluation technique taking into account the relation between gas explosion risk elements and the response of targeted structure. To handle such contents, the research was carried out dividing into three categories of explosion analysis, risk analysis and structural dynamic analysis. Firstly, in the explosion analysis, a great amount of explosion data have been analysed by using developed VBA code, so that distribution pattern for explosion wave properties and correlation between them were examined. Through this analysis, it was revealed that the intensity of rebound pressure is comparable with initial peak pressure in some cases. In addition, the influence of geometrical confinement on the extent of explosion pressure impact was identified. In the risk analysis chapter, explosion risk level and criteria have been described based on relevant principle, but the effect of rebound pressure phase was considered, and difference for explosion risk criteria between proposing method and conventional one was found. Correlation analysis for explosion wave properties indicated what type of explosion wave can be produced more frequently, and its likelihood was computed based on probabilistic approach.

Lastly, the interaction between explosion pressure and structural response was thoroughly investigated along with several issues. The influence of rebound pressure on physical deformation of structure was identified in terms of structural dynamics. Although its impact depends on the relative value for time domain, it has a remarkable effect on structural response. However, rebound pressure properties are usually negligible in the TNT explosion. Typical parameters in such an explosion are initial pressure phase. Whereas two more parameters, in this thesis, are proposed, i.e. rebound peak pressure and its duration time. Through an extensive investigation for a gas explosion in offshore topside platform, it was confirmed rebound pressure phase cannot be ignored in structure analysis related to explosion impact load.

Acknowledgements

First of all, I would like to express a word of my gratitude to my supervisor Professor Xiangyu Wang and co-supervisor Changzhi Wu. They always gave a helping hand for me to focus on PhD study, by offering research resources and opportunities.

In addition, I'm grateful to Dr Yongze Song, my colleague, in this academic journey. He offered very helpful advise and constructive comments for research attitude as well as techniques.

Finally, a family is the most powerful supporter to me, therefore I wish to dedicate this thesis to my lovely wife, daughter, brother, my parents and all in-laws family members.

Related Publication

Kang, K. Y., & Wang, X. (2018). A Stepwise Risk Assessment for Explosion Events considering Probability Distribution of Explosion Load Parameters. Complexity, 2018.

TABLE OF CONTENTS

LIST OF FIGURES

XI

LIST OF TABLES

Chapter 1

Introduction

This chapter has three sections which outline the research. Section 1.1 introduces the research topic, relevant industry field and key issues. It helps understand the direction for this research. Section 1.2 reviews two industry disasters, Piper Alpha in 1976 and Deepwater Horizon in 2010, which generated attention due to the significance of the accidents. Section 1.3 presents the significance and objectives of this study.

1.1 Background

The offshore facilities are multi-functional structure, which is normally used for processing hydrocarbon materials and for the storage of oil. Since such a multitasking require a set of apparatus and installations for the operation, offshore structures are very huge to involve all of them. Therefore, hazards of fire, explosion and potential accidents are bigger than onshore plant and the management of these risks is requiring more focused on. The floating production storage and offloading (FPSO) structure is a representative multi-functional structure in this field, which has both equipment related to gas processing and liquefaction as well as storage system on their topside area. A great amount of combustible gas and substance could be created during the operation, so this facility always has a higher potential risk for an explosion incident [1]. If flammable materials are combusted, an explosion could occur, and heavy losses would result from the explosion pressure and toxic gas. These hazards have a negative impact on the structure itself as well as on other resources.

Explosion incidents are considered a major hazard in the oil and offshore industries. According to offshore oil and gas industry statistics, more than 70% of accidents in offshore facilities are related to explosions [2]. Therefore, theoretical and practical insight for explosion incident are required for the safety of the offshore industry. Most offshore structure systems, in order to operate organically, are mass-processing facilities which have many sets of equipment and installations such as vessels, pipe-racks and storage tanks. The layout of task is also far more demanding compared to onshore structures due to the limited space available. Confined conditions can generate greater combustible gas compared to semi-confined or unconfined conditions, and confinement helps increase turbulence with a higher combustion rate. In confined conditions, a great amount of energy is given off, so that both structures and workers are in danger. In addition, oil leak which result from explosion impact can also cause serious damage to the ocean environment as well as marine ecosystems. Overall, an explosion incident in an offshore structure can be much more dangerous than an onshore explosion incident.

To prevent potential tragedy, explosion risk analysis should be based on feasible hazardous scenarios, and the assessment of structural response exposed to explosion pressure waves is also required. [3-5]. The key interest in ERA is to lower the acceptance level for explosion hazards as much as possible and to offer the explosion design load according to the type of installations. However, implementation of ERA can vary in keeping with

the analyst performing it, and it is totally determined by the accuracy of selected variables like the geometric confinement, leak frequency calculation, ignition modelling and implementation of safety rules like shutdown and blowdown etc. [6-8].

Common sense in ERA is to assess the performance criteria and corresponding explosion design loads based on the overpressure or drag pressure which can be generated by explosion ignition. [9, 10]. This is because explosion wave pressure is the most detrimental threat to structural stability. It can be characterised by a time-varying pressure and its duration, and the interaction of explosion waves and the structure is the main cause of partial or global structural failure. The explosion wave is a time-dependent load, so its influence on the physical behaviour of structures is totally different from static problems. Therefore, the influence of several factors associated with explosion load-time profile on structural response should be extensively investigated considering not only static and dynamic analysis, but also linear and nonlinear analysis.

In analysis, the method for applying explosion load is very important. The oil and gas industry normally pursues conservative design based on the very significant known safety issues, and the industry recognizes that most structural components experience major explosive damage during the initial normal pressure phase. The rebounded pressure phase is often neglected in an explosion-resistant design since its peak pressure is typically much smaller than peak overpressure in the normal phase. However, many studies have shown that rebounded pressure phase can have a very significant influence on structural response [11-13].

Risk assessment is also important issue in ERA process. Generally, assessment can be divided into two types, quantitative and qualitative analysis. Both are vital for the risk analysis of a potential explosion event. As one of explosion risk factors, explosion load parameters can also be examined based on both approaches. In quantitative risk assessment, frequency and consequence results are required, and each risk factor is calculated considering specific scenarios. Each loading parameters such as overpressure, impulse and duration, is quantified and compared under several conditions. On the other hand, from qualitative analysis, the risk degree for each loading parameter can be identified by reviewing the structural response according to loading types. As a result, it means that the risk criteria for the explosion load are specified by applying both types of analysis. This study aims to systematically analyse the explosion risk parameters, especially explosion wave pressure, and assess their risk level considering structural behavior as well as probabilistic distribution of the elements.

1.2 Gas explosion accidents

Explosion accidents that occur on offshore facilities are some of the most devastating accidents that can occur. The injuries and property damage from an incident of this nature are extreme and can have long-term consequences. The most severe recorded offshore incidents are the Piper Alpha accident, which occurred on 6 July 1988, and the Deepwater Horizon accident which occurred on 20 April 2010. Fig. 1 and 2 show the

aftermath from the accidents, and each accident is explained below [14, 15].

1.2.1 Piper Alpha

Piper Alpha was an oil production facility in the North sea, which consists of four separated modules. It was situated on the Piper oilfield, approximately 193 km northeast of Aberdeen, Scotland. It began production in 1976, operated by Occidental Petroleum Limited. At first, it was an oil-only platform but later changed to add gas production module. For worker health and safety, the most risky operations were distant from the residence district. However, the process of converting the facility from oil to gas broke this safety doctrine, considering the other concept that sensitive areas should be located together. As a result, the gas compression caused this tragic accident.

On 6 July 1988, some malfunctioning parts and a small gas leak which ignited under pressure caused an explosion and the resulting oil and gas fires killed 167 people and caused damage of US$3.4 billion. At the time of the disaster, Piper Alpha provided about 10% of North Sea oil and gas production, and the accident was the worst offshore oil disaster in terms of loss of lives and economic damage. There are several reasons for the catastrophic outcomes. Most manager who had the authority to order evacuation were killed by the first explosion, and the platforms continued to pump oil and gas to Piper Alpha until the second explosion happened. The worker who saw that Piper Alpha was burning could not do anything because the worker thought they did not have authority to shut off production, even in such an urgent situation [16-20].

1.2.2 Deepwater Horizon

Deepwater Horizon is the most recent explosion accident in the offshore industries. The accident not only caused an explosion in the topside area but also resulted in oil release for several months. It was wrapping up the well and was in the final stages of completion. An explosion of seawater from the drilling riser was occurred and the erupted seawater was followed by a combination of mud, flammable gas and water.   As a result, several explosions took place on the platform. At the time of the explosion, there were 126 crew on board. Eleven workers were presumed to have died during the initial explosion. The rig was evacuated, with many workers airlifted to receive an emergency medical treatment. The burning continued for about 36 hours after the first explosion, and then Deepwater Horizon sank two days later on 22 April 2010. The remains of the rig came to rest on the seafloor at a location approximately 1,500 m deep, and about 400 m from the northwest of the well. The oil spill reportedly continued for three months after the explosion, and over 4.9 million barrels of oil were released. On 15 July 2010, the wellhead was finally capped. As well as the deaths and injuries of the crew, the released oil had an extremely negative effect on surrounding area, wildlife and coastal ecosystem. During the clean-up work, the coastline was closed, and a range of ships, barriers and many other methods were used to stop the spill from spreading. However, despite concerted efforts, it was estimated that over 450 km of the Louisiana coastline had ultimately been affected.

In January 2011, the oil spill commission team in the US White House released their report on the causes of the Deepwater Horizon accident. The report stated that the companies involved in the Deepwater horizon project had not taken measure to provide safeguards against an incident of this nature happening. The report also showed a chart on the correlation of decisions which possibly saved time and money, but increased the risk to the crew aboard Deepwater Horizon [21-26].

(a)　　　　　　　　　　　　　　　　　(b)
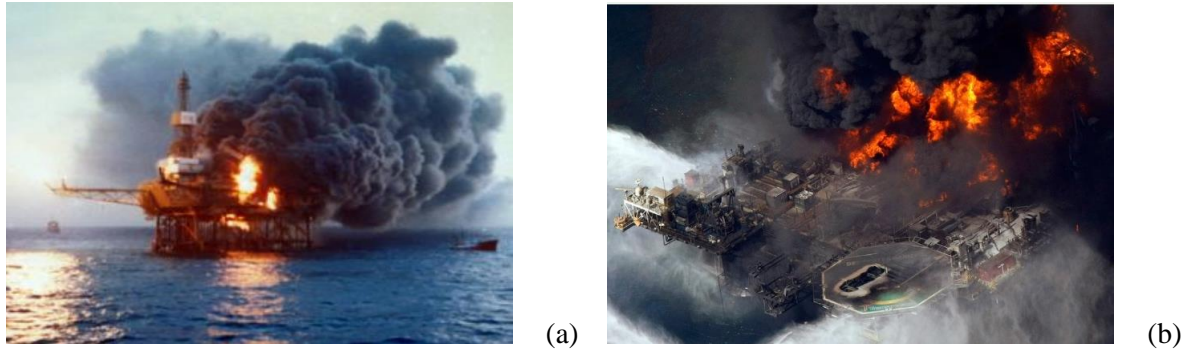
Fig. 1 Major explosion accidents in the oil and gas industries (a) Piper Alpha (b) Deepwater Horizon

(a)　　　　　　　　　　　　　　　　　(b)
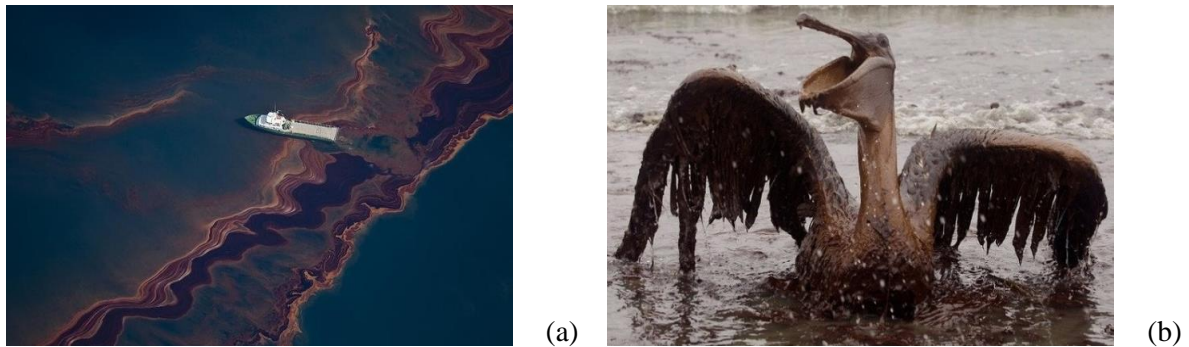
Fig. 2 Aftermath from the disaster (a) marine pollution by oil spill (b) seabird losses from oil spill

1.3 Explosion risk analysis of offshore installations

Hydrocarbon explosions and relevant hazards like fires, blasts and heat are the most frequent accidents that could be occurred in offshore structures [27]. The purpose of risk analysis is to offer required information for safety design and let operators recognize the significance of potential risks. To understand the explosion risk, systematic investigation of the risk from such hazardous activities need to be performed. At first, the most possible explosion scenarios considering operation environments should be assumed based on the statistical data or historical cases, and then the consequence of potential explosion is calculated in terms of overpressure and impulse. To perform more detailed consequence analysis, computational fluid dynamics (CFD) simulation are usually carried out for each of the cases established to characterize the explosion pressure profiles [28, 29]. In case of frequency data, historical data or probabilistic approach is generally used. Throughout the combination of consequence and frequency analysis, the corresponding risk could be calculated quantitatively [30]. On the other hand, qualitative risk assessment is commonly based on

experience or expertise and results in categorical estimates of risk. It may be sufficient for simple operation system which has fewer variables and uncertainties in terms of risk level.

1.4 Significance and objective

This research is intended to be useful in the offshore industries, where the principle of probability statistics is required to define design loads associated with an explosive event. In the industry, conservative design for explosion resistance is normally carried out based on rough estimations which mostly focus on the severity of overpressure. In the case of onshore plant, or unconfined structures, this method can be appropriate since explosion wave profile in such a region generally only has an initial pressure phase. However, the explosion wave which occurs in offshore facilities has other factors, such as rebound pressure phase, also called the negative pressure phase. This is a very controversial issue in this field. Some researchers claim that it is minor, and does not influence structural damage, but others emphasise it should be considered in the design stage. Therefore, the distribution of these factors and influence on structural response need to be thoroughly examined.

In this research, the explosion wave profiles are used, in priority, in order to investigate what factors can influence properties such as peak pressure, duration, normal or rebound pressure phase and each impulse, and then extensive risk analysis including both quantitative and qualitative approaches can be performed. In common risk assessment, a wide range of consequences and relevant probabilistic issues are examined. Probability means the frequency of risk elements, and it is likely to be varied according to the type of incident. For the consequence analysis, it is necessary to compute the probability of the undesired event, and to include knowledge of personnel injury or fatalities, environmental damage and financial loss. However these impacts are often estimated by using databases of statistics and data on accident. After all, risk assessment of explosion event, mainly concentrates on gas dispersion and induced explosion pressure in order to obtain explosion wave loads in a target area.

It is difficult to find previous research which performs risk assessment based on the interaction between explosion wave loads and the structural body even though structural capacity against explosion impact is most relevant to the degree of total damage. The explosion pressure time history has a lot of shapes, each of which can influence the structural response differently. In particular, the time factor is another crucial elements when analysing the structural behavior against the type of short pulse like explosion loading as there are many explosion loadings which have different duration times. The structural damage can be more severe or light with the same duration loading since each structure has a different natural periods according to its material properties. In addition, the superposition effects of initial and rebound pressure phase also have to be investigated carefully.

Based on these issue, the objective of this research is to advance understanding of the interaction between the

explosion wave and structures, and to evaluate and define the gas explosion risk in terms of structural dynamics. The main objectives are:

(1) To decide the primary risk elements in the explosion pressure time history.

Original explosion pressure-time curve is usually oscillated quickly and sometime shows the transition of the pressure phase. Thus simplifying of this curve with reasonable assumption is required to investigate the variables more efficiently. An original curve without simplifying cannot be standardized due to its irregular shapes. Using the simplified explosion wave profile, its properties and influence on structural damage can be studied.

(2) To establish a method for statistical and probabilistic estimation of explosion design load and quantitative risk for gas explosions.

To do this, the probabilistic density function for the main factors and its correlation analysis are considered, so that the explosion load characteristics can be predicted approximatively. To classify the risk level of the target, the safety discipline as well as risk screening need to be investigated in qualitative aspects. Risk matrix diagram and explosion pressure contour analysis are also carried out for that.

(3) To undertake quantitative consequence analysis for structural response by gas explosion loading including rebound pressure phase.

In terms of dynamic response, the effect of rebound pressure phase is investigated using some structural models, and then the results are compared to the structural response with only the initial pressure phase. As a result, the conservativeness of traditional design method can be checked.

1.5 Scientific problem and practical contribution

A gas explosion in fully packed area like a FPSO topside platform is totally different with usual TNT explosion since it does not have much space to allow the blast pressure to escape. Due to such a geometrical condition, a gas explosion pressure wave normally has two types of pressure phase, initial and rebound pressure stages. However, the degree of damage by rebound pressure is highly controversial issue. Some researchers claim that its effect is insignificant since the level of rebound pressure is normally much lower than initial peak pressure level [31-34]. But, others emphasis it could be considerably influenced on the structural integrity, so its effect should be thoroughly considered in the design stage [35-39]. They agreed that rebound pressure is much lower than initial peak pressure, but they pointed its duration is much longer than initial phase, and thus it may have a greater impact on structural damage even though the pressure intensity is relatively small [40]. It is also indicated that the negative peak pressure doesn't vary much whereas the positive peak pressure has big variation depending on the distance from the ignition position and the flammable gas cloud size. Hence, negative pressure phase should be considered as a critical factor to reasonably evaluate structural integrity. This study is with the latter. There are some issues need to be checked

for this topic. At first, the numerical range for rebound pressure should be investigated based on the type of total explosion pressure profile. The length of duration time, peak pressure value and the number of peak point are the most important factors which can be directly related to structural damage level. Second, the relationship between rebound pressure level and geometrical condition should be also identified. It could be checked using distributed monitoring points for recording pressure histories in computation model. Lastly, risk analysis including rebound pressure phase properties should be studied.

1.6 The structure of the thesis

This thesis consists of three main topics which are explosion, risk and structural analysis parts as shown in Fig. 3. In explosion analysis, explosion event and corresponding risk elements would be defined based on computational model for explosion simulation, and then be analyzed massive data-set using developed VBA code. This code is just for sorting and processing output data-set by CFD simulation. When it comes to explosion risk analysis, risk level and criteria would be established based on relevant principle and technical method, but remarkable thing is that this calculation would be based on the rebound pressure properties as well as initial pressure phase. Lastly, a series of finite elements analysis would be carried out to investigate the influence of each explosion pressure parameter on structural damage and performance.

Based on these topics, this thesis is divided into six chapters from introduction to conclusion remarks. In this chapter, basic knowledge and background about this research were introduced.

Chapter 2 shows an extensive literature review related to explosion risk assessment methods based on qualitative and quantitative approaches. In addition, several methodologies to calculate explosion loads are also reviewed.

Chapter 3 presents the computation method for gas explosion simulation using 3D target model. Through the explosion simulation results, the properties of explosion waves and its numerical distribution according to explosion scenarios are analyzed.

In chapter 4, the potential risk issue about explosion wave pressure are handled. After identifying risk elements in explosion wave profile, each explosion risk level and its criterial are described based on typical approach and proposing method. Correlation analysis between explosion wave properties are also performed in order to investigate probability distribution.

Chapter 5 is for practical analysis of interaction between explosion loads and structure. The influence of explosion wave properties such as overpressure and duration time on structural physical damage or deformation are examined using both single degree of freedom model and finite element model. The effect of rebound pressure are also reviewed in terms of linear and nonlinear analysis.

Chapter 6 summarizes the conclusions and new findings from this study.

Gas Explosion Analysis	Explosion Risk Analysis	Structural Analysis
Explosion event definition	Identifying hazards (Quantitative & Qualitative)	Case study for constitutive equation
Explosion modelling – CFD analysis	Risk screening indicator from explosion waves	Numerical model set-up (SDOF & FE models)
Data analysis (VBA sorting and processing)	Risk calculation using practical methods	Structural dynamic analysis (Linear & Nonlinear analysis)
Classifying influence factors (Overpressure, impulse)	Probabilistic analysis of explosion pressure parameters	Investigation of structural response (Damage pattern, displacement, etc.)
Calculation of explosion design load	Correlation coefficient analysis	Evaluate structural performance

"Statistical and Probabilistic Explosion Risk Assessment for Offshore Facilities"

Fig. 3 A framework for the thesis

8

Chapter 2

Literature review

This chapter has seven sections which introduce relevant other studies, theories and methodologies. Section 2.1 and 2.2 describe the mechanism of gas explosion phenomenon in order to understand what kind of factors should be focused in this study. In section 2.3 and 2.4, methods for estimating a gas explosion impact are examined, it helps understand the modeling of gas explosion and dispersion. Section 2.5 and 2.6 present several issues related to gas explosion in offshore facilities. Design principles are primarily covered taking into account the characteristics of offshore modules and explosion wave travel. Lastly, section 2.7 delineates the techniques of explosion risk analysis.

2.1 Gas explosion phenomenon

A gas explosion is regarded as an action in which the burning of gaseous materials, that is, combustible substances, cause a dramatic increase of pressure. It is a very complex phenomenon with several spatial and time issues as well as powerful gradients of field variables such as fluid density, velocity, temperature and pressure. Gas explosions can occur almost anywhere if combustible substances are present, which could be inside process equipment, buildings or offshore platform as well as open and unconfined process area. The level of explosion impact is related to flame speed and the quantity of released wave from the ignition source. [41]. Once an explosion occurs in a certain location, explosion pressure waves are produced, and the pressure build-up can damage not only personnel and facilities but also the environment and ecosystems.

When ignition is occurred, two types of the blaze, deflagration and detonation are generated. The difference between them is the speed of the blaze. The deflagration occurs at subsonic speed (1~1000m/s), and pressure can be increased, up to 5 times higher than the initial value, while the detonation mode propagates at supersonic speed (1000~3500m/s), and its peak pressure can increase to more over 20 times higher than the earlier pressure. Therefore, detonation can create a much more dangerous situation.

Gas explosions are also classified as either confined or unconfined. If the gas cloud is located in an unconfined area, the explosion pressure can be negligible. However, in a confined situation, there is no venting and heat loss or very little relief of the explosion wave propagation, and the overpressure can be high. The detonation mode in a confined area is clearly the most dangerous situation. A gas explosion is very sensitive, its severity is dependent on many factors, making it difficult to estimate the consequences of each explosion case.

2.2 Consideration for gas explosion model

For an extremely short time, the explosion pressure suddenly soars until it reaches the peak value, and is then equilibrated with atmospheric pressure. This state of increasing pressure to just before equilibrium is called the overpressure phase, and the time retained in the overpressure phase means the initial phase duration. Fig.

4 indicates the typical pressure-time history which can appear in an explosion event [42, 43].

At first, Fig. 4-(a) indicates a step rise in pressure from barometric pressure P_0 to the maximum, P_m, followed by a dramatic decrease in value during a duration time of initial phase (t_p). The second peak is related to the rebounded pressure wave from the obstacle. The pressure then reduces to below atmospheric point over a period t_n, which is called the rebound phase duration. Finally, pressure returns back to usual as the shock wave passes by. This type of pressure-time curve can be measured in detonation mode, where the maximum overpressure can be high as 15-18bar.

In Fig. 4-(b), the pressure increases slowly to the maximum point and then gradually decreases. The period of initial phase is longer but the peak pressure value is lower compared to the detonation pressure-time curve. This is because such an explosion mode occurs by a slower burning combustion process, which has relatively low level of overpressure of less than 1 bar. In offshore modules with plate decks, the burned gas could be stuck in the area, and it causes overpressure to increase to 2-3 bar or higher. The common interest in most explosion analysis is to investigate how explosion wave properties (overpressure, phase duration, etc.) depends on a number of variables such as fuel type, ignition source type and location, and size, shape and location of obstacles.

The severity of overpressure in a given geometry is definitely influenced by the reactivity of fuel. Methane gas is normally known as the least reactive gas, whereas acetylene and hydrogen are the most reactive, so they can generate high pressure [44]. The ignition source and location properties also have a great effect on the explosion magnitude. Jet-type ignition source generates much higher overpressure than point type source [45, 46]. The last key factor is the level of confinement. Confining the geometry leads to pressure build-up and affects the propagation of the flame through the geometry by improving the turbulence of the burning flame, so that it helps accelerate the pressure wave travel. In general, there are three types of geometric confinement: fully confined, partially confined, and unconfined areas [47, 48]. A large quantity of flammable material is trapped in the area surrounded by highly congested sets of equipment, so that a more powerful pressure wave can be generated in such an area. Therefore, the degree of confinement should be reflected in great detail to derive a reliable explosion pressure data set [49].

The kinds of the obstacles installed in the geometry can be regarded as another factor which can influence to higher overpressure. The more severe pressure is normally produced in an area with many small objects rather than one large object. This is because such an area causes the turbulence enhancement of the burning speed [50-52]. Therefore, at the primary design stage, such an issue is thoroughly examined taking into account potential explosion hazard and layout design. Lab scale test or computational analysis can be used to figure out the optimal equipment placement and to diminish an undesired damage.
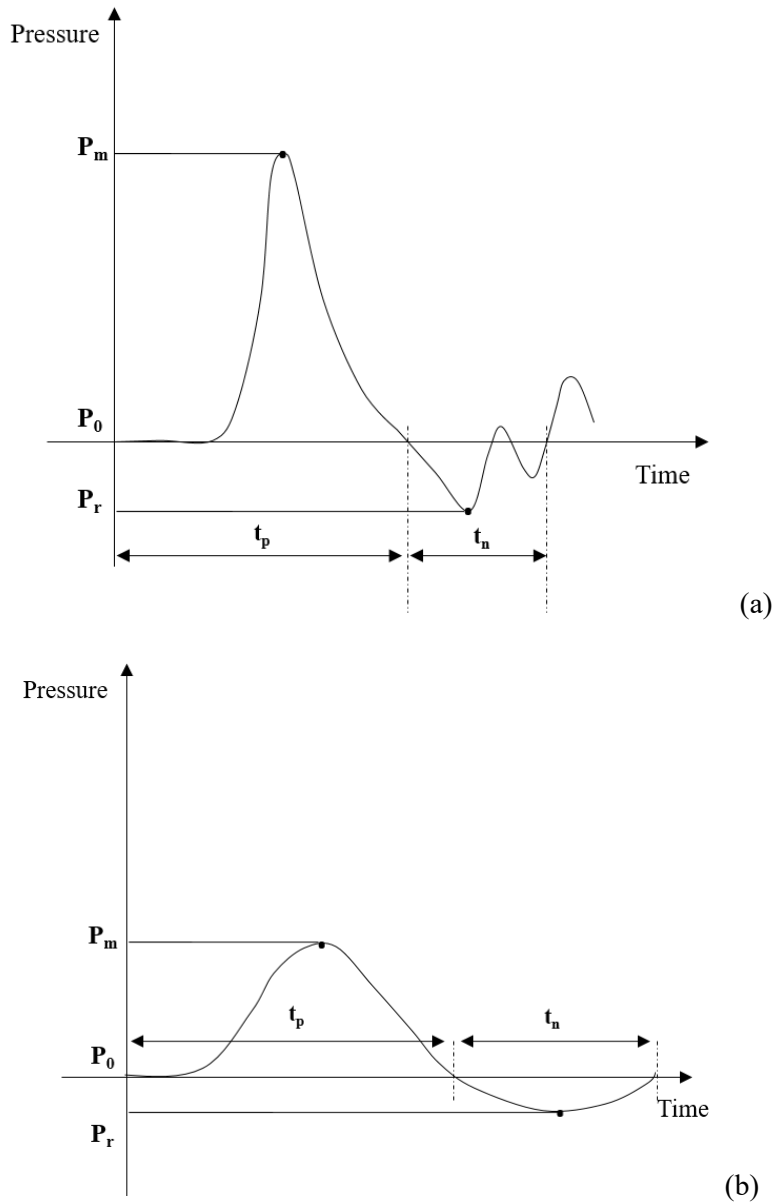
Fig. 4 Typical explosion pressure-time curve:
(a) detonation mode, (b) slower combustion mode

2.3 Methodologies for explosion impact estimation

Four different analysis methods are introduced in this section. Empirical models generally use the results obtained by experiments. Two representative methods (TNT and multi-energy theory) commonly used in the industry are also discussed.

2.3.1 TNT Equivalent method

TNT equivalence is generally used to express the energy released by an explosion. The relationship between the weight of TNT charge and the distance from the ignition is considered. The diagram for TNT detonation

has been used to estimate the gas explosion magnitude, even though there are differences between them [53]. The pressure generated by gas explosion is much lower than TNT detonations, and even the pressure decay from TNT is much more rapid compared to a gas explosion [54, 55]. Nevertheless the reason for using this method is to predict peak pressure from a gas explosion. The TNT model uses a pressure-distance diagram to transform the maximum overpressure of gas explosions, and the equivalence of TNT charge is calculated from the energy content in the ignited gas cloud volume [56, 57]. To find the mass of TNT equivalent to the mass of hydrocarbon in the cloud, the following equation can be used:

$$W_{TNT} \approx 10 \cdot \gamma \cdot W_{HC}, [kg] \qquad \qquad \text{eq (2.1)}$$

Where W_{TNT} is the mass of TNT, γ is a yield factor ($\gamma = 3 - 5\%$), and W_{HC} is the actual mass of hydrocarbons in the gas cloud. The number 10 indicates that most hydrocarbons have ten times higher combustion heat than TNT. For military purpose, ample tests of TNT have been performed by many researchers. As a result, a great amount of data were obtained, explosion wave properties like overpressure, phase duration time and impulse can be described by using the scaled factors. These factors are for an explosion of ground level, and rebound pressure influence on the total overpressure. The scaled factors are described in Table 1. For convenience of calculation, the scaled factors are described using the below equation developed by Brasie and Simpson [58]:

$$log_{10}(z) = 0.082(log_{10}P_0)^2 - 0.529 log_{10}P_0 + 1.526 \qquad \qquad \text{eq (2.2)}$$

Where P_0 is the maximum pressure in bars. This formula is only used when the maximum value is included in the range of 0.01 to 1 bar. In the original TNT equivalency model, however, the geometry was not considered. Therefore, in order to reflect the geometrical effects in the TNT model, another equation was proposed by Harries and Wickens [59]. The yield factor was increased to 0.2 and the weight of hydrocarbon was to accord with the weight of gas in the severely congested area. In case of natural gas, the equivalent TNT mass can be calculated using the following equation:

$$W_{TNT} \approx 0.16V_{eff}, [kg] \qquad \qquad \text{eq (2.3)}$$

Where $V_{eff} = min(V_{con}, V_{cloud})$ indicates the smaller of either the total volume of the congested part or gas cloud volume.

Table 1. The scaled factors in TNT method

Scaled factors	Equation
Scaled overpressure	$P_s = P_o/P_a,$ (P_o: Peak over pressure, P_a: Ambient pressure)
Scaled positive phase duration	$T_d = \dfrac{t_p}{W^{1/3}}$ (t_p: Positive phase duration)
Scaled arrival time	$T_a = \dfrac{t_a}{W^{1/3}}$ (t_a: Arrival time)
Scaled impulse	$i_s = \dfrac{i_p}{W^{1/3}}$ (i_p: Positive phase impulse)

2.3.2 Multi-energy method

The multi-energy method proposed by van den Berg [60] is normally used to predict the level of gas explosion with variable strength. It estimates that only part of the gas cloud would contribute to the blast. The reason for this assumption is that an unconfined gas cloud only has a small effect on increasing pressure, and the level of confinement is regarded as the most important factor for increasing the overpressure. In the numerical analysis for this technique, the generation condition of explosion wave is regarded as formulaic type. It is only ignited at the central position in the spherical cloud with constant flame speed. There are two variables in the formula: a combustion-energy scaled distance and the strength of the explosion. The scaled distance, R_{ce}, can be defined as:

$$R_{ce} = R_0/(E/P_0)^{1/3}, \qquad [m] \qquad\qquad \text{eq (2.4)}$$

Where R_0 is the distance from the ignition centre, E is the total combustion energy and P_0 is the barometric pressure. Most hydrocarbon type materials have similar total amount of energy, therefore the total combustion energy can be calculated by the following equation.

$$E \approx 3.5V_{cloud}, \qquad [MJ] \qquad\qquad \text{eq (2.5)}$$

The extent of the explosion impact is considerably different according to the position of ignition source. The charge strength is expressed using a number from 1 to 10, where 10 denotes a detonation mode.

A correlation for the charge strength has also been proposed, based on the three factors of the volume blockage ratio (B_r), the flame length (L_f) and the average obstacle size (O_s) [61]. This approach also considered not

only the scale of the situation but also the fuel type by using the laminar combusting velocity (V_l) and a scale factor (D). The correlation is:

$$P_{CS} = a \left[\frac{B_r \cdot L_f}{O_s} \right]^b V_l^{2.7} D^{0.7}$$

eq (2.6)

When it comes to offshore structures, another researcher [62] has proposed a method for determing the charge strength using three variables:

- Congestion: If congestion level is over the 30% of the limitation, it can be regarded as "High"
- Ignition source: Low in spark and hot surfaces, High in naked flames and welding
- Parallel confinement: Low for granted decks, High for plated decks.

2.3.3 CFD method

Computational fluid dynamics (CFD) analysis is a useful and effective method, which can describe the circumstance related to engineering phenomena including detailed geometrical condition. The main objective of such an analysis is to compute the numerical solutions using relevant governing equations for the phenomenon. To obtain the computation results, a series of mathematic techniques are required taking into account space and time domains. Through the discretisation process, several coupled algebraic equations are generated, and then they are applied to each sub-domain. Therefore, the outputs obtained by CFD model mean a great deal of information about the phenomenon. In general, CFD analysis is widely used to model an explosion event and calculate the explosion wave loads. It can not only investigate many different scenarios but can also repeat the same analysis with little extra effort. The consequence of a gas explosion depends on many variables, but explosion simulation using a CFD model can reflect this complexity with more realistic and accurate input data. In addition, the complex geometries can be designed by importing the 3D target model as shown in Fig. 5.

One of the most popular CFD tools is the FLame ACceleration Simulator (FLACS) software developed by Global Explosion Consultants (GexCon). It is generally used to model the dispersion and combustion of flammable materials considering the geometries of the target and to generate explosion pressure responses by counting possible scenarios [63]. The validation of the model and the accuracy of simulation results has been confirmed by many studies [64-66]. Wang et al. [67] applied the FLACS model to analyse the shock wave propagation process in a building and to compare the blast-wave curve at different locations. Li et al. [68] used the FLACS model to assess the effect of safety gab in gas dispersion as well as the explosion risk for heavily congested offshore facilities. Hansen et al. [69] studied the explosion loading on different types of equipment with various shapes by using the FLACS explosion model. Dadashzadeh et al. [70] applied FLACS to investigate the dispersion of flammable hydrocarbon release and the explosion consequence of BP's Deepwater Horizon accident. Das and Weinberg [71] used the FLACS code to present a project result for improving the application of correlation models in quantitative risk assessment (QRA) considering vapour

cloud explosion (VCE) events in offshore platforms. There are many previous research studies based on CFD analysis, but they have drawbacks. The main flaw is caused by the limitations imposed by the available computing hardware.
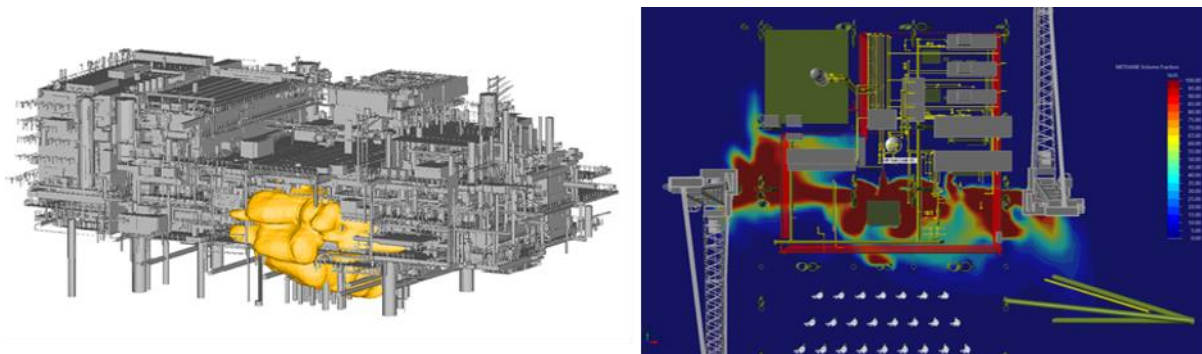
Fig. 5 3D model for gas explosion analysis

2.3.4 Experimental method

The test method is the most accurate method for generating an explosion consequence database if all the variations in environmental conditions and operational systems in target structures can be reflected. However, explosion tests have many constraints such as space limitations, safety issues and excessive cost. Therefore, laboratory scale tests are normally performed to compare to computational simulation results. Some experimental studies for gas explosion are introduced as follows. Gieras et al. [72] carried out a lab-scale experiment on methane gas explosions. Fig. 6 shows the test apparatus of this study. A chamber which has a 40-dm^3 volume with 140 mm in diameter and 441 mm in height was used and the initial gas temperature inside the explosion chamber was varied, at 297, 373 and 473 K. A pressure gauge and temperature sensor were attached to the chamber's outer surface.

Jingde et al. [73] tested vented gas explosion with different separation gaps between tanks. Explosion-proof fans were used to mix the methane and air. The pressure measuring range is from zero to 150 kPa. Several pressure sensors were installed on the tank wall in order to measure internal pressure, while two other sensors were mounted on the neighbouring tanks for external pressure. The ignition system was remotely controlled, and only the ignition scenario in the central area was considered. Fig. 7 shows the explosion testing equipment.
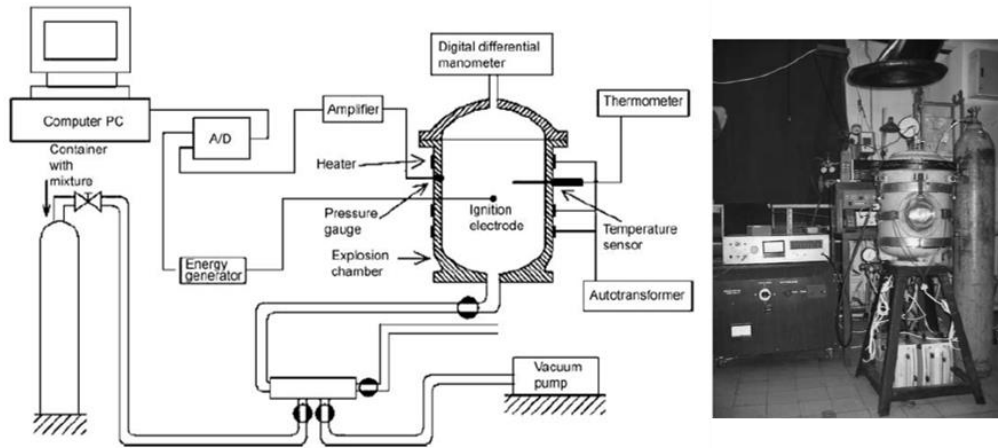
Fig. 6 General view of 40dm^3 explosion chamber and layout of the test facility. [72]
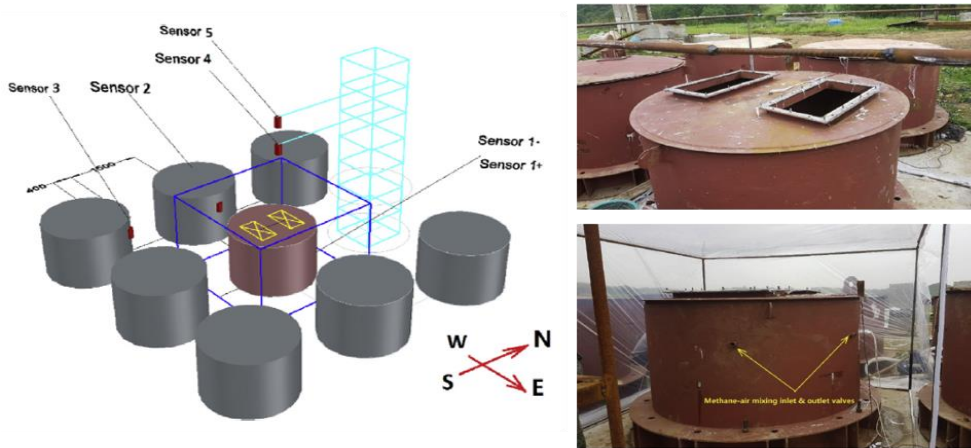
Fig. 7 The explosion test set using a series of tank groups [73]

2.4 Gas dispersion analysis

A series of gas release and dispersion is one of event before explosion. The release condition can be divided into two cases: regulated release and accidental release. Regulated release events include those from power stations or boilers combusting natural gas and oil, while accidental releases are events due to external factors such as equipment or operational failure issues, such as the release of a toxic gas from storage tanks or vessels [74]. In these conditions, it is important to carefully consider the downwind concentration levels which might cause economic or environmental damage. The following section provides information on the level of exposure and useful data for emergency response procedures.

2.4.1 Release modes

Understanding the mode of gas release and its behaviour is difficult, but very important, since gas is a very sensitive material and its behaviour hinges on the chemical properties of the material [75]. The type of gas release is divided into two categories according to release period. The first type is a release during a short period. It is normally occurred when the pressure in an apparatus is controlled by a safety device. In this case, gas dispersion is influenced by the environment conditions at that moment. The other type of release is a continuous release mode. It usually occurs from a broken pipe or a crack in a storage tank. Unlike the first type, this release occurs at relatively slow speed.   Another issue is the density of the released gas relative to that of the nearby air [76].

There are three types of dispersion mode depending on the level of gas density. The first type is the case of lower density than air, such as hydrogen releases, called positive buoyant dispersion. The second type, neutrally buoyant dispersion, occurs when the gas density is similar to the surrounding air. The third case is denser than air, but very different from the two other types. Many hazardous materials, such as chlorine, liquid petroleum gas (LPG) and ammonia, are involved in this dense gas dispersion. These dense gaseous materials are usually remained on the ground, so they can more easily affect to personnel. In addition, the dispersion of dense gases should be examined taking into account the congestion level of obstructions since they are much more dependent on the geometrical condition than elevated passive releases. Therefore, different models are required for each case. Sometimes, a series of models should be used in sequence.

2.4.2 Main factors in gas dispersion

The gas dispersion in the atmosphere is a complex issue influenced by many variables. However, atmospheric structure and turbulence are the dominant factors in gas dispersion. Other relevant factors are the material properties, storage types, meteorological conditions and the geography of the area. These factors are summarised below.

1. Storage vessel type

A liquefied gas in storage tank under pressure is normally at the room temperature. The representative gases stored in such a condition are ammonia, chlorine, propane and butane. These substances need to evaporate before being an airborne vapour. However, if these gaseous materials are stored at a higher temperature than their boiling point, it can cause a catastrophic rupture resulting in a two-phase release or aerosol, with much air being mixed into the gas cloud. The gas dispersion may therefore already be diluted by the significant quantities of surrounding air. In some cases of refrigerated storage, the low temperature on release results in the formation of a denser-than-air cloud. The dispersion condition also depends on whether the gap in the storage tanks is above or below the liquid level, the size of the gap in relation to the cross-sectional area of the storage, the actual storage conditions, and the material properties [77].

2. Wind conditions: Speed and direction

The wind condition is a significant factor in dispersing any gas released to the atmosphere. A higher wind speed can generally result in improved dilution compared to the heavy dense gas release case, so that the range of the hazard region can be smaller. However, in certain conditions, especially instantaneous or transient release cases, a high wind speed is able to transport a gas cloud further downwind, and then the potential hazard may increase [78]. Wind speed also affects the evaporation rate of non-boiling liquid pools, giving a higher evaporation rate for a higher wind speed. Contrary to this, a very low speed wind in stable or neutral conditions is able to make vapour flow very slowly. Therefore it may block gas diffusion to a more distant area, but it cannot have much influence on the rapid evaporation rate.

The main influence of wind direction is whether the gas dispersion proceeds downwind or upwind. If the wind direction is toward an area containing many combustible materials and many operation systems, it can be much more dangerous. Therefore, the direction of prevailing wind should be considered when analysing the potential risk. In most areas, any direction of wind can produce, even though there are dominant conditions for speed or direction which can occur more frequently.

3. Geographical conditions

As mentioned in chapter 2.4.1, the release type can be varied according to the location of the apparatus and the kind of obstacles or installations. Barriers, like storage tanks, pipe-racks and buildings, have an effect on the dispersion, either by funnelling the gas in certain directions or by increasing the turbulence. As a result, enhanced mixing can occur. The issue is crucial in the case of dense gaseous materials affected by an inclination of ground. The surface roughness of the surrounding area included in the gas dispersion range can also influence the atmospheric turbulence and thus the rate of dilution.

4. Gas density

The released gas will rise until it make a thermal equilibrium condition if the gas density is lower than surrounding air. But, in the opposite case, the gases are likely to remain on the ground and to disperse with a different manner. The major roles for this trend are gravitational effect, wind speed and deflection. The gravitational effect is related to the potential energy, kinetic energy and the buoyancy effect. The potential energy can be calculated by the dispersing cloud and kinetic energy is described by wind speed. Lastly all gaseous materials are influence by upward force called buoyancy. In the case of a dense gas cloud, it is dragged to the ground, and thus it remains within a lower wind speed part of the atmosphere. In the initial phases of a large dense gas dispersion, the wind would be deflected by the presence of the cloud, so that it has the other micro-climate of reduced flow speed and turbulence. The density gradient at the top edge of the gas cloud also acts in a similar manner so that the atmospheric turbulence is suppressed, which results in a slower dilution of the gas cloud.

2.4.3 Modelling approach

There are many different kinds of models for predicting gas concentrations and dispersion, but the models have been developed with only one or a few representative gas compositions, which are normally chosen based on buoyancy considerations and gas reactivity [79, 80]. In general, the worst case composition is used for dispersion modelling unless the likelihood of leaks from this composition is very low. The C3 and C4 are largely occupied in the worst case composition, and these gases tend to cause higher overpressure [81].

Two basis models for describing the steady release and momentary release are used to discuss the dispersion modelling approach: the positively buoyant model and the neutrally buoyant model [82]. The positive buoyancy case can occur when either the temperature of gases are higher than room temperature or the weight of gases are lower than the air. The hot stack gases and other residual gases are able to act in a positively buoyant manner [83, 84]. The stack gas is often used in estimating leeward concentrations of pollutants from stack releases. The neutrally buoyant model can predict the downwind concentration based on the Gaussian model for continuous dispersion as follows:

$$C(x, y, z; H) = \frac{Q}{2\pi\mu\sigma_y\sigma_z} exp\left[\frac{-y^2}{2\sigma_y^2}\right]\left\{exp\left[\frac{-(H - z)^2}{2\sigma_z^2}\right] + exp\left[\frac{-(H + z)^2}{2\sigma_z^2}\right]\right\} \qquad \text{eq (2.7)}$$

Where C is the concentration leeward at location (x,y,z) (kg/m3), Q is the release rate (kg/s), H is the release height (m), σ_y is the horizontal dispersion coefficient (m), σ_z is the vertical dispersion coefficient (m), μ is the speed of wind (m/s), x is the leeward distance, y is the crosswind distance (m) and z is the vertical distance (m). The coordinates x,y,z indicate the distance leeward, current of air and vertical distance from an origin at the beginning of the release point at ground level. In addition, stability input is used in air quality dispersion modelling to facilitate estimates of horizontal and vertical dispersion parameters used in the models [85]. The commonly used air quality modelling application for stability input scheme was proposed by Pasquill in 1961 [86]. The dispersion coefficients are obtained graphically or numerically using the leeward distance and stability class of the atmosphere. This stability mark, from A to G, denotes the extent of vertical mixing in the atmosphere. Class A indicates an extremely unstable condition, D is the neutral stable state, and the last one, G, describes an extremely stable condition. Table 2 provides the parameters for the Pasquill stability classes as originally defined.

It is unsuitable for general application, while the original scheme offered a criterion associated with dispersion modelling. It is essential to evaluate the extent of insolation present and note the range of wind speed. It is clear that some incompatibilities exist, such that high wind speeds (> 6m/s) with very unstable conditions like class A do not normally co-exist. It is common to report stability wind speed categories as A2 or D5. To establish the dispersion scenario, various leak and release conditions should also be defined, since the range of the gas cloud can be generated by various release conditions. It is important that the release location should not necessarily be based on the most likely leak area, but rather should be chosen by a range of release cases.

Leak properties is determined in the preventative range of feasible combinations of relevant variables, and the direction relative to the wind, leak point and free field jet. The duration of the leak, and therefore the mass of released gas, is determined by the gas detection time, shutdown procedures and inventory characteristics. If oil is present, it may contribute to cloud build-up by evaporation, flash-off or formation of suspended oil droplets. The latter is typically produced by the leak of pressurised oil containing a substantial portion of dissolved gas. The contribution of oil leakage to an explosion incident rests on the characteristics of segments, the corresponding leak frequencies and even the installation layout. The relevance of including a heavier gas composition in the explosion risk analysis, representing the oil, should therefore be evaluated further when information about segment characteristics and leak frequencies is available.

The heavier gas dispersion is an important class of gas release scenarios, but difficult to calculate. To consider such an event, there are some release cases which can lead to dense gas behavior [87, 88]. The first case is the gas with molecular weight greater than air, such as liquefied petroleum gas (LPG) and chlorine. The second case includes liquefied gaseous materials at cryogenic temperature such as liquefied natural gas (LNG). The last case includes liquefied gases under pressure with boiling point below atmospheric, such as ammonia. It is possible to analyse the heavy gas dispersion in detail if the gas passes through a simple area. However, it is not modelled well if the targeted area has many obstacles, complex terrain or sloping ground.

Table 2 Meteorological conditions defining Pasquill stability classes

Surface Wind speed (m/s)	Daytime insolation			Night-time conditions	
	Strong	Moderate	Slight	Thin overcast or > 4.8 low cloud	≤3/8 Cloudiness
< 2	A	A–B	B	E	F
2–3	A–B	B	C	E	F
3–5	B	B–C	C	D	E
5–6	C	C–D	D	D	D
> 6	C	D	D	D	D

2.5 Gas explosion in offshore facilities

Offshore structures have a variety of geometrical conditions with much equipment. Once an explosion occurs in this facility it can be very dangerous. A high-density equipment layout and a partly-open area can develop an explosion pressure build-up and support flame acceleration. This is because condensed explosive energy can be generated if the gas cloud is not able to escape from the ignition position. If a large gas cloud stays in a certain area, it is likely the explosion damage is much greater. This section considers the basic physics of

explosion cases to help develop a comprehensive understanding of the explosion phenomenon in offshore facilities.

2.5.1 Offshore modules and compartments

The internal area of an offshore module is regarded as a hazardous area since emissions of flammable and explosive gaseous materials could be the cause of ignition. If fuel or combustible gas is accidentally released in this area, a gas explosion may occur. Although gas detection equipment and safety installations should be capable of detecting such an issue every time, an explosion can occur in an instant, and an accident can always happen at an unexpected moment. The degree of explosion damage depends on several elements such as fuel type, gas cloud properties, geometrical conditions and congestion level. In particular, an explosion occurring in a confined area can be more serious.

In an offshore module, with compartments and fully confined or partly confined areas containing installations related to operating systems, there are many kinds of equipment and objects, so that a gas cloud will be condensed into the inward area. In addition, equipment engulfed by the gas mixtures will play a role as obstructing objects during an explosion. Fig. 8 shows the example of a gas explosion which occurred in a partially restricted area with some objects. In such an area, flame acceleration is turbulent mixing caused by the creation of turbulent flow fields ahead of the flame. The flame will definitely be towards the right side since that is the only vent area in this compartment. When the flame dissipates the cloud, the gas expands. After the gas finishes expanding, the unburnt gas is propelled forward by the flame, and a flow is provoked within the compartment. In this process, some of the unburnt gas will move out through the opening vent. On the other hand, the gas left in the compartment flows around the installations, and then this equipment can interrupt the flow and make turbulence ahead of the flame. In this way, the relative location between the opening area and the ignition point is a dominant factor in how the explosion pressure and turbulent flame acceleration develop during an explosion. Therefore rational layout and compartment design should be required to substantially reduce potential explosion risk.
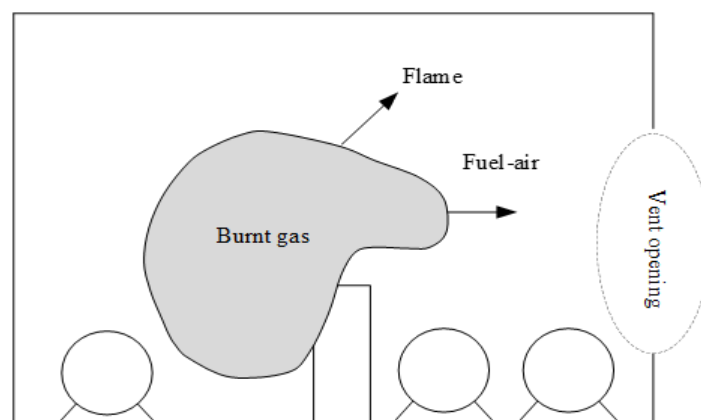
Fig. 8 Gas explosion in a partly confined area with several pieces of equipment [89]

2.5.2 Pipe-racks, vessels and tunnels

A pipe-rack is an elevated truss structure designed to support pipes, cables or other instrumental equipment on the offshore platform module to another structure. It also transports oil and gaseous materials, and needs to be connected to other process systems. Therefore, failure of pipe systems can lead to an escalation of an initial explosion event, and cause secondary damage that can influence the entire system's failure, which may in turn have much more severe consequences. Under basic physics in this case, turbulence is also the dominant parameter in developing flame speed in pipe-racks [90]. After the gases burn, it enlarges and propels residual gas to the front of the flame. The flow to the front of the flame can help a turbulent boundary layer to develop and the turbulence then increases the burning rate. The highest velocity of the flame is when the gas is ignited in the semi-closed foam. In this case, the gas at the front of the flame is propagated through the pipeline and can cause much turbulence. In the fully-closed foam, the flame accelerates quickly at the very beginning, but then decelerates later since the flow in front of the flame is blocked by the closed end.

There are two types of storage vessels: horizontal and vertical vessels. Both types usually have small openings such as the connection part with the pipe and relief valve, and pressure can be relieved by them during an explosion. However, the relief process is very slow, and it is difficult to reduce the pressure quickly, so pressure build-up can occur like the event in fully-closed foam, and interconnections may contribute to a strong pressure build-up. This phenomenon is called pressure piling. Where multiple vessels are connected by pipes, tanks and unit operations, ignition in a vessel and pressure piling may lead to a deflagration to detonation transition and a very large explosion shock wave, and this wave travels through the passageway into the next enclosure. The first explosion pressure together with secondary one in the other part produces a combined huge explosion beyond the equipment's control. Explosion pressure can be further more increased by fuel type, concentration level, the filling ratio, the number of vents and the combustion rate. Although all of vessels are not filled with combustible gaseous materials, even a small difference in filling ratio may have big variations in explosion consequences.

2.6 Principles of design philosophies for offshore facilities

Offshore facilities are likely to be affected by several loads and structural deformations arising from service requirements including from the general to the extreme. Therefore, the task is to build a structure that is able to withstand all requirements throughout the projected lifetime. In structural design, it is very important to use a proper design philosophy considering structure properties to ensure structural integrity since specific design guidelines and the safety discipline depends on the service environment during the design life. This philosophy can be generally divided into two categories of limit state design (LSD) and permissible stress design (PSD) concept. In the permissible stress design, the maximum stress in structural members by service loads should not exceed the elastic limit state. This limit is generally defined by ensuring that stresses remain within the limits through the use of safety factor. By using the safety factor, it is possible to consider many

uncertainties due to natural variability, inaccurate evaluation and variation in design procedure. Therefore, the design criterion of the PSD method can be expressed as follows:

$$\sum \sigma_w \leq \sigma_p = \sigma_n f_s \qquad \text{eq (2.8)}$$

Where σ_w is a working stress due to the design load, which is based on the loading value in elastic limit, σ_p is the permissible stress of the design material, σ_n is the material's nominal stress, and finally f_s indicates the safety factor specified along with the design rule. Selection of permissible stress depends on successful similar past experience and the relevant design code. It is very simple to use, but it is difficult to consider various uncertainties and the true safety factor against failure modes. Nevertheless, the PSD method is still used in several industries.

In contrast to the permissible stress design, the LSD method considers all actions likely to occur during the design life. A limit state means a state of a structure beyond which it can no longer perform the intended function. For these conditions, the applicable strength can be assumed and employed in design as a limit for such behaviour. The load-carrying capacity of a structure is normally evaluated using simplified design formula or by using a computation method such as nonlinear finite element analysis including detailed modelling related to geometric conditions, material properties and loading condition. Internationally most structural design concepts have now shifted from the permissible stress design to the limit state design since the LSD method leads to more rigorous design and is even more economical. In dealing with uncertainties, the LSD method incorporates uncertainties in the design into an approach of partial safety factors [91]. The partial safety factor is related to the design 'demand' load and resistance effect. The fundamental principle of partial safety factor based design criterion can be described as follows:

$$D_d < R_d \qquad \text{eq (2.9)}$$

Where D_d is factored design demand load and R_d is design resistance. Each factor can be expressed as:

$$D_d = \beta_0 \sum_i D_{ki}(F_{ki}, \beta_{fi}) \qquad \text{eq (2.10)}$$

$$R_d = R_k / \beta_m \beta_c \qquad \text{eq (2.11)}$$

Where β_0 is a partial safety factor considering the level of seriousness of the particular limit condition associated with safety and durability arising from economic, social consequences and any other special situation. $D_{ki}(F_{ki}, \beta_{fi})$ is the distinguishing measure of demand for loading type i, calculated from the distinguishing measures of loads, F_k, and amplified by the partial safety factor, β_f, taking into account the uncertainties in regard to loads, R_k is the distinguishing measure of resistance, β_m is a partial safety factor considering the uncertainties owing to material properties, β_c is a partial safety factor for the uncertainties on the resistance of the structure, e.g., construction quality, corrosion, method considered for determination of the capacity and so on. Fig. 9 indicates the relationship between partial factors for demand load and

resistance in the LSD. The design demand load and resistance are types of stress which can be represented by a statistical distribution. If the design load is larger than the resistance load, the system would fail. LSD is a reasonable design method based on the limit state condition that limits the continued safe operation of the target structure. Generally, four limit states are considered in the relevant design process [92]:

1. Ultimate limit state (ULS): This state is associated with the collapse of a structure due to the loss of structural integrity. It means loss of equilibrium in the structural system or local buckling and collapse due to pressure.

2. Serviceability limit state (SLS): This state indicates the failure modes for normal operations due to the non-functionality of routine operation. It is not related to catastrophic failure but reduces the operation capability.

3. Fatigue limit state (FLS): This is associated with fatigue crack occurrence of structural details due to stress concentration and damage accumulation under the cyclic loading. It can be divided into two types: low-cycle fatigue involving plastic deformation, and high cycle fatigue not involving plastic deformation.

4. Accidental limit state (ALS): This is a condition related to excessive structural damage caused by accidental load, such as explosion, fire, dropped object, collision and so on. Accidental cases normally directly influence the structure, the environment and personnel.

By comparing each limit state, it is evident that a different safety level or design criteria may be used according to the type of limit state. Therefore, it is important to use a rational design method considering the operational environment and the intended structure's properties.
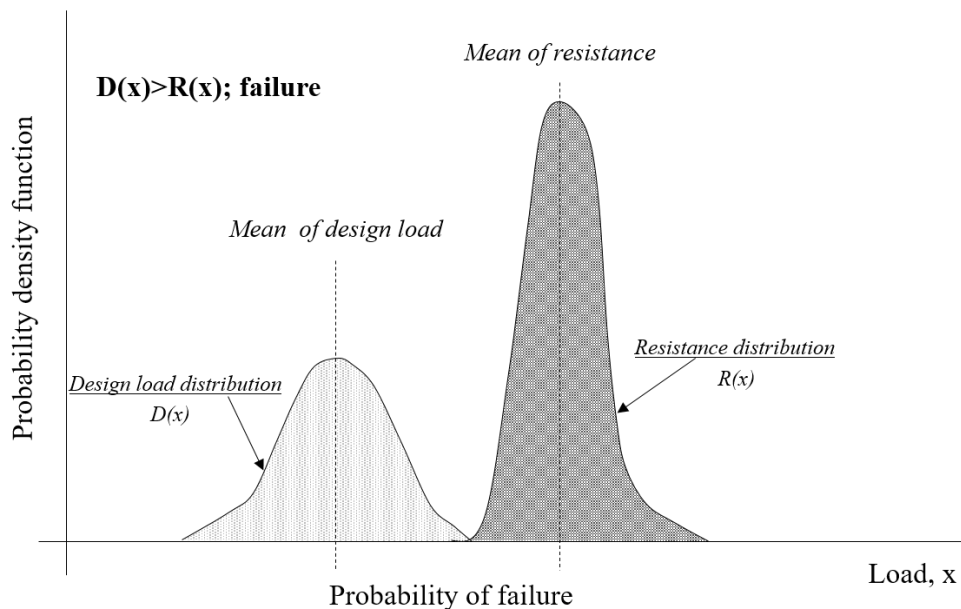
Fig. 9 Partial factors in limit state design

2.7 Gas explosion risk evaluation

Explosion risk assessment identifies the vulnerable components of an offshore facility under a possible explosion event and investigates methods to alleviate damage to personnel, structural members and the environment. This section discusses general risk assessment methodology and explosion risk assessment with relevant issues.

2.7.1 Design philosophy for gas explosion

As noted in the previous section, explosion is regarded as an accidental limit state, so an accidental load based design method can be used in explosion-resistant design. Accidents in offshore oil and gas facilities are defined as undesired events during the operational process. The objective of analysing accidental cases is to evaluate the level of initial damage and check if the particular hazard could progress toward the worse case in terms of personnel, environmental impacts and financial damage. The worst accidental event occurs when the local damage causes a series of additional following events. For example, an initial explosion may have an effect on the failure of primary structural systems. It could be regarded as a minor event if this issue is resolved by repairing that system, but any additional failures including subsequent global damage could lead to the potential loss of life or devastation of the environment.

Under the explosion, pressure would increase rapidly, and it often increases to a load where nonlinear structural response is expected. Therefore, explosion design criteria should be modified to consider the acceptability of the nonlinearity including large deformation. To define the explosion design criteria, explosion risk assessment is also required since an explosion event has a random probability distribution characteristic. The method for assessing gas explosion risk follows the typical risk assessment for offshore facilities including existing risk identification and structural response assessment [93].

There are several methods for identifying risk in facilities. A number of industry databases on accidents or operation failures are available. With this data, possible risk scenarios related to undesired events can be identified. Potential explosion risk is examined by considering the combined effect of the frequency of the accident and its consequence. This process is called preliminary risk assessment. In the detailed assessment, the events checked in the preliminary stage are categorised considering risk tolerance, and events with very low frequency and insignificant consequence can be removed. The final assessment aims to reduce the level of conservatism in the initial stage. It highlights mitigation activities for risk exposure and makes a conclusion that sufficient structural capacity or operational constraints exist to reduce the risk.

2.7.2 Terminologies in risk assessment

Several terms are used in risk analysis, but there is some inconsistency in applying them. For example, 'hazard' and 'risk' are often used to have the same meaning even though they are different. As this confusion may reduce the reliability of the results, key terms related to general risk assessment are defined.

Hazard

Hazard is usually defined as a source of potential damage. It means all situations that could lead to an undesired event. Hazards in offshore facilities include abnormal high pressure or temperature in any operation system, the occurrence of smoking in a dangerous area, flammable materials and storage tanks with toxic substances.

It is important to note that 'hazard' indicates potential damage or harm, not a realised one. The purpose of risk analysis is to ensure this very potential damage does not appear and if the damage does appear, then mitigation methods are required.

Risk

The risk is expressed as the product of the likelihood with which events are predicted to happen and the consequence of their outcomes. Although risk consists of both dimensions, general understanding for risk tends to be related more to the severity rather than the probability. But risk is two-dimensional and this means risk can be controlled by minimising the extent of loss or severity of the undesired event, and by reducing or eliminating the likelihood of the event. Therefore probabilistic concepts should be included in 'risk' assessment.

Likelihood

The likelihood of a certain risk is defined as events per unit time (normally per year). The likelihood of an event can be acquired from industry information or historical data. If this data are not available or cannot be used, the likelihood is computed using risk assessment models.

Consequence

The consequence can be defined as the number of injured or killed people, environment and property damage, money lost, and so on. Regardless of the measurement, the consequence should be defined for each event.

2.7.3 The principle of risk assessment

Several activities are included in the risk analysis process, but risk assessment is a key issue since it means identifying the extent of risk which must be managed adequately. Representative technical reports stress the importance of the relationship between the level of effort in assessing risk and the extent of the risk [94-96]. The purpose of risk assessment is to ensure that all potential hazards are investigated quantitatively or qualitatively. Fig. 10 shows the general risk management process.
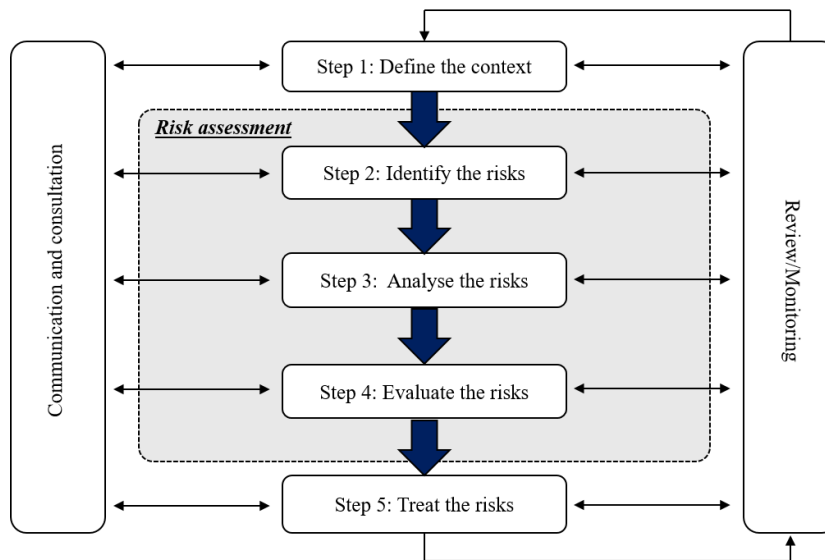
Fig. 10 The procedure of typical risk management

The methodology for risk assessment can be categorised into two types: quantitative and qualitative approaches.

Quantitative risk assessment

Quantitative risk assessment is a systematic approach of identifying a major accident hazard with its likelihood and consequences. This methodology is usually required for production or process systems including extreme operational environments. The results are expressed quantitatively for how certain risk is dangerous to people, the environment and other properties. The validity of quantitative results is assessed by identifying key assumptions and risk driving factors. Acceptable risk criteria could be required if there are significant changes to system operations or major hazard plant construction plans. Quantitative risk assessment can be divided into four key stages. Each stage is summarised below [97, 98].

Step 1 System definition

System definition is divided into three elements of system boundary, the purpose of the system, and activities within the system boundary. The definition of the system boundary is important to analyse systematically, because if it is not investigated clearly, the result can be confused with interacting systems. The system objective describes the intent of the target system with inputs and outputs. The last element is to make a list of activities that could occur within the system during operation.

Step 2 Hazard identification

Hazard identification includes all aspects associated with the safety discipline, environmental issues, economic loss and so on. This step is the most significant step in the entire risk assessment process. By using several techniques like 'What if' analysis or Hazard and Operability (HAZOP) analysis, potential factors in the system are checked.

27

Step 3 Frequency and consequence analysis of hazards

This stage involves investigating the frequency at which the identified potential hazards are expected to happen. Some hazard events, such as explosion, fire and collision, can directly have a negative effect on the system, but other events, like oil leak or gas release, may not be a direct hazard but can be the cause of a catastrophic event. Therefore this type of hazard requires further analysis based on relevant principles like event tree analysis technique. Consequence analysis evaluates the magnitude of the physical effect of hazardous outcomes identified in the hazard identification stage. It investigates the structural response or system damage to the hazard, and lists how an event can escalate. It also provides a basis for estimating the fatalities that could happen as a result of the event. Computational methods can be used to describe the effect of a hazardous event. The representative computational models are fire, explosion and gas dispersion.

Step 4 Risk evaluation and decision making

Based on the results of the previous stage, each risk level is compared using established criteria, and evaluated as either tolerable or dangerous. The decision making stage for risk reduction should identify whether the risk level is included in the "As Low As Reasonably Practicable (ALARP) region". If it is exceeds the ALARP, the most effective and efficient risk reduction measures are prepared.

Qualitative risk assessment

On the other hand, qualitative risk analysis is used to quantify the risk related to a particular hazard. This approach also uses the frequency and consequence concepts even though they are not numerically estimated. Instead, each indicator is assessed by verbal expression, such as high frequency, low frequency. It may often be difficult to provide exact numerical outputs for probability distribution or consequence estimation for a certain risk with the quantitative approach. However, the qualitative assessment method can be a good substitute for risk screening and comparing several alternatives in this situation. If numerical information is used in the analysis by quantifying the frequency and consequence for potential risk, the analysis would change to a semi-quantitative or quantitative risk assessment.

Qualitative risk analysis methods can be employed relatively easily. They can consider potential hazards from the early stage in the life-cycle of the target system since they provide ways to assess the relevant issues systematically. The representative application, the risk matrix method, provides a list ranking the potential hazard elements based on the acceptance criteria. Although this result may not directly influence the safety issue, it may have an effect on the availability and reliability of the target. Many previous practical cases have shown this approach can identify a large amount of useful information.

Qualitative analysis has many benefits, but also disadvantages. Due to relying heavily on the experience and knowledge of analysts, the results may not be comprehensive and may also be biased to particular factors.

2.7.4 Risk assessment techniques

There are several practical techniques for risk assessment. The What-if analysis method is roughly structured and similar to the brainstorming approach. Multidisciplinary skill and information are used to consider unexpected events involving potential negative consequences. The method investigates latent difference between design, fabrication, alteration and operating intent. The application range is vast and flexible, so the "what-if" method can be used in any stage in the process life-cycle based on available knowledge. But the analysis is too unsystematic for use in new designs and evaluation of operating plants. Considerable time is required to prepare the "what-if" questions.

Fault tree analysis (FTA) is a top-down method that is widely used to describe the events and component failures related to the main undesired events. The fault tree construction starts with the top event, generally a major potential risk. In the case of the top event, the conditions required for producing the event are recognised and regarded as new events at the next level of the tree. It continues until the root cause or primary events that instigate the occurrence of the top event are detected. To describe the sequence of each event, component failure and the correlation between them, fault tree analysis uses OR logic and And logic. At each level, if one or more events can cause an event on an upper level, they are combined with OR. Alternatively, if one or more events must occur simultaneously to produce the higher event, they are combined through an AND gate. Fault tree analysis can be used to evaluate or predict the reliability of highly complex systems.

The Hazard and Operability (HAZOP) analysis technique is a structured and systematic examination of a complex planned or existing operation in order to examine and assess safety risks in a process installation and potential operability problems [98]. HAZOP is rest on a principle that estimates risk events are occurred by potential abnormality from the design specification. Identification of such issue is facilitated by using sets of guidewords as an organized list of abnormality perspectives. The guidewords are made by adding predefined adjectives (i.e. high, low, etc.) to the properties of process parameters, and a group of analysts and experts discuss the causes and consequences of each deviation. If a certain concern is discovered, the group must ensure there are the appropriate safeguards to prevent the deviation from happening.

Event tree analysis (ETA) is a logical model to combine the success and failure from individual factors. It has various pathways leading to all the possible outcomes of the particular event. It can be applied to investigate the effects of functioning or failed systems after the event has happened [99, 100]. In many cases, the same result may be measured, but it is important to check the different paths in spite of the same outcome. Event tree analysis is available for systems early in the design process to check latent issues that may occur, rather than correcting events after they happen. Therefore it can help to prevent undesirable events by providing a risk assessor with the probability of occurrence.

Although the logic of event tree analysis and fault tree analysis seems similar in some parts, the methods are different. Both methods involve the identification and classification of events and factors, but with a different

focus on undesired events. The main objective of fault tree analysis is to prevent any loss, while event tree analysis focuses on mitigating negative outcomes. Therefore event tree analysis should offer all paths including a successful outcome, while fault tree analysis just focuses on the failures of a particular component. Event tree analysis can be used in both quantitative and qualitative approaches. In the qualitative approach, its value is in the structure of the tree itself. By analysing the structure of an event tree, the analyst can understand how the results of a negative event can escalate and how safety measures are applied to mitigate such an event. In the quantitative approach, a probability concept is used for each branch. Therefore it is very important to have probability data. If it is not available, the analyst should use other analytical tools based on reliability theory.

2.7.5 Application in offshore explosion risk

An explosion accident is a potential hazard that can lead to very destructive damage of the total system. Particularly in the offshore oil and gas industry, explosion risk analysis (ERA) is compulsory in the design stage since the entire system in an offshore facility is exposed to hazardous and flammable hydrocarbon materials. The main purpose of ERA is to identify and mitigate vulnerable members in the target system that could lead to fatal damage if exposed to an unexpected situation. An explosion event occurs through accidental release of gaseous materials into the area followed by an ignition source. Therefore ERA for such a target should take into account a series of events associated with the explosion like gas leak, dispersion and ignition. Based on the principle of quantitative risk assessment, it is possible to systematically identify events for that issue [101]. But the ERA is usually performed in a probabilistic manner since there are a great number of scenarios together with geometries or operational conditions.

The basic concept of the probabilistic ERA is to use the computational fluid dynamics (CFD) methodology. By using CFD, it is possible to consider relevant factors involving their probability or frequency distribution with possible scenarios. Although there are almost infinite scenarios in the real world, fewer practical scenarios are used in the CFD. But reasonable scenarios can be used by dividing the possibility of real values into several intervals, and then selecting representative data at each interval. In this way, gas dispersion or explosion scenarios including hazard elements can be established, and then potential explosion wave pressure data caused by explosion ignition can be derived.

Fig. 11 shows the schematic overview for ERA using CFD methodology. As described in the figure, it is divided into two categories according to the distribution of the gas cloud. The first section focuses on deriving the probabilistic distribution by considering the combination effect of gas dispersion analysis and its probability investigation. Leakage cases as the initial event should be studied based on the probabilistic approach, and then the frequency of established leak scenarios should be computed considering any relevant factors like wind direction, leak rate and distribution [102-104]. Ventilation analysis should be carried out prior to gas dispersion simulation to get the flow geometries influenced by wind conditions [105]. In the

second part, explosion overpressure is assessed using the exceedance curve which consists of frequency distribution and the pressure range. It is normally used in the explosion-resistant design stage to determine the explosion design load.
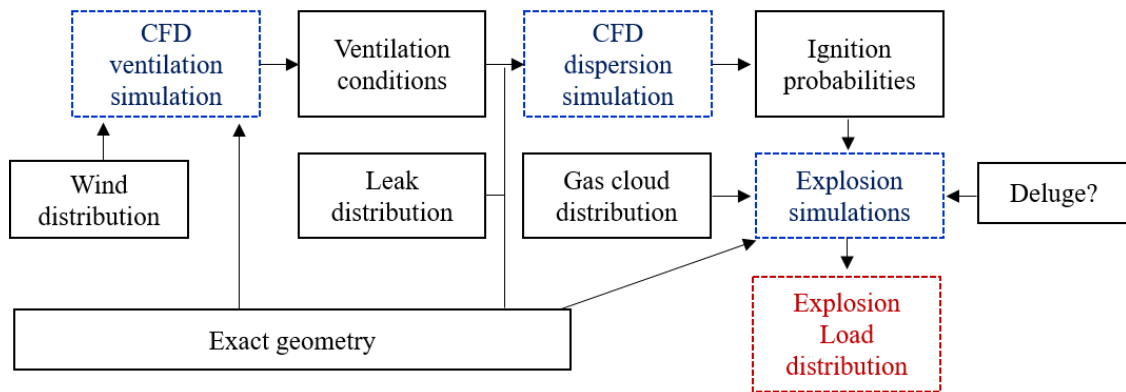
Fig. 11 Schematic overview of typical ERA based on CFD method [106]

Chapter 3

Gas explosion analysis

3.1 Introduction

In the offshore oil and gas industry, explosions by flammable gaseous material release are the most hazardous undesired events. To assess this accidental case, structural designers may need to investigate thousands of possible scenarios in order to get explosion loading information. The methodology is divided into two approaches: experimental analysis and computational analysis. Due to the many limitations and assumptions, the experimental approach is not appropriate for large scale structures with complex systems, while the computational method can reflect many conditions and reduce limitations compared to experiments. This chapter discusses the entire process from gas explosion computational analysis to applying a design load. To create an explosion pressure data set, CFD analysis was conducted using flame acceleration simulator (FLACS) software, and then these data were investigated using a data processor program developed based on VBA code.

3.2 Methodology for gas explosion analysis

3.2.1 Explosion simulation by FLACS code

The remarkable issue in a gas explosion is a dramatic pressure increase within an extremely short time. The fuel-oxidiser mixture can amplify this pressure increase. The extent of pressure is influenced by the flame speed and how the pressure enlarges away from the ignition position. A gas explosion can happen anywhere if there are combustible substances. However, the extent of a given gas explosion may vary according to the environmental conditions (e.g. wind direction, speed or leak rate) and geometric conditions (e.g. layout principles, confinement level and obstacles). To establish gas explosion scenarios based on these parameters, the CFD methodology is used with a very detailed 3D model. It is a very useful and effective method that can reflect mechanical phenomena in complicated flow geometries. The representative software, Flame Acceleration Simulator (FLACS), can model a potential explosion event caused by flammable fluid release based on user defined characteristics. It requires a complex computing process since it is associated with a range of influence factors such as environmental conditions, leak conditions, geometry, fluid materials and ignition resources [107, 108]. It is not possible to set up an actual experimental apparatus for offshore facilities involving a semi-confined geometry where a large quantity of flammable gaseous materials are confined in such an open area due to highly congested obstacles, but the CFD method can overcome this limitation by using a computational model based on most of the relevant parameters.

In this study, the target FLACS model is a geometrical floating production, storage and offloading (FPSO) facility which is a very detailed model including stairs, handrails and equipment as well as the main modules and installation as described in Fig. 12. In general, the FPSO structure is classified into two main parts based on the extent of the explosion influence: the turret module and the process module. The turret is moored to

the seabed with chains, wires and anchors. It allows the FPSO to use the direction that minimises the impact of waves, wind and currents. The topside platform is of key interest in this study since it has a much higher explosion risk compared to other parts of the FPSO facility because a great quantity of flammable gaseous materials are produced in the operational procedures of the process module. Therefore, it is important to understand the relationship between gas cloud size and explosion pressure intensity. In the FLACS model, a box-shaped stoichiometric gas cloud concept is used to define different amounts of gas cloud volume. Although it has some uncertainties, it is widely used to find a connection between leak frequencies and the intensity of pressure. Finally, this study covers hundreds of explosion scenarios as shown in Table 3. For 0.5 m of grid size, the four smallest cloud sizes were considered up to 1,560 m^3, while the three largest cloud sizes have been considered for 1.0 m of grid size.

Based on these established scenarios, explosion analysis was conducted using FLACS to produce explosion pressure responses. To measure explosion wave pressure data, two types of measurement tools were used as described in Fig. 13. A thousand point monitors were evenly distributed on all the modules, and local panel monitors were also distributed on both deck and explosion-resistant wall areas. Once ignition occurred at a user defined location, the explosion wave can then propagate to all directions within the sweep of the effect. At this time, a shock wave goes through the porosity monitoring tools mentioned earlier, so that each wave's pressure variation with time can be recorded at each position.
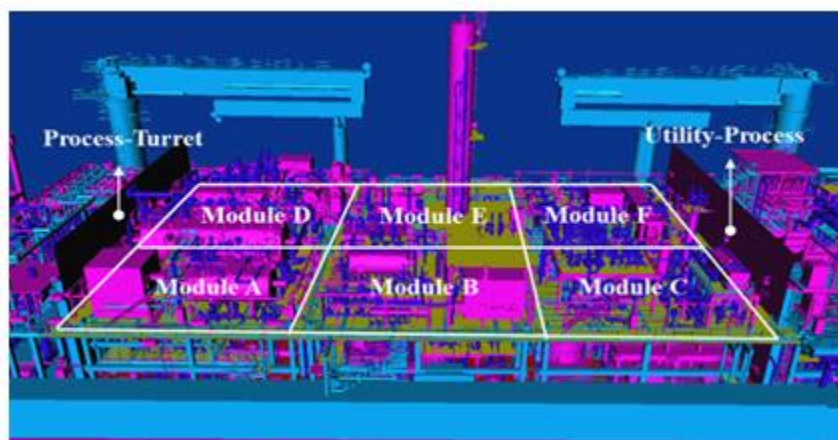
Fig. 12 3D FLACS model for explosion analysis [109]
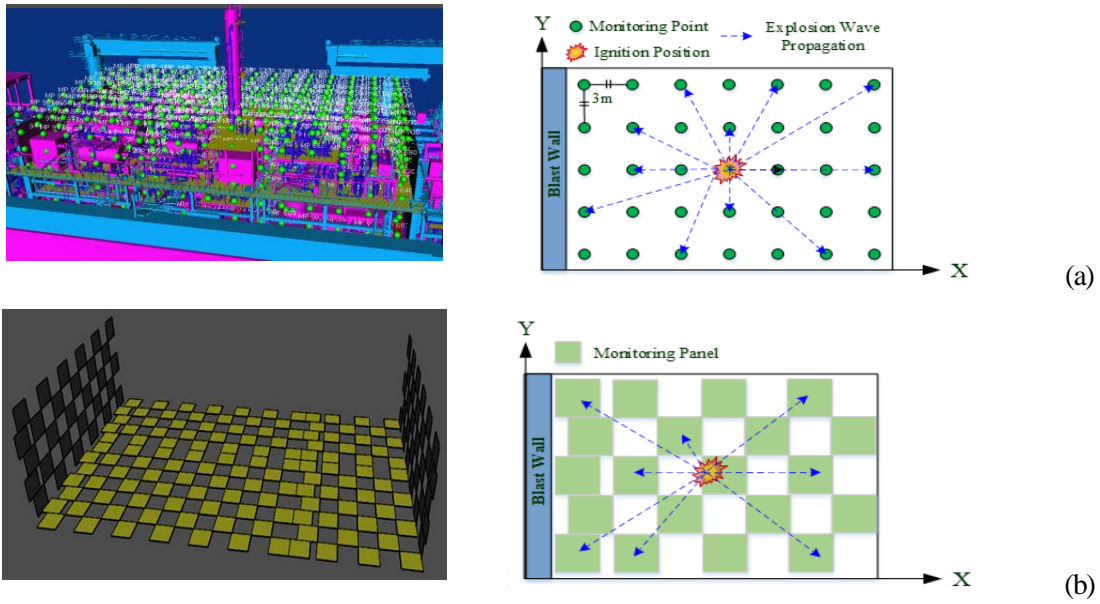
Fig. 13 The measurement tool for explosion pressure data (a) monitoring point (b) monitoring panel [110]

Table 3. Details of explosion scenarios for each module [109]

Module positions	Grid sizes	Ignition positions at elevation view	Cloud positions[†]	Cloud sizes	Ignition positions at plan view
1. A 2. B 3. C 4. D 5. E 6. F	1. 0.5 m	1. Bottom 2. Top	1. Center 2. Left 3. Right 4. Bottom 5. top	1. 199 m^3	1. Center
				2. 465 m^3 3. 900 m^3 4. 1560 m^3	1. Center 2. Edge[††]
	2. 1.0 m	1. Bottom 2. Top	1. Center	5. 2480 m^3 6. 3730 m^3	1. Center 2. Edge
				7. 5320 m^3	1. Center 2. Left 3. Right 4. Bottom 5. top
			2. Left 3. Right 4. Bottom 5. top	5. 2480 m^3 6. 3730 m^3	1. Center 2. Edge

[†] Cloud positions – within a module
[††] Edge – same position as the cloud position index

3.2.2 Validation for gas explosion model

The corresponding explosion computational analysis was carried by the developer of FLACS, which is one of the best validate tools for modelling flammable gas releases or explosion incidents in the oil and gas fields [64, 111-113]. To validate the accuracy of FLACS computation results, many efforts have been made by both academic fields and industries. As a result, FLACS software is often used in explosion analysis or relevant industrial project. There are several studies to investigate the effect of geometrical congestion to the FLACS explosion loading computation. Most results indicated that the level of pressure in congested area packing with piping of smaller diameter is much higher than the pressure of a geometry including larger diameter piping rack in the same volume [114]. The gas explosion simulation performed in this study were conducted to identify the potential explosion loads based on the detailed geometry and processing fluid material information at the final design phase of FPSO structure. Since the modeling details are the most critical factor affecting the explosion pressure wave response, 3D model using in this study includes minor obstacles such as small piping, stairs, vessel, and storage tank as well as all the equipment and structural systems on the FPSO topside area. All of structural modeling and required computational analyses basically have been followed the recommendation by the FLACS manual.

3.2.3 Gas explosion parameters

In explosion analysis, dispersion is the phenomenon in which materials spread within a fluid. Materials are generally diffused from high concentration regions to relatively low concentration regions, and diffusion can happen in liquids or gaseous materials. Therefore, dispersion analysis is required to define representative gas cloud properties which can be produced in possible release scenarios. Table 4 shows the gas composition used in the computational analysis. Based on these properties, dispersion analysis was conducted to establish gas cloud size and leak information considering possible leak scenarios and environmental conditions.

Of environmental factors, the representative element is wind conditions involving direction, speed and turbulence level. In this study, wind speed was assumed taking into account a linear correlation estimation between external wind speed and internal flow, and then a dispersion study was performed to determine the spread of gases in several conditions including wind properties, ventilation, observations about installations, and the features of surrounding area. The leak state was also considered by a preventive range of possible combinations of leak properties and includes variations in directions relative to the wind directions, leaks impinging on objects, free field jets and dispersive leaks. The leak locations were determined to be close to a specific installation or in an area with several leak sources. The eight leak rates considered in the analysis are: 0.75, 1.5, 3, 6, 12, 24, 48 and 96 kg/s. In addition, six different directions of $+/- X$, $+/- Y$ and $+/- Z$ and dispersion conditions were used for specific leak locations. For turbulence modelling, FLACS code uses a Reynolds-Averaged Navier-Stokes approach. This assumption rests on the principle of classifying the velocity term of fluid and scalar quantities like pressure and gas concentrations into the average and fluctuating

elements. The transport equations can be solved for the average values, and a model is used to describe the influence of variations of elements on the average. The average values for velocity, pressure and concentrations computed by using the FLACS model are regarded as the results in statistically steady flows.

Table. 4 Fluid compositions (mole fraction)

Compositions	C_1	C_2	C_3	C_4	C_5	CO_2	H_2O
Portions	40%	14%	25%	19%	2%	0%	0%

3.3 Explosion design load factors

As offshore facilities have a possibility of experiencing a gas explosion accident during the design life, the structural members in facilities should resist such potential loads. Therefore, it is necessary to satisfy the performance criteria of offshore safety discipline subjected to a specific level of risk-based explosion load by international standards [115-117]. A structure that is exposed to an explosion pressure is normally subject to a differential pressure load. An explosion causes the formation of incident shock waves and reflected waves. Generally, explosive energy can make the ambient pressure increase instantaneously until reaching the peak overpressure. At this time, an incident wave of pressure influences on structures that are not parallel with the wave route, and it is reflected and strengthen, generating rebounded pressure. Although the duration time of the explosion pressure is very short, interaction between the overpressure in shock waves and the actual loading applied to the structure is not simple. If the pressure wave generates in a closed area, and the incident wave energy is then reflected, the initial peak pressure would also increase more. Hence, many analysts in relevant fields take into account initial peak pressure as the most dominant design factor.

However, gas explosion pressure-time history measured from computational analysis for complicated offshore facilities is a little different. Although the level of initial peak pressure is higher than the rebound peak pressure, it fluctuates more. In some cases, the rebound pressure phase had a larger portion of the entire shock wave's pressure-time history. The gas explosion pressure curve can have many different shapes based on the rate of pressure rise, fluctuating cycles and so on. Therefore, it is very important to apply these factors to design formula. Fig. 14 shows idealised explosion design load profiles with different approaches. Fig. 14(a) shows the general design concept focused mostly on the initial peak pressure. In this case, the analyst only wants to get the level of peak overpressure. The point is to determine the critical point of peak pressure in terms of structure failure. Fig. 14(b), however, has a few more factors. For this method, the properties of the rebound pressure phase should be considered. The interaction between the initial and rebound phases needs to be considered since these two different phases would apply almost coincidentally in terms of the structure itself. Therefore, in this study, explosion design parameters were established which included these issues.

Fig. 15 illustrates the entire procedure for risk-based explosion-resistant design. Ideally, for extensive numerical analysis about explosion wave factors, all feasible potential explosion cases are meticulously

examined, and CFD analysis is carried out in order to model gas dispersion and explosion. Although scenario assumption is very important part, it remains beyond the scope of this study. The accidental load generally considered acceptable is influenced by the safety functions which correspond to 10^{-4} or 10^{-5} per year for a single accidental event. It normally corresponds to an overall frequency of 5×10^{-4} per year as the impairment frequency limit of the system. Explosion design load could be assumed based on this frequency range. But a different safety discipline should be required according to the extent of potential risk. For example, extra safety measures may be needed in high risk areas or the residential area. After identifying all of the safety critical elements, a possible undesired explosion event is assessed with explosion wave load parameters. The next step is to perform the structural analysis using computed design loads. For more accurate analysis, nonlinear analysis is recommended. If the outcome satisfies the safety rule or guideline, this stage is terminated. However, if the result is not acceptable, the analysis returns to the "re-selection design load" stage. Here, two methods can be considered according to the control of the design layout. If there is modification of the structural geometry condition or configuration, re-assessment is required, but additional analysis is just required if there is no critical change.
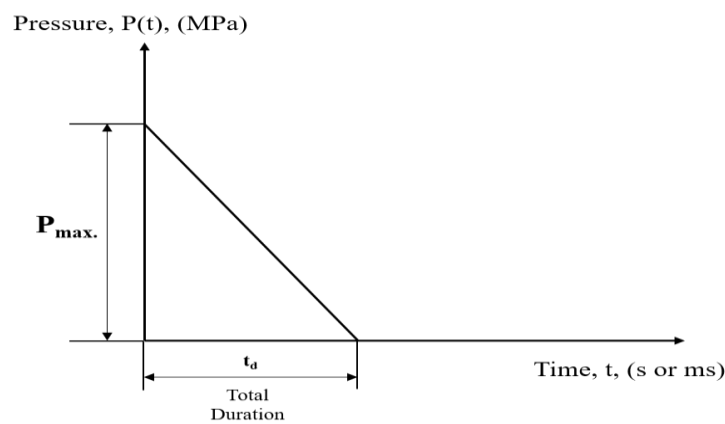
(a)
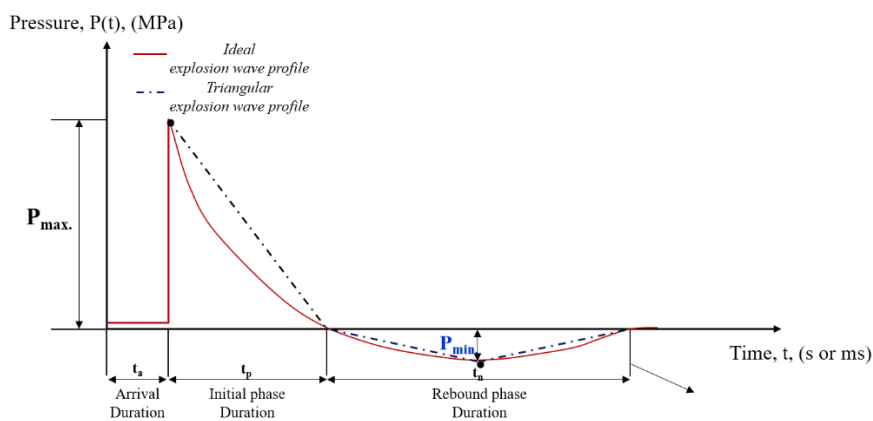
(b)

Fig. 14 Approaches for determining design load parameters: (a) initial peak pressure based, (b) combination of initial and rebound pressure phase [110]
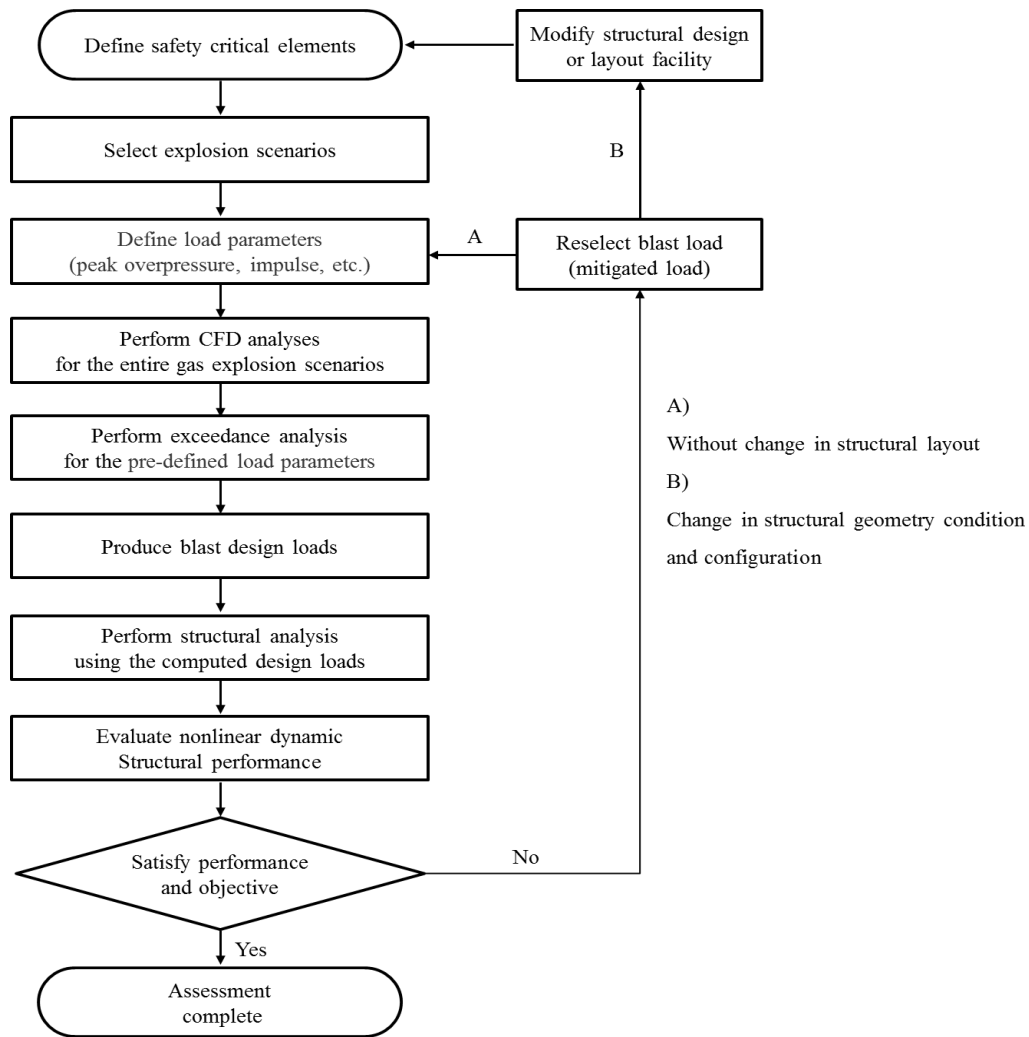
Fig. 15 The typical procedure for risk-based explosion resistant design [109]

3.4 Explosion simulation data sorting method

In the explosion computational analysis, a thousand monitoring points and panels were used to record explosion pressure data with hundreds of explosion scenarios. As hundreds of thousands of explosion pressure-time history data can be generated as outcomes, it is not possible to investigate the numerical information in such a large data set using a simple method and a data processor was required. In this study, Visual Basic Application (VBA) code based on Excel software was used to develop a program to analyse the enormous data set. Fig. 16 shows the algorithm and several functions of this developed code. First, the text type files can be generated as an outcome in the CFD analysis software. They are original files before classifying based on user defined properties, and include the record for pressure variation with time. After extracting all of the data from the CFD analysis program, the VBA commander can bring up all of the extracted files. The next stage is to sort these a great amount of data set as user wanted. The most important

factors which should be investigated are the numerical properties associated with pressure, impulse and the time domain in each stage. The developed VBA code offers the several functions which can bring such values from the output data, and even compares these parameters based on user defined scenarios and data types. In addition, the original fluctuating explosion pressure-time curve can be transformed to an idealised triangle shape curve which is generally used as the loading condition in finite element analysis (FEA). This issue is discussed in more detail in Chapter 5.
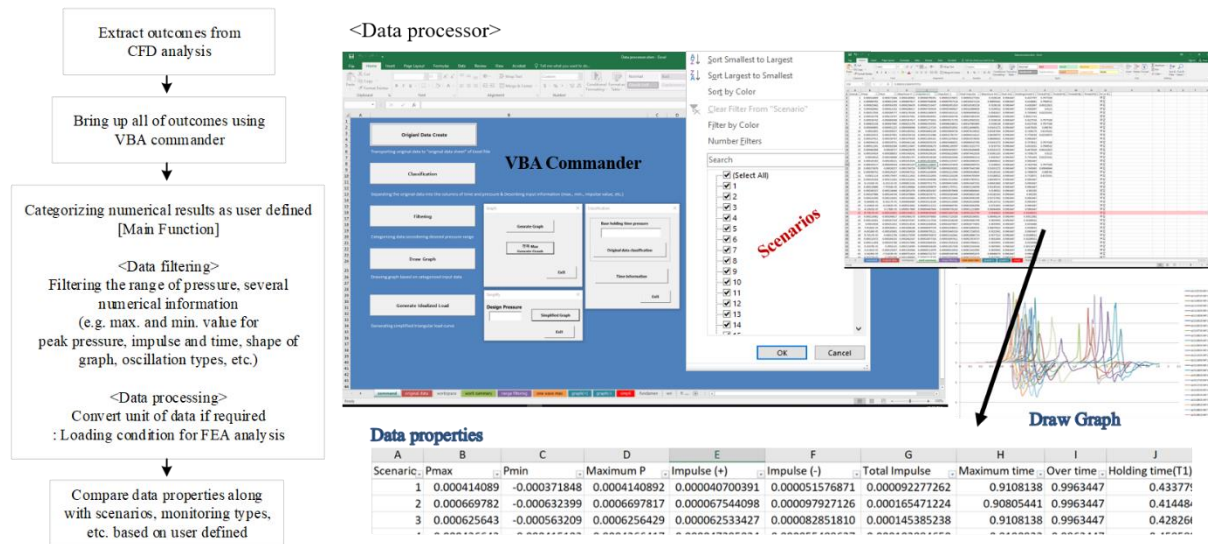
Fig. 16 Descriptions of the developed data processor based on VBA code

3.5 Data analysis for explosion simulation results

3.5.1 Initial peak pressure

First, the distribution of explosion pressure according to different gas cloud volumes and distance from the ignition was investigated as shown in Fig. 17. In each case, the level of average peak pressure in both the initial and rebound phases was marked with different colours, and the ratio between the initial and rebound peak pressure was depicted with a black dotted line. It is clear that the variation of initial peak pressure was large with regard to factors such as gas cloud volume and ignition distance, while rebound pressure had relatively small variation. The gas cloud volume which contributes to the explosion energy source directly influenced the level of peak pressure. However, the relationship between peak pressure and ignition distance was not linear. As described in Fig. 17, a larger gas cloud indicated a higher peak pressure. Although rebound peak pressure had a little fluctuation, initial peak pressure definitely increased with gas cloud volume. But the relationship between peak pressure and distance from ignition position was different. Peak pressure at 25 metres from the ignition position was higher than the peak value 15 metres from the ignition location, and then decreased again at the location further than 25 metres away. Peak pressure at closer locations to the ignition is expected to be high, but the analysis result shows there may be other factors which can contradict

common knowledge. This is because the intensity of the explosion wave pressure can be influenced by several factors like geometrical congestion and other obstacles [118].

Fig. 17 Significance of rebound pressure (a) for different flammable gas cloud volumes, (b) for different distance from the ignition positions

3.5.2 Rebound peak pressure

There is controversy about whether to include the rebound pressure phase in the explosion wave profile when performing the explosion-relevant analysis. Some researchers have claimed the rebound pressure phase is not generated in most real situations or its impact is so insignificant that it could be ignored [119, 120]. However, extensive explosion pressure data analysis showed that the rebound pressure is sometimes quite significant and should not be neglected. This means the interaction between the rebound pressure phase and structural damage should also be considered. In this study, the distribution between the initial and rebound peak pressure was examined based on a large explosion pressure data set.

Fig. 18 shows the comparison results for the quantitative difference between both pressure types. It is evident that initial peak pressure is higher than rebound pressure in many cases, but some cases show the rebound pressure is almost similar or even higher than the initial peak pressure level. For the point-pressure (NP) data case, entirely, the level of rebound pressure is quite low compared to the initial pressure data, but some data are similar to the initial pressure group included at a relatively low level as shown in Fig. 18(a). Fig. 18(b) shows each pressure distribution measured by panels, and most rebound pressure levels are higher compared to the earlier case, and even comparable with initial peak pressure. The occurrence of the rebound pressure phase depends greatly on the location of ignition. The representative case is a tunnel. If the explosion source is ignited in a tunnel with a closed end, there would be overpressure first, and then the shock wave travels to the opening, where a high level of rebound pressure can then be produced inward. On an offshore facility, the offshore topside area is very complicated, and has a suitable geometrical environment to generate rebound pressure. Therefore, the rebound pressure phase should be applied for reasonable explosion analysis and

structural assessment except when the level of the rebound pressure is very low compared to the initial peak pressure.
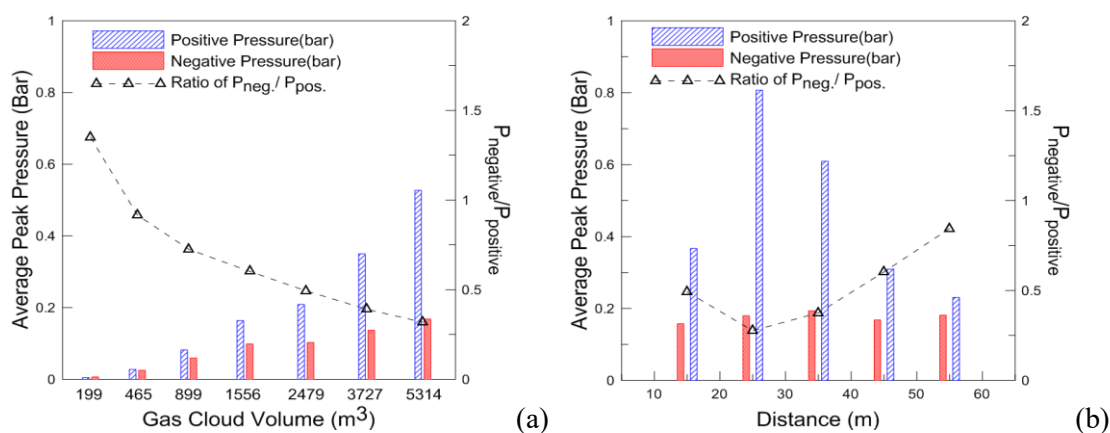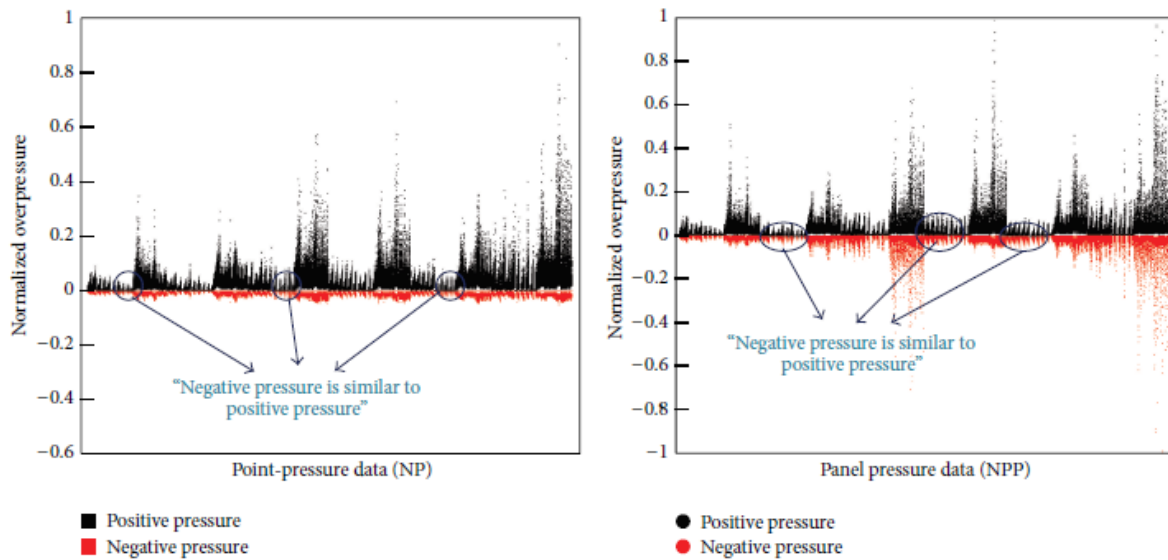

Fig. 18 Significance of rebound pressure (a) for different flammable gas cloud volumes, (b) for different distance from the ignition positions

3.5.3 Contribution of geometrical condition

The panel monitors on the gas explosion-resistant wall were grouped into three sections in both the horizontal and vertical direction. The horizontal direction monitors were divided into three areas of compression module, piping-rack connected area and separation module. The vertical groups were categorised as the air-affected area, deck-connected area and support-connected area. As a result, a total of nine sections were distinguished to investigate the distribution of explosion pressure properties based on geometrical difference. Tables 5 and 6 show the comparison results of each parameter depending on the geometrical division. All the numbers in each table denote the average value. The tables show the distinctions evident among each section. The highest pressure and impulse level was measured at the support-connected area and piping-rack connected area, and both of them were more similar to the closed type section than other areas.

As mentioned earlier, the intensity of an explosion pressure wave can be more powerful in such an environment. The FPSO structure is usually designed to produce and store hydrocarbon, so there is an arrangement of process and utility modules alongside a central pipe-rack which typically has very confined geometry. Arranging the piping-rack along the longitudinal centreline allows for process and utility equipment to transfer oil and gaseous materials to modules either side [121]. Both the support-connected area and the piping-rack connected area were influenced by the reflected pressures, which were generated by the pipelines and surrounding equipment. Fig. 19 indicates one example for the explosion pressure contour diagram

showing the wave propagation. As described in the figure, the higher pressure was generated near the obstacles or installations. But the pressure level was definitely low when there was empty space or a gap between equipment since the pressure wave can move out along the opening. To clearly understand this issue, the numerical pressure distribution of each module was investigated. As described in the FLACS 3D model, each module has a different congestion level and layout features. These conditions can result in different consequences even if the level of ignited explosive energy is similar. Therefore, how explosion pressure and impulse vary in this situation should also be analysed.

Table 5 Numerical results for explosion wave parameters dependent on the direction of height

Division	Pmax. (MPa)	Pmin. (MPa)	Time (initial, s)	Time (rebound, s)	Impulse (initial, MPa·s)	Impulse (rebound, MPa·s)
Air-affected	0.017	0.006	0.06	0.13	0.000513	0.0004
Deck-connected	0.030	0.013	0.062	0.11	0.00093	0.00071
Support-connected	0.045	0.016	0.063	0.12	0.00143	0.00097

Table 6 Numerical results for explosion wave parameters dependent on the direction of width

Division	Pmax. (MPa)	Pmin. (MPa)	Time (initial, s)	Time (rebound, s)	Impulse (initial, MPa·s)	Impulse (rebound, MPa·s)
Air-affected	0.017	0.006	0.06	0.13	0.000513	0.0004
Deck-connected	0.030	0.013	0.062	0.11	0.00093	0.00071
Support-connected	0.045	0.016	0.063	0.12	0.00143	0.00097

Fig. 19 Explosion pressure contour diagram with wave propagation
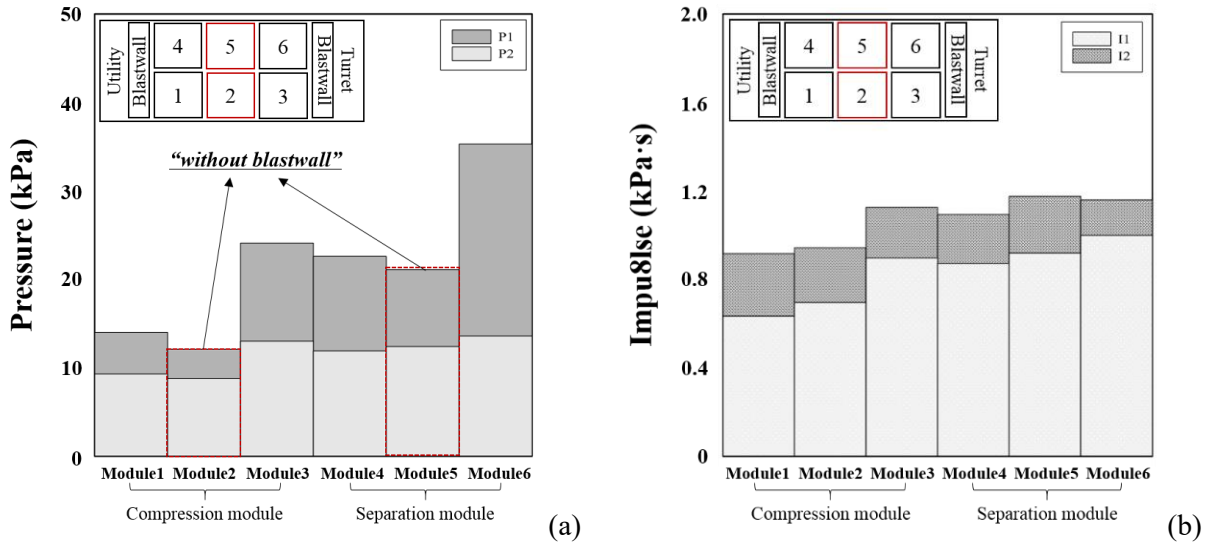
Fig. 20 The average peak pressure and impulse in each pressure phase at the modules

(a) average peak pressure (b) average impulse

Table 7. The consequence for risk elements of explosion wave in each module

Module	Risk elements from blast wave					
Types	P1 (kPa)	P2 (kPa)	I1 (kpa·s)	I2 (kpa·s)	R1 (s)	R2 (s)
Module 1	14.12	9.25	0.63	0.92	0.045	0.099
Module 2	12.08	9.12	0.07	0.94	0.058	0.107
Module 3	24.34	13.15	0.09	1.13	0.037	0.087
Module 4	23.16	12.47	0.087	1.09	0.041	0.088
Module 5	21.19	12.21	0.092	1.18	0.040	0.099
Module 6	35.27	14.01	0.102	1.16	0.028	0.085

Chapter 4

Stepwise Explosion Risk Analysis for induced gas explosion event in FPSO facilities

4.1 Introduction

With demand for energy increasing, the offshore oil and gas industry is using more developed installations to be possible obtaining resources in more remote and dangerous region. These environments inevitably lead to more hazardous accidental events and engineering difficulties in using preventive design [122-127]. The FPSO structure, the representative facility in this field, has a multi-functional structural system. It does not need to include many external support components, and therefore allows oil and gases to be changed into forms more capable of being moved using manufacturing facilities of its own. To connect a series of systems on each module efficiently, many types of equipment and systems associated with the operational process are required, making the topside area of a FPSO facility very congested. Many flammable carbon materials remain due to the repeated manufacturing process. These operational conditions not only increase the potential for explosion accidents, but also aggravate the extent of system damage or mechanical structure damage by high pressure explosions. Ignition occurring on the FPSO process area could cause serious engineering problems with devastating effects. Workers could be killed or seriously injured and all system components could fail. Oil leakage due to breakage of storage tanks could also have catastrophic impacts on the ocean environment and marine ecosystems.

To minimise latent hazards, FPSO structures should be designed taking into account the feasible risk cases of explosion incident and technical guidelines preventing from increasing these undesired issues.

An explosion risk assessment (ERA) is very helpful in making risk-informed decisions to reduce undesired accidents. ERA is performed during the initial design stage as part of safety inspection and is done to lessen the acceptance level for risk elements as much as possible and to offer the numerical range of explosion pressure affecting to the structural damage of safety critical apparatus. Typically, technical reports are produced considering safety measures in order to offer design input parameters. The reports address the performance criteria and corresponding explosion design pressure influenced by overpressure and drag pressure [128-130]. Although many studies have explored ERA, there are still several unresolved issues. This chapter presents a practical method to evaluate the explosion design load considering the extent of peak pressure and duration time, in both the initial and rebound pressure stages, using probability distribution functions with correlation analysis, and compares it to conventional industry practices.

4.2 Explosion risks assessment (ERA) general approach

Explosion risk assessment follows the typical risk assessment principles. Since all the attention is concentrated on the explosion hazard, target issues are much more specific and some stages can be excluded. In the ERA process, the most important element is explosion risk identification. Based on the cause of the explosion, the influencing factors and their probability, the most dominant hazard elements are identified. As

mentioned earlier, these analyses can also be used in qualitative and quantitative approaches. Qualitative explosion risk description is expressed by words. It focuses on the definition of potential explosion circumstances, and the combined effect of likelihood and consequence for each event rather than numerical detailed analysis for outcomes. On the other hand, quantitative explosion risk assessment gives quantitative estimates of explosion risk considering the elements composing them [131, 132]. Each explosion risk output is computed based on specific scenarios with comparison analysis for explosion risk acceptance criteria. Both approaches are needed to identify high explosion risk areas and to manage the system efficiently.

The research in this chapter is similar to a semi-quantitative concept. Explosion wave pressure is regarded as the most important aspect of analysis since it has a decisive influence on structural mechanical damage. In the worst circumstance including a higher gas leak rate and geometrical confinement, it can produce a more powerful explosion wave despite a similar extent of explosion. Thus explosion wave properties should be more clearly quantified to define the explosion risk level and acceptance criteria.

A typical ERA model for an explosion event was summarised in Fig. 20. The first step is to define the targeted potential explosion event. The boundary condition for the target area should be described clearly considering interfaces with other installations. All the activities that could happen within the system and may directly have an effect on the potential explosion need to be listed. The next step is to assess the explosion risk factors which then determine the whole content of the ERA, since establishing the risk elements directly affects what data are analysed. Subsequent consequence and likelihood investigations are carried out based on the identified risk elements, and the explosion risk level is described through the analysis results. Once the explosion risk is computed by the earlier stage, the next step is to assess whether that risk is tolerable or not. If the explosion risk level is regarded as tolerable, then it is managed by the safety design discipline. Otherwise, risk reduction measures are needed. This research also followed this typical process, but the core contribution is the boxed area in Fig. 21. Most analysts pay more attention to the potential impact of an explosion incident on the environment, equipment assets and personnel rather than on an explosion's immediate cause, while this research concentrates more on the root of an explosion which can have catastrophic impacts.
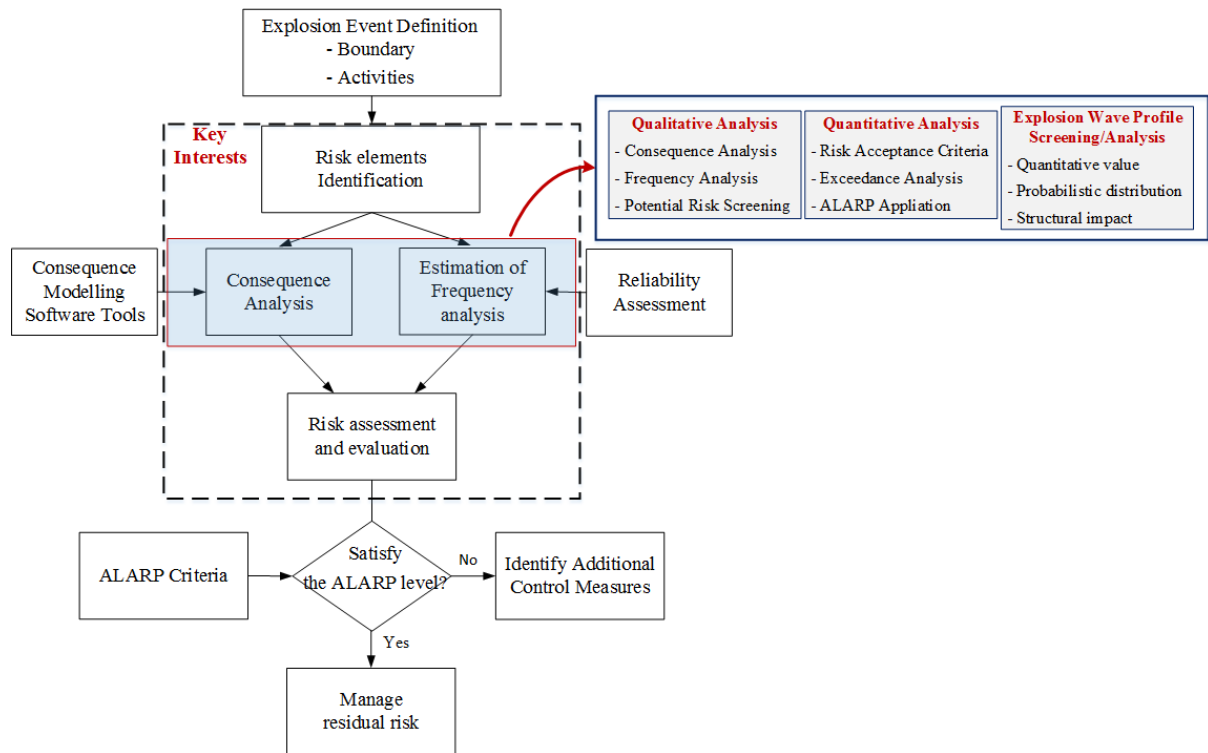
Fig. 21 The flowchart of explosion risk assessment model

4.3 Explosion event and target area definition

The targeted issue in this chapter is gas explosion shock waves which are likely to generate in the topside process module of an FPSO structure. Typically, the FPSO topside area is built with several modules for different purposes. Each module has many equipment and interface systems in order to perform gas compression, oil processing and storage and treatment tasks [133]. Many flammable gaseous materials can be produced during operations, and they are a potential risk for ignition and explosion. Once an explosion occurs, an explosion wave travels into the air, and then the surrounding structure components are exposed to the explosion wave impact load. This impact directly influences the physical damage of structure [134]. The level of impact loading exerted on the structure varies along with external and internal elements. External elements are the variables associated with the explosion source, such as ignition types and explosion material types, while internal factors are related to the structure itself, such as material properties and structural shape [135].

4.4 Identifying risk elements

4.4.1 Limit state concept risk estimation.

After an explosion event, explosion pressure waves are produced which can directly influence, significantly or insignificantly, structural physical damage even at a distance. Due to the geometrical dependency on explosion pressure level, extensive parameter analysis for explosion waves based on applying detailed input

materials is needed to identify explosion wave risk elements. Unlike previous studies which only focused on initial peak pressure, this research designated risk factors more broadly. These key elements are the duration time, impulse and peak pressure in two opposite pressure phases as described in Fig. 22. The figure shows both original explosion pressure-time history and its idealised curve. All the explosion wave curves were transformed into this type, and then comparative analysis was performed on the risk aspect. It is remarkable that the area under the curve of each pressure phase is the same even though the pressure-time history was simplified as a triangular shaped loading condition. This means both of them are identical in terms of impulse which is represented by the integral of force with respect to time. There are three reasons for this simplification as follows. First, the original curves oscillate frequently, so it is hard to establish the target variables for identifying risk elements. Second, in setting a time step for finite element analysis, the oscillated loading curve requires a very fine segment at each step, which takes too much computational time. Third, by applying this idealisation based on reasonable assumptions, it is possible to compare and evaluate not only explosion wave properties but also their influence on the physical damage of the structure for all explosion pressure data on the same basis.

The pressure-time history information is input data to assess the extent of an explosion event. It can be used as a loading condition to investigate the target model's response and damage pattern. Since the foremost purpose of present research is to extract the risk elements included in explosion wave and to evaluate their effect to structural stability in terms of physical damage, the application of advanced theories or technical aspects in structural analysis is not primarily focused in this study. The main task, therefore, is to classify the dominant factors in the explosion load time history, and then the extent of hazard for each variable is assessed using both qualitative and quantitative approaches.
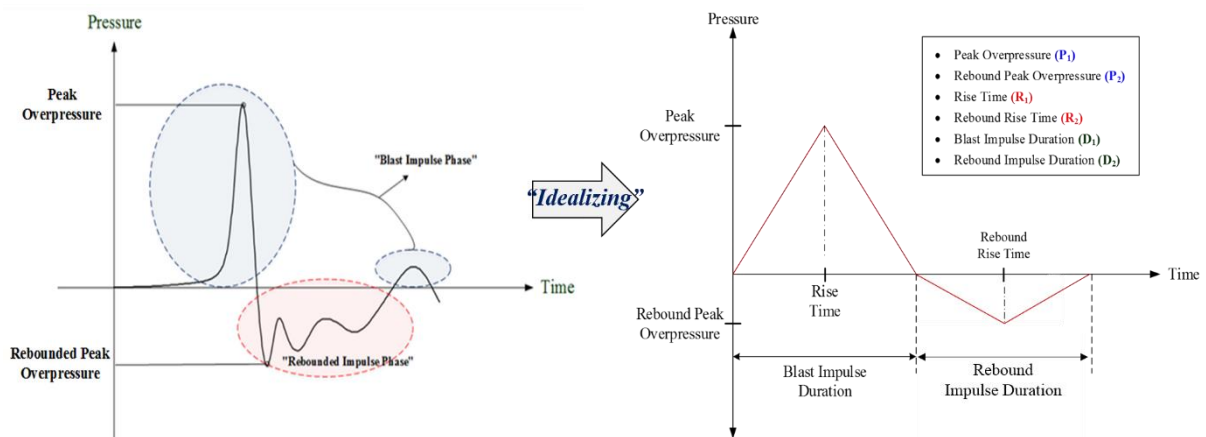
Fig. 22 Idealized explosion wave profile and the definition of its risk elements

4.4.2 Qualitative ERA

In the qualitative explosion risk assessment of FPSO facility, both safety function and risk monitoring are required concurrently. Such a multi-functional structural system has a lot of components, installation, connection system for operation effectively [136]. Therefore, it has a host of possibilities of undesired event in several parts. As described in the qualitative ERA approach, first, the safety function and risk screening were considered simultaneously to establish the risk level of the target area. The reason for this multiple analysis is that FPSO facilities are normally managed using both guidelines. The safety function includes design philosophies and operation rules or maintenance issues to prevent explosion incidents. On the other hand, the potential risk screening task can be performed considering risk frequency and consequence.

The objective of risk screening is to investigate which part is regarded as a low risk area for an explosion incident and whether or not it requires additional action for more detailed structural analysis [137]. Table 8 lists the risk screening categories according to safety measures and maintenance guidelines. Not only are consequence and frequency classified based on the risk level, but the influence of safety installations as per each risk level has also been assessed. Meanwhile, the potential explosion hazard was separated using the risk matrix shown in Table 9. The high and low-risk area can be identified given the matrix. Low risk areas are definitely less complicated due to fewer installations and other components, so these areas can be unstaffed facilities with low intervention frequency by workers, which can then facilitate more focus on the relatively high risk areas.

Fig. 23 indicates the explosion pressure contour when ignition occurs in the centre of the module. From this diagram, it is evident which areas should be prioritised to prevent an undesired explosion event, and it is also clear that the high risk area showing a high level of explosion pressure is around obstacles like the blast wall. On the other hand, weak pressure was measured in the less congested zone due to the secured space for escaping pressure waves.

Table 8. Risk screening index considering safety function

Ⅰ. Risk level		Description for consequence severity
A	Low	• No loss of production and damage to equipment • Negligible
B	Moderate	• Safety installation can cover most of area • Minor damage to equipment and/or facility
C	Major	• Safety installation can cover some parts only, requiring significant preventative action • Serious loss of production
D	Critical	• Urgent remedial action required
Ⅱ. Risk level		Description for likelihood or frequency
1	Almost Certain	• Expected to occur in most circumstances • Safety installation for only human living areas.
2	Likely	• Probably occur in most circumstances • Safety installation covers critical potential area of FPSO structure
3	Possible	• Must occur at some time • Safety installation covers most of area of FPSO structure
4	Unlikely	• May occur at some time • Requiring medium level of maintenance and intervention
5	Rare	• May occur, but only under exceptional circumstances • Requiring high level of maintenance and intervention

Table 9. Risk matrix diagram for potential risk screening

Likelihood or Frequency		Consequence Severity			
		Low	Moderate	Major	Critical
		(A)	(B)	(C)	(D)
Almost Certain	1	High	Extreme	Extreme	Extreme
Likely	2	Moderate	High	Extreme	Extreme
Possible	3	Low	High	Extreme	Extreme
Unlikely	4	Low	Moderate	High	Extreme
Rare	5	Low	Moderate	High	High
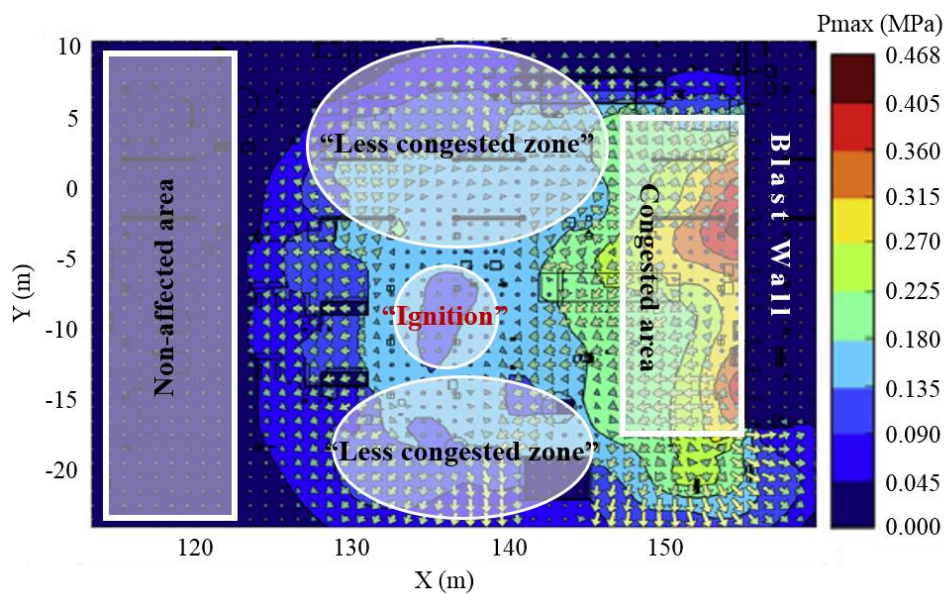
Fig. 23 Explosion pressure contour according to wave propagation

4.4.3 Quantitative risk assessment: As Low As Reasonably Practicable (ALARP) application

In quantitative risk assessment, the ALARP concept is used as a hazard acceptance basis. The ALARP is a concept of quantitative risk expressing that undesired hazard should be made less to a certain level which is as low as reasonable practicable [138]. Whether certain risk is tolerable or not is generally judged based on the three regions described in Fig. 24. Each boundary is defined by target safety levels. In the upper "unacceptable region" the risk is regarded as being intolerable and further safety measures are required. In the lower "ALARP region" risk is regarded as being widely acceptable, so no further safety measures are needed. To determine this region for an explosion event, the overpressure versus frequency exceedance curve is typically used. In this curve, the risk level can be regarded as the ALARP region by considering Individual

Risk Per Annum (IRPA), which is a measure of the annual risk to an individual working on the facility. In general, the proper ALARP region range is from 10^{-5} to 10^{-4} per year in terms of IRPA. Based on this range, a reasonably practicable extent of overpressure is obtained numerically, and it is often used as the design strength of offshore structures. The last region is the "negligible region", normally called the intermediate ALARP region. The risk included here is considered to be tolerable only if it is revealed to be ALARP, namely, if it is demonstrated that no further reliable reduction measures could be applied cost effectively.

However, the principle of ALARP should not only be understood as simply a quantitative measure for the hazard, since it is also used for a practical judgement of the balance between potential risk and benefit in design aspects. Although it is a very useful tool to evaluate certain risks quantitatively, the mechanism of ALARP should not only be understood as merely a quantitative measure for potential hazard. The other important purpose is to judge the proper balance between potential hazard and design benefit [139-141]. However, in the typical ERA approach, the limitation of this principle is to only use the overpressure (initial peak pressure) as the measurement of the risk. Even though initial peak pressure is the main cause of structural physical damage in an explosion pressure wave, there are definitely other properties that could influence on the damage, like the rebound pressure phase. This approach is not a limit state concept, which should consider all factors related to the event. Therefore, the more in-depth analysis based on all explosion loading parameters should be implemented to fully understand the relevant risk of physical damage from explosion waves.

Fig. 24 The application of ALARP principle; the overpressure versus exceedance frequency

4.5 Probabilistic analysis

Many assumptions used in the explosion analysis procedures are required to determine the variation in the probabilistic analysis results. Even though probabilistic concepts are commonly used in the offshore oil and gas industry to evaluate accidental loads from explosion and fire, a firm instruction has not been established [142-144]. This section introduces sever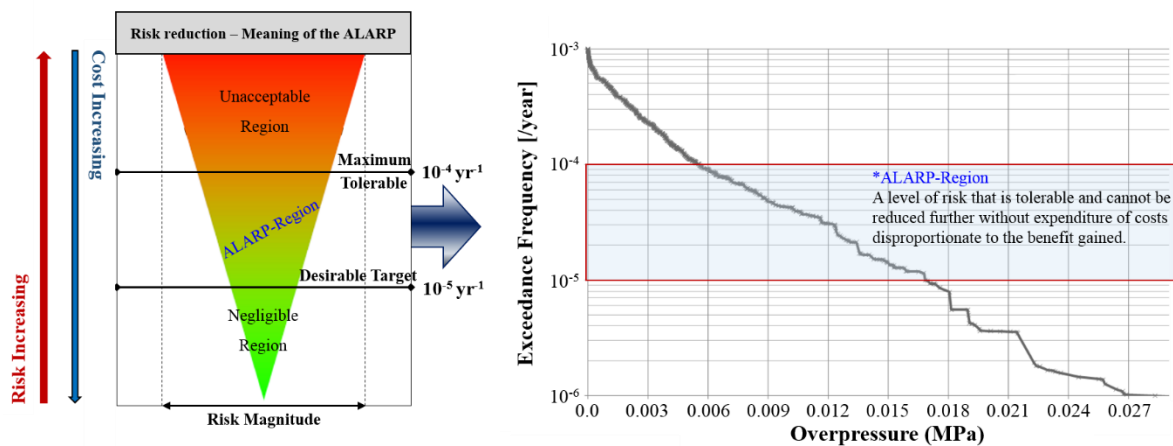al methods to study probabilistic issues of explosion wave properties. Based on probability theory, numerical distribution characteristics and correlation between each variable were investigated and explosion wave history was assessed by considering a pressure phase progressively with the event tree analysis technique.

4.5.1 Probability distribution of explosion pressure parameters

An explosion event is a complex phenomenon, since several variables with uncertainties should be considered. Explosion wave pressure, which is regarded as the most crucial risk factor here, varies according to the extent of explosion source energy and ignition condition. This means, in terms of the probabilistic approach, explosion wave properties could be considered as random variables affecting the intensity of an explosion. A random variable is defined as a variable which can be obtained by a random phenomenon, and the relevant factors mentioned earlier such as wind direction and speed or leak rate do not have any rule for their formation. Therefore, all factors associated with the explosion pressure profile are outcomes generated by random variables [145]. Thus, peak pressure, duration time and impulse of both the initial and rebound phases were used as random variables, and their probability distributions were analysed to understand the variability of numerical properties. Probability density functions (PDF) were computed using the entire explosion pressure data set. A PDF is generally used to describe the probability of random variables included in a particular range, as opposed to taking any one particular value [146]. Applying a PDF to the explosion pressure data set can be helpful in understanding the variation in established scenarios. Based on the numerical analysis results for explosion wave time history, each PDF was computed. The resulting median value and deviation of each data point are marked in the graph (Fig. 25 and 26).

In addition, the coefficient of variation was computed to compare the probability distribution for each property. It means the ratio of the standard deviation to the average, and it can be used to compare the degree of variation from one data series to another type, even if the average values are completely different. The coefficient of variation (CV) for parameters in the initial pressure phase is 0.86, 0.7 and 0.85, respectively. For parameters in the rebound phase, the CV is 0.28, 0.32 and 0.34. They were relatively small compared to the initial phase because the scattering extent of initial peak pressure data was bigger than the rebound pressure group and even sensitive to explosion scenario factors mentioned in the previous chapter. As a result, in the initial peak pressure data group, all the distributions were close to the log-normal distribution type as shown in Fig. 25, while rebound peak pressure data showed a completely different style. Furthermore, Fig. 26 shows that only the peak pressure data set indicated a normal distribution, but for duration time and impulse in the rebound

phase, there was no clear relationship between the input data.

Fig. 27 shows the reason for the relationship by indicating the relationship between peak pressure and the corresponding impulse properties. The duration time effect made an irregular distribution. While there is no clear linear relationship, it is evident that the initial pressure-impulse dependence was more linear than the rebound phase combination. Most data that have a higher initial peak pressure value have longer duration than the relatively small peak pressure group. However, this feature was not found in the rebound pressure phase data set. Hence, the distributions of the initial peak pressure and their impulse were similar, while the rebound wave properties were different for each factor. The results corresponding to each distribution are summarised in Table 10.
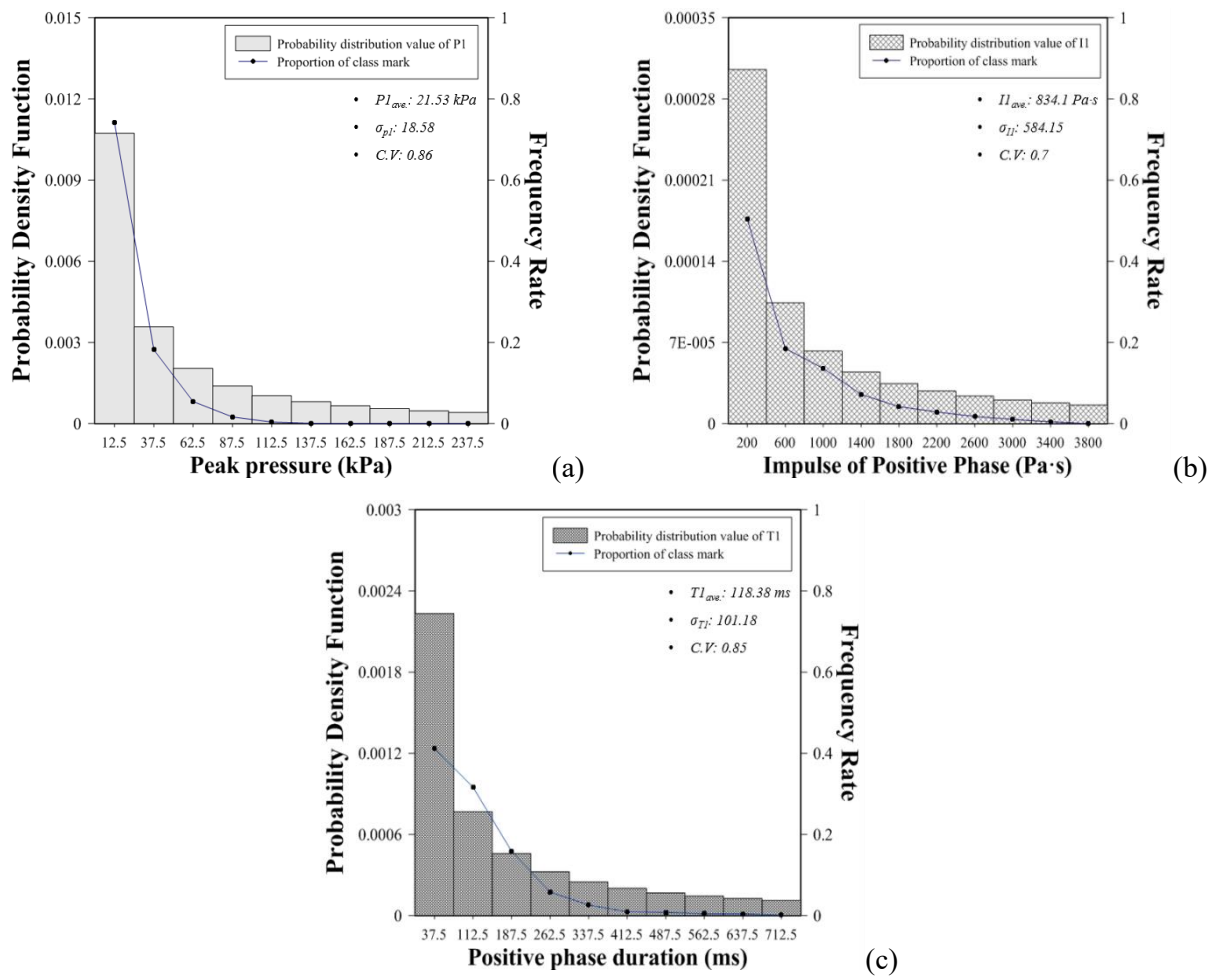
Fig. 25. Probability density function for parameters in positive pressure phase (a) for the peak pressure, (b) for the impulse (c) for the duration time

53
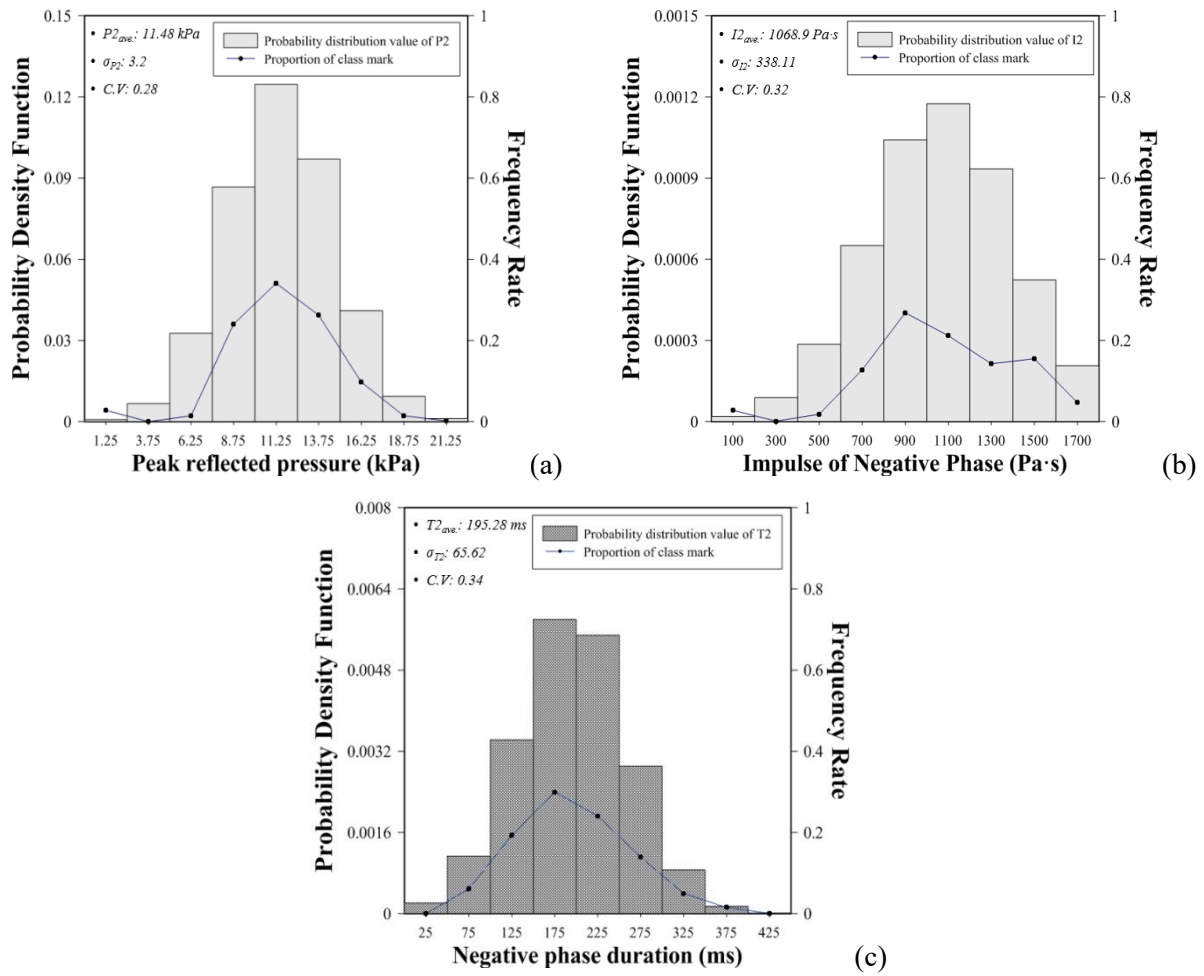
Fig. 26. Probability density function for parameters in positive pressure phase   (a) for the peak pressure, (b) for the impulse (c) for the duration time
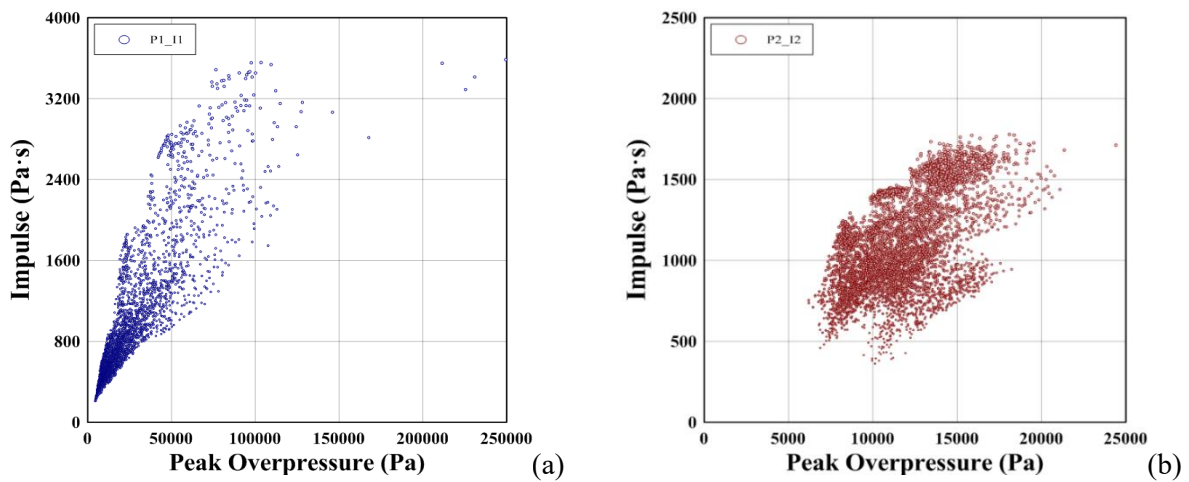
Fig. 27. Scatter diagram between peak pressure and impulse (a) initial peak pressure and impulse (b) rebound peak pressure and impulse

Table 10. Results for probability distribution of parameters in both pressure phases

1) Probability distribution for parameters in positive phase								
Initial peak pressure			Initial phase impulse			Initial phase duration time		
$P_{1ave.}$ (kPa)	σ_{P1}	C.V	$I_{1ave.}$ (Pa·s)	σ_{I1}	C.V	$T_{1ave.}$ (ms)	σ_{T1}	C.V
21.53	18.58	0.86	834.1	584.15	0.7	118.38	101.18	0.85

2) Probability distribution for parameters in negative phase								
Rebounded peak pressure			Rebound phase impulse			Rebound phase duration time		
$P_{2ave.}$ (kPa)	σ_{P2}	C.V	$I_{2ave.}$ (Pa·s)	σ_{I2}	C.V	$T_{2ave.}$ (ms)	σ_{T2}	C.V
11.48	3.2	0.28	1068.9	338.11	0.32	195.28	65.62	0.34

4.5.2 Correlation coefficient analysis

In the ERA, the general approach of correlation analysis for explosion wave load is to evaluate the relationship between peak pressure and its impulse. The explosion pressure-impulse diagram shows the three loading zones of impulsive, quasi-static and dynamic domain according to their duration time and peak pressure intensity [147-149]. The diagram is usually used to categorise the explosion wave loading type and to assess the structural damage as well as the human injury based on each loading condition [150]. But this classification considers only initial peak pressure and its impulse and it cannot be defined as short or long term based only on its digit comparison. In this study, long or short duration should be separated by considering the relative ratio between the natural period of the structure and the total duration time of applied loading. It is essential to investigate explosion pressure properties in detail before considering the structural eigenvalue. Pearson product-moment correlation coefficients were used to assess the extent of correlation between different explosion pressure profiles. The correlation coefficients were computed by the following equations.

$$\text{COV(X, Y)} = \frac{1}{n-1}\sum_{i=1}^{n}(X_i - \bar{X})(Y_i - \bar{Y}), \ (\bar{X} = \frac{\sum X_i}{n}, \bar{Y} = \frac{\sum Y_i}{n}) \qquad \text{eq (4.1)}$$

$$\sigma_X^2 = \frac{1}{n-1}\left\{\sum_{i=1}^{n}X_i^2 - \frac{(\sum_{i=1}^{n}X_i)^2}{n}\right\} \qquad \text{eq (4.2)}$$

$$\sigma_Y^2 = \frac{1}{n-1}\left\{\sum_{i=1}^{n}Y_i^2 - \frac{(\sum_{i=1}^{n}Y_i)^2}{n}\right\} \qquad \text{eq (4.3)}$$

$$r(X,Y) = \frac{Cov(X,Y)}{\sigma_X \cdot \sigma_Y} = \frac{n \sum_{i=1}^{n} X_i Y_i - \sum_{i=1}^{n} X_i \sum_{i=1}^{n} Y_i}{\sqrt{n \sum_{i=1}^{n} X_i^2 - \left(\sum_{i=1}^{n} x_i\right)^2} \cdot \sqrt{n \sum_{i=1}^{n} Y_i^2 - \left(\sum_{i=1}^{n} Y_i\right)^2}} \qquad \text{eq (4.4)}$$

Where COV (X, Y) is the covariance of X and Y, σ_X and σ_Y mean the standard deviation of X and Y, respectively. Thus, the correlation between each factor is computed using those equations. If the correlation coefficient (r) is close to either +1 or-1, it means a positive or negative linear relationship. The correlation analysis results are summarised in Table 11. Each variable was defined as follows:

- $r(P_p, P_R)$: correlation between initial peak pressure and rebounded peak pressure
- $r(I_p, I_R)$: correlation between initial and rebound phase impulse
- $r(T_p, T_R)$: correlation between duration times in each stage.

The results showed all factors have a strong association, and this indicates that the initial phase has a significant effect on the following rebound phase. The higher initial peak pressure is more likely to produce stronger rebound pressure, and it is also the same in the relationship between the duration times of both stages. Typically, when designing the structure to have the potential risk for accidental impact load, the resonant frequency range should be ascertained to prevent the oscillation with larger amplitude when the loading is applied. Around resonant frequencies, even small accidental loads have the ability to produce large deformation due to the storage of vibrational energy. Also, the structural dynamic effect is totally dependent on the relationship between structural frequency and loading duration. If the natural period is shorter than the expected impact loading, the dynamic effect can be reduced by the effect of the rebound phase, but in the opposite case, the dynamic effect would be large. Therefore, it is important to determine the possible range of explosion impact loading duration. Since total duration time is determined by combining the two pressure phases, the correlation investigation of duration time is needed for resonance avoidance design. In addition, quantifying explosion pressure properties and predicting their correlation conservatively is necessary to estimate explosion risk and to have a practical use in the design stage.

Table 11 The correlation coefficient analysis result

Strength of Association	Range (Positive)	Coefficient, r	Value
Small	.1 to .3	$r(P_p, P_R)$	0.458
Medium	.3 to .5	$r(I_p, I_R)$	0.798
Large	.5 to 1.0	$r(T_p, T_R)$	0.554

4.5.3 Event tree analysis

Most damage criteria related to accidental explosion loads are based only on the intensity of initial peak pressure as described in Table 12 [151]. However, in the limit state design concept, all actions likely to occur should be considered together. The extensive investigation of numerical properties of explosion wave profiles identified that the rebound pressure phase also has a considerable proportion in them. Therefore, its influence on structural damage should be assessed. According to previous studies, the initial pressure phase can last for about 0.01–0.25s, and its counter phase is usually longer. The extent of damage could be significantly different according to the duration time even if the wave has the same amplitude. This section explores the types of explosion pressure profiles that could be more hazardous and investigates their probabilistic issue.

In the two physical phases in an explosion pressure wave, structures experience different physical effects. Major deformation firstly occurs during the initial pressure phase, followed by the secondary effect of the rebound pressure phase. Although it appears each phase is independent, it is not long enough for structures to respond separately in each stage. However, it can be regarded as a sequence of events despite the short time from the risk assessment aspect. Event tree analysis (ETA), which is generally used to assess the outcomes of a certain system which has a probability of occurring after an initiating event, could be used. In the explosion wave travel, initial peak pressure is regarded as the initiating event, and then subsequent factors are produced in regular sequence. The ETA analysis result for the explosion pressure wave is summarised in Fig. 28. As the initiating event, the standard for initial peak pressure intensity was classified into three cases based on the criteria in Table 6. For the next event, rebound peak pressure was divided into two branches considering its normal distribution features. In normal distribution type, data converged into a mean value, so the data can be divided into less than or more than mean value. Finally, duration time is categorised in the same manner. Duration time can independently influence damage to structural members or installation systems to some extent regardless of the peak pressure intensity. The extent of structural damage or failure mode can vary according to the relationship between the natural period of structure and the total duration time of explosion wave. If the pressure waves have a similar time period to the targeted structure's natural period, it can result in excessive vibration, which can cause very serious physical damage. This is the worst case scenario for equipment like reciprocating compressors. Therefore, the investigation for resonance frequencies is required to avoid this undesired event.

It is noted that the ETA results have something in common with the correlation analysis result. The rebounded peak pressure is more likely to be less than its average if the initial peak value is less than or equal to the ALARP range. The explosion risk level, however, should not be determined based solely on this issue. Impulse property is also an important factor associated with structural physical damage and failure. If a relatively lower peak with a long period of time is applied to certain structures, it can cause a more hazardous situation than its counterpart scenario. The level of impulse for each case was used to evaluate the extent of explosion risk, as shown in Fig. 29. This criteria is changeable as it is analyst defined. If different scenarios

are used, it must be modified. The new finding is in the overlap area between ALARP and dangerous damage criteria. The negligible region could be acceptable, but it is difficult to clearly separate the ALARP and dangerous region, since there is overlap between them considering the total impulse range. Therefore, judgement of explosion risk criteria based only on the initial peak pressure is not enough. To be clearer, structure response analysis for the total impulse should be investigated.

Table 12 The influence of peak overpressure

Peak overpressure (MPa)	Description of damage	Criteria
0.001	Crack in glass	Negligible
0.003	Shattering of glass	
0.01	Repairable damage to equipment and structural member	ALARP Region
0.02	Minor damage to steel frame	
0.03	Major damage to equipment and structural member	Dangerous
0.17	Severely damaged or demolished	

Peak Pressure (P1) $P(E_1)$	Rebounded Peak Pressure (P2) $P(E_2)$	Total Duration Time (T) $P(T)$	Outcome $P(E_1) \times P(E_2) \times P(T)$
I. P1<ALARP $P(E_1)$: 0.0032	P2>P2ave. $P(E_2)_1$: 0	T<0.25s $P(T)_1$: 0	$P(E_1) \times P(E_2)_1 \times P(T)_1 = 0$ ...①
		0.25s<T>0.35s $P(T)_2$: 0	$P(E_1) \times P(E_2)_1 \times P(T)_2 = 0$ ...②
		T>0.35s $P(T)_3$: 0	$P(E_1) \times P(E_2)_1 \times P(T)_3 = 0$ ...③
	P2<P2ave. $P(E_2)_2$: 1	T<0.25s $P(T)_1$: 0.055	$P(E_1) \times P(E_2)_2 \times P(T)_1 = 0.00018$ ...④
		0.25s<T>0.35s $P(T)_2$: 0.664	$P(E_1) \times P(E_2)_2 \times P(T)_2 = 0.00213$ ...⑤
		T>0.35s $P(T)_3$: 0.280	$P(E_1) \times P(E_2)_2 \times P(T)_3 = 0.0009$ ...⑥
II. P1=ALARP $P(E_1)$: 0.516	P2>P2ave. $P(E_2)_1$: 0.373	T<0.25s $P(T)_1$: 0.217	$P(E_1) \times P(E_2)_1 \times P(T)_1 = 0.042$ ...①
		0.25s<T>0.35s $P(T)_2$: 0.306	$P(E_1) \times P(E_2)_1 \times P(T)_2 = 0.059$ ...②
		T>0.35s $P(T)_3$: 0.478	$P(E_1) \times P(E_2)_1 \times P(T)_3 = 0.092$ ...③
	P2<P2ave. $P(E_2)_2$: 0.627	T<0.25s $P(T)_1$: 0.092	$P(E_1) \times P(E_2)_2 \times P(T)_1 = 0.030$ ...④
		0.25s<T>0.35s $P(T)_2$: 0.390	$P(E_1) \times P(E_2)_2 \times P(T)_2 = 0.126$ ...⑤
		T>0.35s $P(T)_3$: 0.517	$P(E_1) \times P(E_2)_2 \times P(T)_3 = 0.167$ ...⑥
III. P1>ALARP $P(E_1)$: 0.481	P2>P2ave. $P(E_2)_1$: 0.664	T<0.25s $P(T)_1$: 0.583	$P(E_1) \times P(E_2)_1 \times P(T)_1 = 0.243$ ...①
		0.25s<T>0.35s $P(T)_2$: 0.178	$P(E_1) \times P(E_2)_1 \times P(T)_2 = 0.047$ ...②
		T>0.35s $P(T)_3$: 0.238	$P(E_1) \times P(E_2)_1 \times P(T)_3 = 0.029$ ...③
	P2<P2ave. $P(E_2)_2$: 0.336	T<0.25s $P(T)_1$: 0.057	$P(E_1) \times P(E_2)_2 \times P(T)_1 = 0.050$ ...④
		0.25s<T>0.35s $P(T)_2$: 0.255	$P(E_1) \times P(E_2)_2 \times P(T)_2 = 0.064$ ...⑤
		T>0.35s $P(T)_3$: 0.687	$P(E_1) \times P(E_2)_2 \times P(T)_3 = 0.048$ ...⑥

Fig. 28 Event tree analysis for explosion pressure considering both initial and rebound pressure phase parameters.
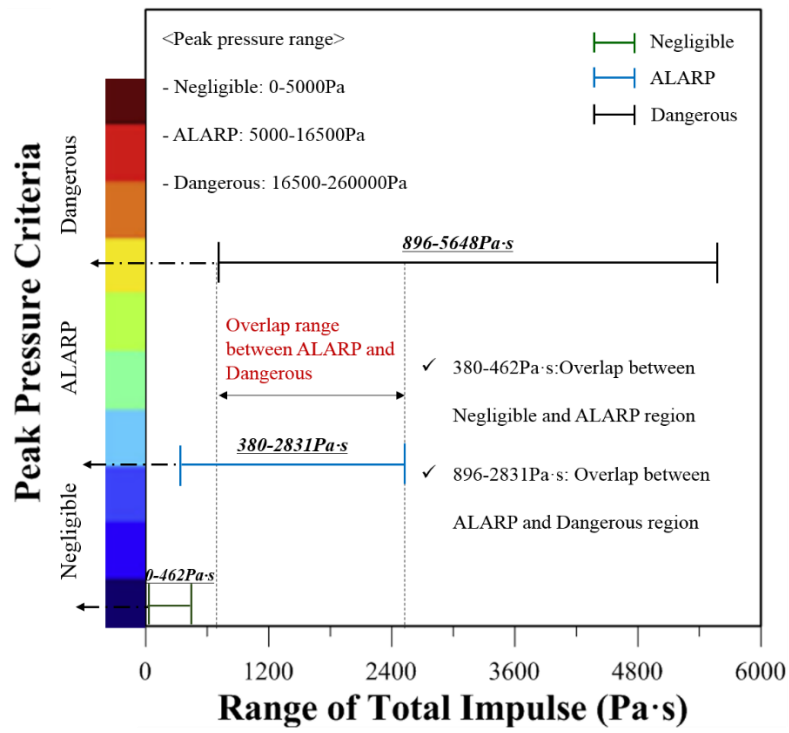
Fig. 29 Impulse range based on the peak pressure criteria

Chapter 5

Structural Response analysis

5.1 Introduction

To analyse the structural response against accidental impact load which is dependent totally on time, several conceptual idealisations and simplifying assumptions based on physical systems are required. Three assumptions are about material, loading and geometrical conditions. Material assumptions mean simplification of material behaviour considering homogeneity or isotropy. The loading assumption considers the external force to be a periodic or simple type. Geometric assumptions point to simplification of target structures by unidirectional elements, and also assume that a continuous structure may be separated as a discrete model by specifying relevant information. The main objective of this chapter is to investigate what type of explosion loading can be more dangerous to structural physical damage. Appropriate assumptions and theories are taken into account and the extent of structural damage is identified in more detail by comparing it with the typical explosion loading-structural response analysis method. Lastly, the limitations of the typical approach are described.

5.2 Analytical model 1: single and multi-degree of freedom system or target model

Single and multi-degree of freedom systems are normally used to simplify complex structures to a simple type model. They can be conveniently described using four elements as shown in Fig. 30 and Table 13. By combining several springs and dampers, a multi-degree of freedom model can also be easily established. Models using the above four elements may provide a reasonable result on the structural response of the model itself, but only limited and inaccurate information on issues related to real structural behaviour. If specific values or exact descriptions for that response were the main focus, this approach would not be useful. However, this study is not focused on such a quantitative analysis, as it is more interested in the qualitative comparison analysis for response and deformation to distinguish the more severe type of explosion loading conditions in terms of the structure itself. Therefore, from a practical point of view, the result from this analytical model can be sufficient for satisfying the objectives and understanding the characteristics of structural dynamic behaviour as well as design and safety requirements.
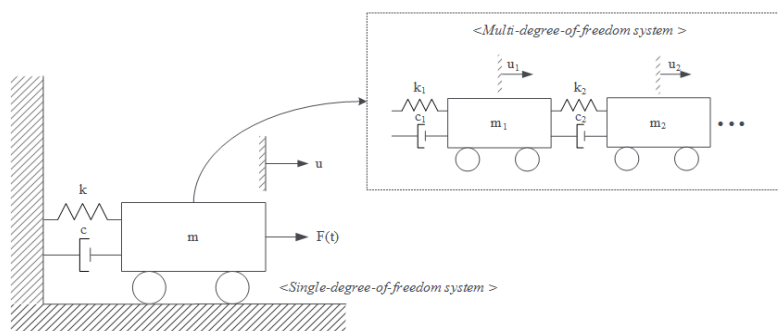
Fig. 30 Single and multi-degree of freedom models

Table 13 Four elements of single degree of freedom system

Element 1 (mass, m)	Mass and inertial characteristic
Element 2 (external force, F(t))	Elastic restoring force and potential energy storage
Element 3 (spring stiffness, k)	Frictional characteristics and energy dissipation
Element 4 (damping coefficient, c)	Loading acting on the structural model

5.2.1 Motion equation for analytical model

The system motion can be expressed using D'Alembert's principle which explains that a mass generates the force of inertia with its acceleration to oppose its motion, so that a system may be set in a dynamic equilibrium state (see Fig. 31). Through the sum of forces along the direction u, the second order differential equation can be obtained as follows [152]:

$$m\ddot{u} + c\dot{u} + ku = F(t)$$
eq (5.1)

Where F(t)=0 means that the response is free vibration caused by initial excitation.

Assuming a solution $u(t) = Ce^{st}$ and substituting equation (1), we obtain:

$$mCs^2e^{st} + cCse^{st} + kCe^{st} = 0$$
eq (5.2)

After abbreviation of the common factor, Ce^{st}, the characteristic equation for the system is:

$$ms^2 + cs + k = 0$$
eq (5.3)

By applying the quadratic formula, the roots of that equation can be obtained:

$$s_1, s_2 = \frac{-c \pm \sqrt{c^2 - 4mk}}{2m}$$
eq (5.4)

Three cases may occur for the quantity under the radical. It may be zero, positive or negative.

Case I. Critically-damped system (c=c_{cr})

If a system oscillates with critical damping (c=c_{cr}), equation (4) can be written as:

$$s_1, s_2 = \frac{-c_{cr} \pm \sqrt{c_{cr}^2 - 4mk}}{2m}$$
eq (5.5)

The expression under the radical in the above equation is equal to zero:

$$\frac{\sqrt{c_{cr}^2 - 4mk}}{2m} = 0, \quad \therefore c_{cr} = 2\sqrt{mk} = 2mw_n, \because \left(w_n = \sqrt{\frac{k}{m}} \right); natural \ frequency$$

In a critically damped system, the roots are equal, that is:

$$s_1, s_2 = \frac{-c_{cr}}{2m} \qquad \text{eq (5.6)}$$

Case II. Overdamped system (c>c_cr)

In this case, the damping coefficient is greater than the critical damping value, and the expression under the radical of equation (4) is positive. Therefore, there are two roots of equation (1), and consequently the solution is given as follows:

$$u(t) = C_1 e^{s_1 t} + C_2 e^{s_2 t} \qquad \text{eq (5.7)}$$

There is no oscillatory motion in the overdamped system. The extent of oscillations decays exponentially with time to zero.

Case III. Underdamped system (c<c_cr)

The last case is when the damping coefficient is less than the critical value, so that the expression under the radical is negative. The solutions of the characteristic equation are as below:

$$s_1, s_2 = \frac{-c \pm i\sqrt{4mk - c^2}}{2m} \qquad \text{eq (5.8)}$$

Euler's formula and Taylor series expansion can be applied:

$$e^{ix} = cos \ x + isin \ x$$

$$e^{-ix} = cos \ x - isin \ x \qquad \text{eq (5.9)}$$

The general solution of the underdamped system can be derived by substituting the roots (s1 and s2) into equation (5) considering the above relationships.

$$u(t) = (C_1' cos \ w_d t + C_2' sin \ w_d t) e^{-\left(\frac{c}{2m}\right)t} \qquad \text{eq (5.10)}$$

Where $C_1' \ and \ C_2'$ are redefined constants of integration and w_d is referred to as damped natural frequency, and is given by:

$$w_d = \sqrt{\frac{k}{m} - (\frac{c}{2m})^2} \qquad\qquad \text{eq (5.11)}$$

or

$$w_d = w_n \sqrt{1 - \zeta^2} \qquad\qquad \text{eq (5.12)}$$

Where $\zeta = \frac{c}{c_{cr}}$ points to the damping ratio of the system.

Applying initial condition as u(t=0)=u_0 and u(t = 0); u_0 and $\dot{u}(t = 0)$; $\dot{u}_0$ into equation (8) gives:

$$u(t) = \left(u_0 \cos w_d t + \frac{v_0 + u_0 w_n \zeta}{w_d} \sin w_d t \right) e^{-\zeta t} \qquad\qquad \text{eq (5.13)}$$
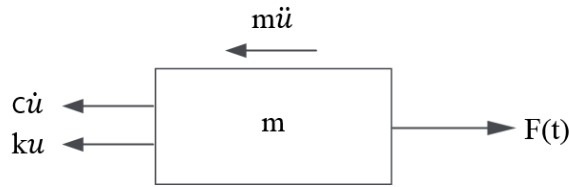
Fig. 31 A system dynamic equilibrium state

5.2.2 Validation for structural model: undamped system

The present research of structural dynamic response with the analysis of a fundamental and simple type of system uses the undamped SDOF model because the energy dissipated is quite small in the case of an extremely short excitation like explosion pressure [153-155]. The damping ratio of a steel structure is also very small, about 2%, compared to other materials such as concrete, therefore the damping coefficient can be ignored. For validation, a series of response analyses were carried out as shown in Fig. 32. It compares results between the response of the damped and undamped SDOF models. The maximum value of Dynamic Load Factor (DLF) means the peak value of displacement divided by the static displacement. The figure shows there is only a small difference for the structural response by damping effect, so that it was ignored in this study and an undamped SDOF model was used for analysis. If the damping device is left out of the practical model, the model can be re-organised as below (see Fig. 33).

Lateral stiffness (k) is obtained using equation (12):

$$k = \frac{3EI}{L^3} \qquad\qquad \text{eq (5.14)}$$

The motion equation of the undamped SDOF model can be expressed using the following equations:

64

$$m\ddot{u} + ku = F(t) \qquad\qquad \text{eq (5.15)}$$

The general solution of this differential equation can be obtained using the superposition of sine and cosine functions:

$$u = A\cos wt + B\sin wt \qquad\qquad \text{eq (5.16)}$$

By differentiating the above equation with regard to time:

$$\dot{u} = -Aw\sin wt + Bw\cos wt \qquad\qquad \text{eq (5.17)}$$

The constants of integration A and B are determined by the initial conditions of displacement and velocity. At time t=0:

$$u_{t=0} = A, \qquad v_{t=0} = Bw \qquad\qquad \text{eq (5.18)}$$

Substituting A and B into equation (14) gives:

$$u = u_0 \cos wt + \frac{v_0}{w}\sin wt \qquad\qquad \text{eq (5.19)}$$

This expression is a simple type function of the time variable t. Therefore, the response of the undamped system can be described using a single degree of freedom.

(a)   (b)
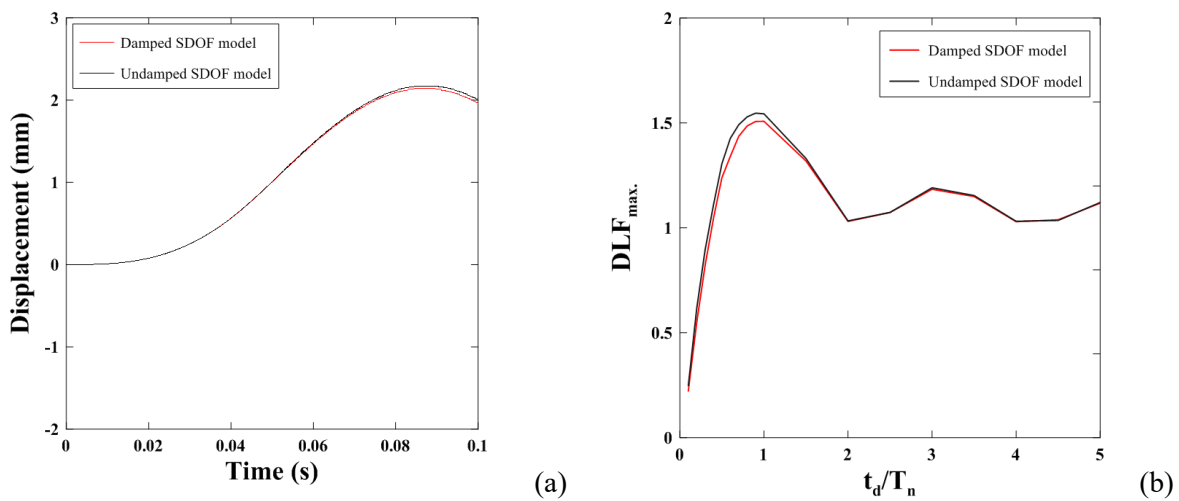
Fig. 32 Comparison between the response of the damped and undamped model
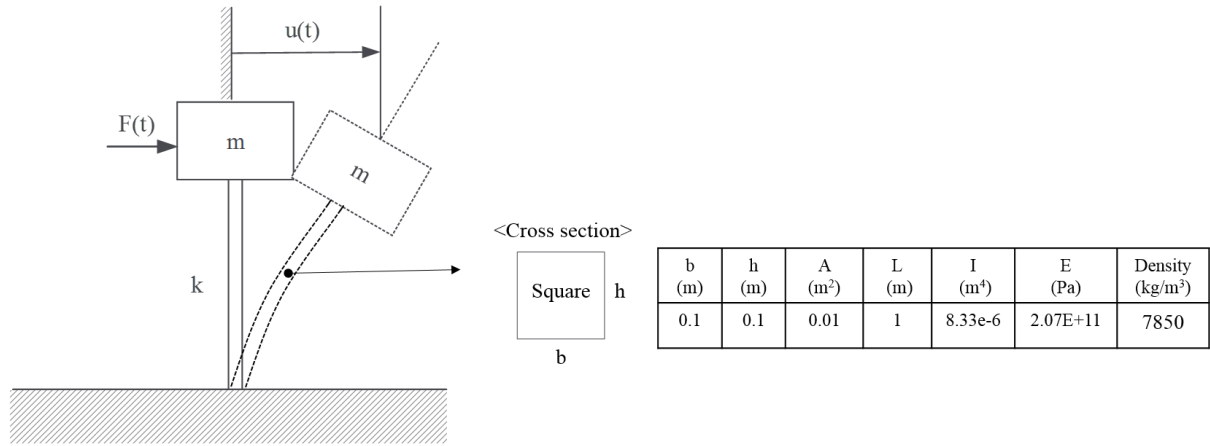
Fig. 33 Undamped single degree of freedom model

5.3 General equation for beam model

The basic equation of beam theory is a differential equation of its behaviour, linking the function of external force, initial and boundary condition [156].

$$m\frac{d^2u}{dt^2} + EI\frac{d^4u}{dx^4} + P\frac{d^2u}{dx^2} = Q(x,t) \qquad \text{eq (5.20)}$$

Where u(x,t) means the deflection, EI is the flexural stiffness, P and Q mean the compressive load and lateral excitation load, respectively. By assuming a uniform cross-section area, mass (m) and bending stiffness (EI) can be regarded as constant along the longitudinal direction.

The free vibration of an undamped model in individual modes can be described mathematically as follows:

$$u(x,t) = \varphi_n(x)q_n(t) \qquad \text{eq (5.21)}$$

Where the deflected shape (φ_n) is not varied according to time. The time variation of the displacements (q_n) is described as the sum of the complementary solution (q_n^c) and the particular solution (q_n^p), that is:

$$q_n = q_n^c + q_n^p \qquad \text{eq (5.22)}$$

This equation leads to the following formulation for deflection of the beam.

$$u = \varphi_n\left(q_n^c + q_n^p\right) = \varphi_n q_n^c + \varphi_n q_n^p = u_c + u_p \qquad \text{eq (5.23)}$$

Considering a deflection of the beam in the nth natural mode:

$$u_n(t) = q_n(t)\varphi_n \qquad \text{eq (5.24)}$$

The corresponding acceleration is:

$$\ddot{u}_n(t) = \ddot{q}_n(t)\varphi_n \qquad\qquad \text{eq (5.25)}$$

And the associated inertia forces are:

$$f_n = -m\ddot{u}_n(t) = -m\varphi_n\ddot{q}_n(t) \qquad\qquad \text{eq (5.26)}$$

By using a generalised single degree of freedom system, it can be formulated with work or energy principles. The virtual displacement theory can be used to describe the system's equilibrium. In other words, the external virtual work (δw_E) is identical to internal virtual work (δw_I). The external virtual work for the forces $f_I(x,t)$ acting on the virtual displacements ($\delta u(x)$) is:

$$\delta W_E = \int_0^L f_I(x,t)\delta u(x)dx \qquad\qquad \text{eq (5.27)}$$

The internal virtual work is due to bending moments $M(x,t)$ acting on the curvature ($\delta k(x)$), and it can be described as follows:

$$\delta W_I = \int_0^L M(x,t)\delta k(x)dx \qquad\qquad \text{eq (5.28)}$$

Substituting

$$M(x,t) = EI(x)u''(x,t) \qquad \delta k(x) = \delta[u''(x)] \qquad\qquad \text{eq (5.29)}$$

Therefore

$$\delta W_I = \int_0^L EI(x)u''(x,t)\delta[u''(x)]dx \qquad\qquad \text{eq (5.30)}$$

These functions of virtual work can also be expressed in terms of the generalised coordinate z and shape function $\varphi(x)$. From equation (2) we obtain:

$$u''(x,t) = \varphi''(x)z(t) \qquad \ddot{u}(x,t) = \varphi(x)\ddot{z}(t) \qquad\qquad \text{eq (5.31)}$$

Substituting the above equations in the external virtual work's formula:

$$\delta W_E = -\delta z[\ddot{z}\int_0^L m(x)[\varphi(x)]^2dx + \ddot{u}_g(t)\int_0^L m(x)\,\varphi(x)dx \qquad\qquad \text{eq (5.32)}$$

and also,

$$\delta W_I = \delta z[z\int_0^L EI(x)[\varphi''(x)]^2dx] \qquad\qquad \text{eq (5.33)}$$

Through the equilibrium for internal and external virtual work:

$$\delta z\left[\tilde{m}\ddot{z} + \tilde{k}z + \tilde{L}\ddot{u}_g(t)\right] = 0 \qquad \text{eq (5.34)}$$

Where $\tilde{m}$ is the generalised mass, $\tilde{k}$ is the generalised stiffness, and $\tilde{L}$ is the generalised force. They are defined as:

$$\tilde{m} = \int_0^l m(x)[\varphi(x)]^2 dx \qquad \text{eq (5.35)}$$

$$\tilde{k} = \int_0^l EI(x)[\varphi''(x)]^2 dx \qquad \text{eq (5.36)}$$

$$\tilde{L} = \int_0^l m(x)\varphi(x)dx \qquad \text{eq (5.37)}$$

Equation (11) should be valid for every virtual displacement, therefore:

$$\tilde{m}\ddot{z} + \tilde{k}z + \tilde{L}\ddot{u}_g(t) = 0, \quad \tilde{m}\ddot{z} + \tilde{k}z = -\tilde{L}\ddot{u}_g(t) \qquad \text{eq (5.38)}$$

This is the formula for the behaviour of the beam-column deflecting according to the shape function. By dividing $\tilde{m}$, it gives:

$$\ddot{z} + w_n^2 z = -\widetilde{\Gamma}\,\ddot{u}_g(t) \qquad \text{eq (5.39)}$$

This equation is the same as the governing equation of the single degree of system, except for the following factor:

$$\widetilde{\Gamma} = \frac{\tilde{L}}{\tilde{m}} \qquad \text{eq (5.40)}$$

Where $\varphi(x)$: shape function

$\tilde{m}$: Generalised mass

$\tilde{k}$: Generalised stiffness

$\widetilde{p}\,(t)$: Generalised force

U(t): the function describing the displacement corresponding to the free end of the beam.

5.4 Amplitude-frequency relation of explosion wave load

In an explosion, a great amount of energy is released in several forms like high temperature, fire, shock wave and gaseous materials. All of them are harmful for structures, but the explosion shock wave accompanying high pressure and large impulse is regarded as the most dangerous in an explosion. The explosion pressure, commonly called overpressure, is expressed relative to ambient pressure rather than an absolute value. In an offshore facility, structural failure may lead to environmental destruction, like the aftermath of the Deepwater Horizon accident. Therefore, a firm understanding of explosion wave load is required. This section analyses explosion load in a structural dynamic aspect rather than ERA aspect. Fig. 33 shows the distribution of amplitude and frequency for several load cases. The explosion wave clearly has a much higher amplitude than the other cases. Although wind load is also included in high amplitude in some cases, its frequency range is very small. Generally, higher amplitude has a more severe effect on structural damage or deformation. However, frequency is also an important factor in damage and deformation. Resonance is a good example related to frequency. Resonance is a phenomenon caused by an external force which can drive another structural system to oscillate with bigger amplitude at specific frequencies. This phenomenon normally occurs when the natural frequency of a structure is in accord with the external force duration. Under this condition, large amplitude oscillations can be generated despite small periodic force. As described in Fig. 34, explosion wave load has a large frequency range from low to very high frequency. Therefore, structural response analysis based on the extensive scope of the amplitude-frequency relation is required.
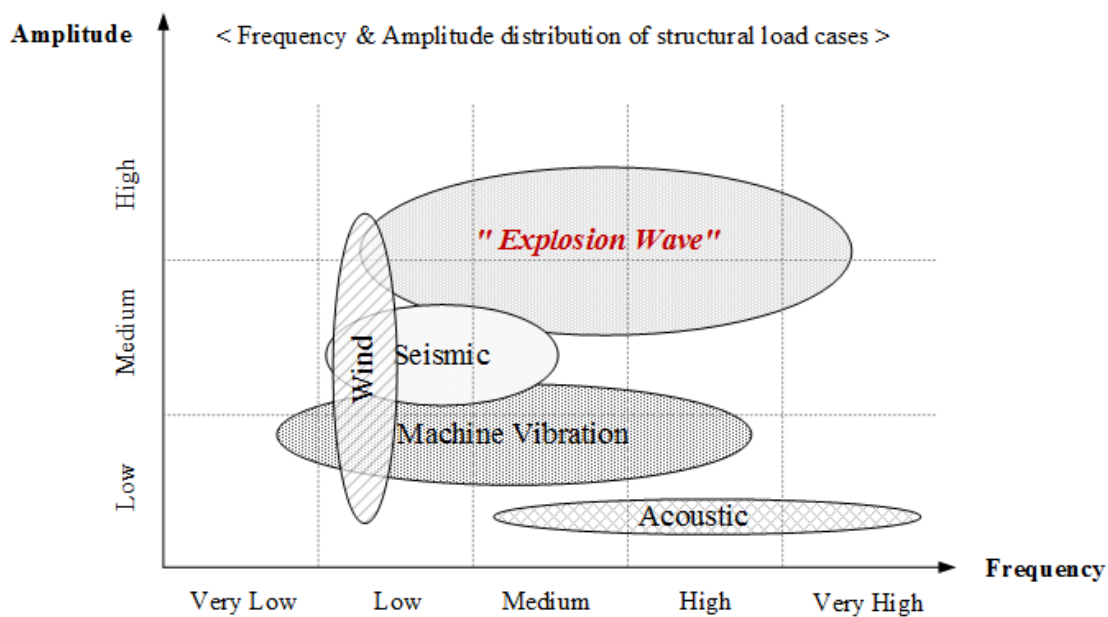

Fig. 34 Comparison for amplitude-frequency relations of structural load cases

5.5 Contribution of amplitude based on pulse shape to dynamic load factor

As mentioned above, the dominant factors of explosion loading are amplitude (overpressure) and its frequency (duration time). First, the influence of pressure on dynamic response was investigated. The pulse shape and the level of peak pressure should be considered together to discuss this issue. The influence of pulse shape on dynamic properties is shown in Fig. 35. It indicates the relation between maximum Dynamic Amplification factor (DAF) and pulse shape for different loading amplitudes. DAF is defined as the displacement at any time t divided by the static displacement (μ_{st}) which occurs by a force of magnitude F_0 [157]. As shown in Fig. 34, two different types of triangular pressure-time curve have been used. Each triangular pulse has the same duration and peak load, but the time to reach peak pressure is different. The bigger number next to the curve means a higher amplitude acted on the target. For the result in Fig. 35(a), the higher amplitude generates the larger dynamic effect and the bigger values of t_d/t_n have a greater dynamic load factor. However, the other pulse, the symmetric triangular pulse in Fig. 35(b), shows a different pattern. Except for the highest amplitude case ($F_0/R_m=1.5$), all of the cases fluctuated over the values of t_d/t_n, and the range of fluctuation was larger in higher amplitudes.

The boxed area is noteworthy in these results. This area means the smaller values of t_d/t_n, that is, pulse duration is shorter than the natural period of the target. In this area, both cases clearly showed a similar pattern. But the other area, which has a longer duration than the natural period, showed a very different pattern. This is because the maximum deformation is influenced by the rapidity of the loading only if the pulse loading duration is longer than the structure's natural period. Therefore, no matter how strong the peak pressure is, if its length is very short compared to the natural period, structural dynamic movement is never influenced by the loading shape.

Fig. 36 gives an additional description of this result by showing the response spectra for three different load shapes: rectangular, half-cycle sine and triangular shapes,. Fig. 36(a) is the result for different shapes but the same amplitude, and Fig. 36(b) is the result for different amplitudes but the same area (impulse). Under the same amplitude, the rectangular-shaped load generated the largest deformation, since this loading case increased suddenly from zero to peak load (P_0), that is, it has the most rapid rising time to peak load compared to the other shapes. The triangular-shaped load, however, is initially the slowest, so that it produces the smallest deformation. The response of the half-cycle sine load was in between the rectangular and triangular-shaped loads. In Fig. 36(b), each load case has the same area in pressure-time history. Therefore, the rectangular-shaped load's amplitude is $P_0/2$, the amplitude of triangular load is P_0, and the half-cycle sine load is $(0.25\pi)P_0$. As described in the figure, in the range of short length load ($t_d < t_n/4$), the maximum deformation is never influenced by the loading shape, but it is definitely dependent on the pressure-time curve's area.
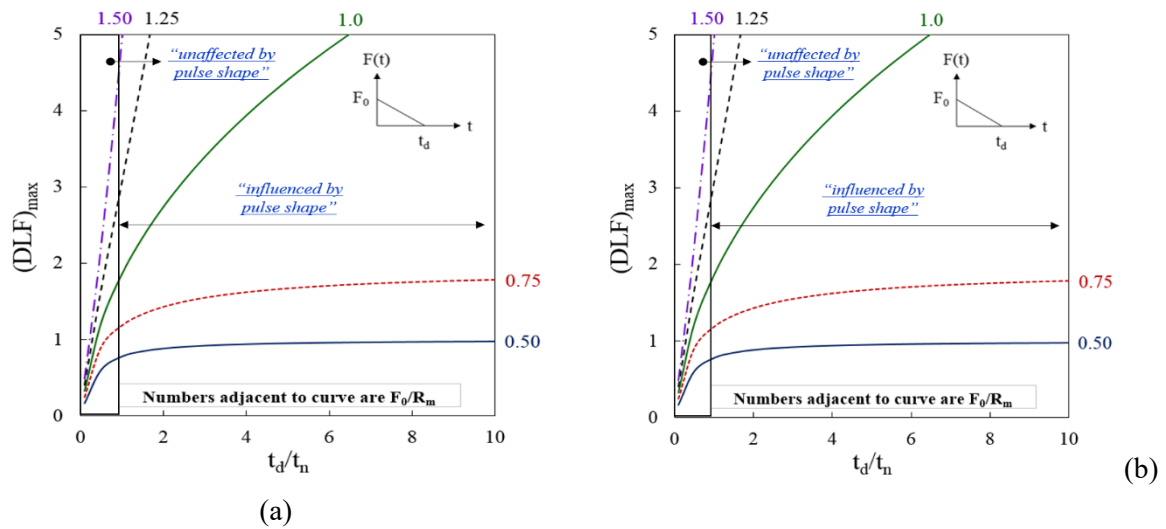
Fig. 35 Maximum dynamic load factor for the undamped SDOF model acted on by a triangular pulse (a) extremely increased types (b) normal increased types
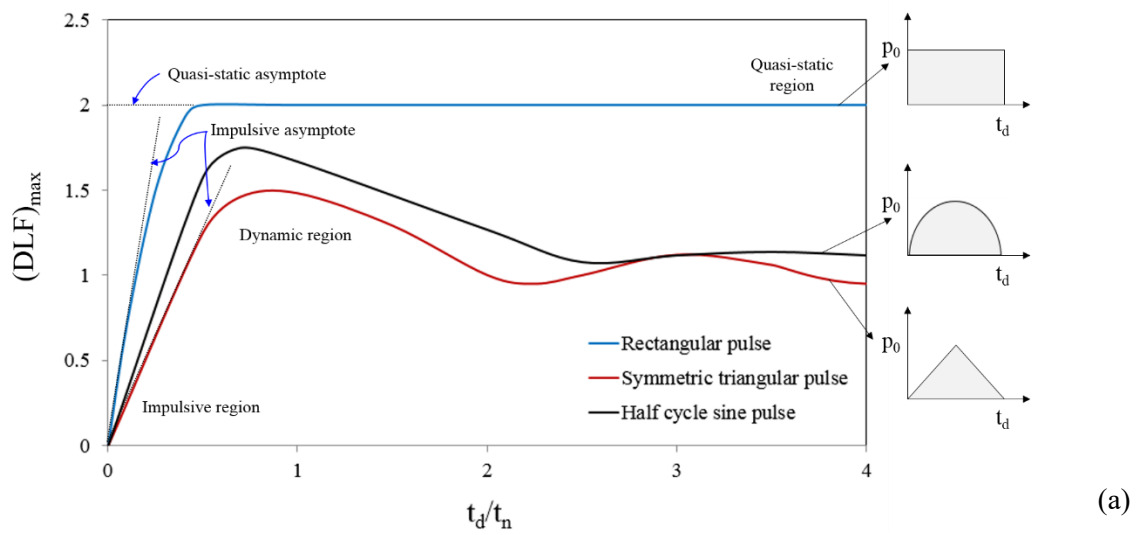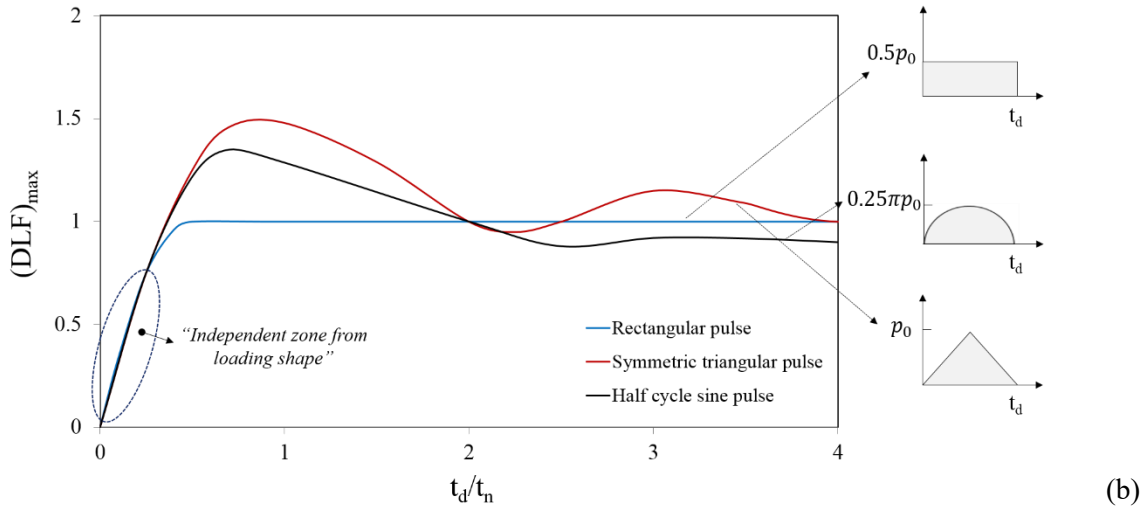
Fig. 36 Maximum response for three different kinds of loads:

(a) same amplitude (b) same area

5.6 Contribution of higher frequency to dynamic response properties

To investigate the influence of higher frequency load on structural response, the following analysis was carried out. By comparing loads with the Eigen frequency of the SDOF model, relatively higher frequency and lower frequency loads were considered.

The Eigen frequency is calculated by:

$$f_1 = \frac{1}{2\pi w_1} \quad ; \quad w_1 = \sqrt{\frac{k_1}{m_1}} \qquad \text{eq (5.41)}$$

Where w_1 is the angular natural frequency, and the corresponding period is then calculated:

$$T_1 = \frac{1}{f_1} \qquad \text{eq (5.42)}$$

While the frequency of acted load was constant, the Eigen frequency of the SDOF model was controlled by changing mass. As a result, different values for the ratio between Eigen periods and loading duration time were derived as described in Table 14. By using this coefficient, each frequency mode can be classified and the influence of different frequencies on structural dynamic response can be understood. However, such modes are very different if the properties of rebound phase are taken into account. Table 15 shows the classification of loading cases acted upon the SDOF model including the rebound phase. Although eigenvalues and loading duration are different from earlier cases, the value of t_d/t_n is the same. Therefore, it

72

is possible to investigate the influence of the rebound phase together with the effect of different frequency modes in the target model.

Fig. 37 shows the results based only on the initial pressure phase. It indicates the dynamic response which can be expressed as total response divided by static displacement as a function of normalised time t/t_d for each case. It is clear that each case shows a different type of dynamic response. The case where the Eigen-period is the same as the loading duration ($t_d/t_n=1$) showed the highest amplitude of dynamic property, and the farther away from this case, the lower the amplitude. The effect of higher frequency mode means that structural behaviour has enough time to react against the pulse, so that its highest value is observed within the pulse duration. On the other hand, for the lower frequency effect, its behaviour does not have enough time to reach peak amplitude. Therefore, in the range right after the arrival of pressure, the higher frequency mode's influence on the structural behaviour is more significant compared to its counterpart. The contribution of the rebound pressure phase is also closely related to a high frequency mode.

As described in Fig. 38, in the lower frequency modes which have a shorter period (t_n) than the pressure duration (t_d), it also does not reach the highest amplitude in the short time ($t<t_d$). In addition, the peak values within the duration time were smaller compared to the same conditions focused only on the initial pressure phase. This means that the rebound phase overlaps with the prior pressure stage, so that its response looks as though the initial pressure phase is weakened. However, as for the other cases (with shorter than loading duration), the response was also generated in the opposite direction from the initial pressure stage because the displacement in the higher frequency mode has enough time to react in both the initial and rebound pressure phases.

Table 14 Classification of loading frequency based on Eigen values of SDOF model (initial phase only)

Case No.	Eigen frequency (1/s)	Eigen period (s)	Duration time (s)	td/tn
1	3.2	0.312	0.078	0.25
2	6.4	0.156	0.078	0.50
3	12.8	0.078	0.078	1.0
4	19.2	0.052	0.078	1.5
5	25.6	0.039	0.078	2.0
6	32.3	0.031	0.078	2.50
7	38.5	0.026	0.078	3.0

Table 15 Classification of loading frequency based on Eigen values of SDOF model (inclusion of rebound phase)

Case No.	Eigen frequency (1/s)	Eigen period (s)	Duration time(s)	td/tn
1	1.67	0.599	0.15	0.25
2	3.3	0.303	0.15	0.50
3	6.7	0.150	0.15	1.0
4	10	0.1	0.15	1.5
5	13.4	0.075	0.15	2.0
6	16.7	0.060	0.15	2.50
7	20	0.050	0.15	3.0
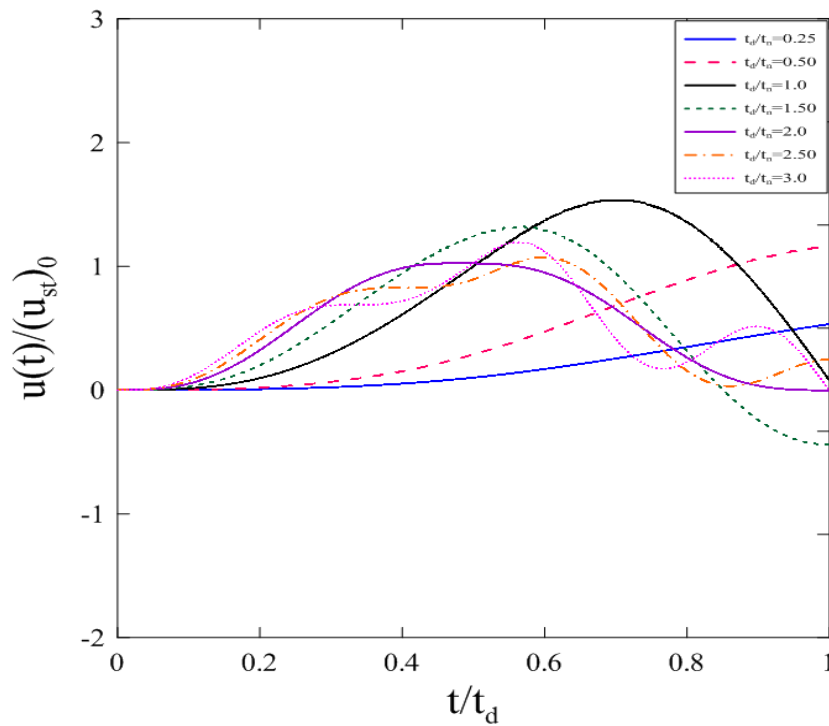
Fig. 37 Dynamic load factor (DLF) in function of normalized time (t/t_d) for the different loading frequency (Only positive phase)
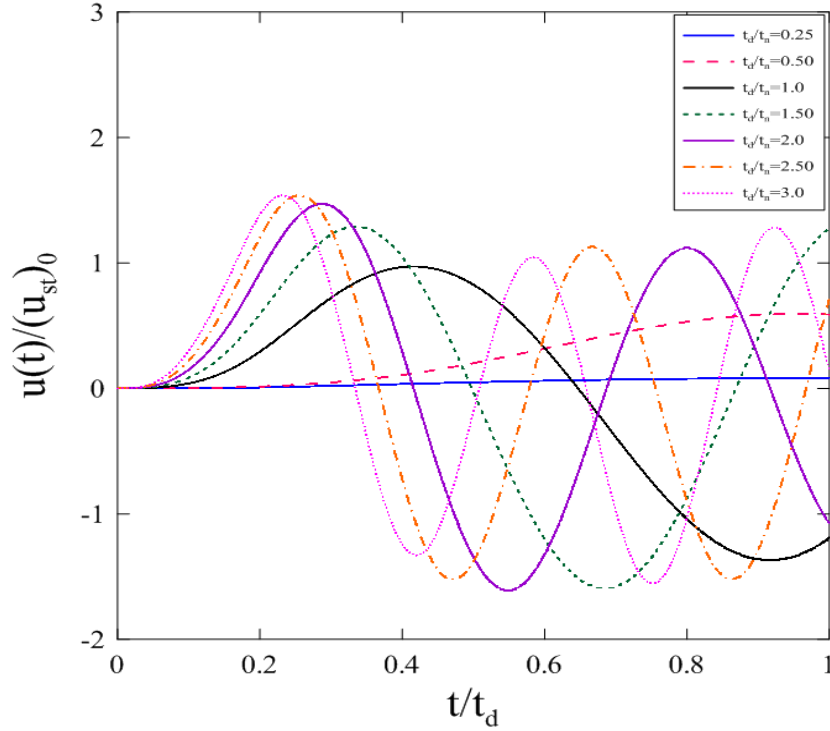
Fig. 38 Dynamic load factor (DLF) in function of normalized time (t/t$_d$) for the different loading frequency (Including negative phase)

5.7 Pressure-Impulse diagram

This section presents a pressure-impulse diagram of the analytical model subjected to explosion loading. It is one of the tools for assessing the structural elements, which indicates the combinations of pressure and impulse that generate the same level of damage to a target structure under the specific loading profile. Therefore, the specified damage level can be recognised based on the combination of pressure and impulse. Fig. 38 compares two different pressure-impulse diagrams according to explosion loading condition. The left and below region in this diagram mean the damage would not be induced, but those regions on the right and above the curve indicate damage in excess of the allowable limit would be produced [158]. The actual level of damage depends on the characteristics of both loading profiles and structural type, and the pressure-impulse diagram established here is based on the SDOF model and a triangular-shaped explosion pressure-time history. For an undamped linear SDOF model under a symmetric triangular load with duration td, the functions of displacement are as follows:

$$u(t) = \frac{2P_0}{K}\left(\frac{t}{t_d} - \frac{t_n}{2\pi t_d}sin2\pi\frac{t}{t_n}\right) \qquad 0 \le t \le \frac{t_d}{2} \qquad \text{eq (5.43)}$$

$$u(t) = \frac{2P_0}{K}\left\{1 - \frac{t}{t_d} + \frac{t_n}{2\pi t_d}\left[2sin\frac{2\pi}{T_n}\left(t - \frac{1}{2}t_d\right) - sin2\pi\frac{t}{t_n}\right]\right\} \qquad \frac{t_d}{2} \le t \le t_d \qquad \text{eq (5.44)}$$

$$u(t) = \frac{2P_0}{K} \left\{ \frac{t_n}{2\pi t_d} \left[2sin\frac{2\pi}{t_n}\left(t - \frac{1}{2}t_d\right) - sin\frac{2\pi}{t_n}(t - t_d) - sin2\pi\frac{t}{t_n} \right] \right\} \qquad t \geq t_d \qquad \text{eq (5.45)}$$

where K is the spring stiffness, P0 is the peak load and tn is the Eigen-period of the SDOF model.

In addition, the dimensionless force and impulse terms are defined as below:

$$\hat{P} = \frac{P_0/K}{x_{max}} \qquad \text{eq (5.46)}$$

$$\hat{I} = \frac{I}{\sqrt{KM}\ x_{max}} \qquad \text{eq (5.47)}$$

The horizontal asymptote of the pressure-impulse diagram means the resistance of the target model for quasi-static loads, and vertical asymptote indicates the resistance against the impulse of applied loads. Both asymptotes of the pressure-impulse curve can be obtained based on the principle of energy conservation. In the case of the impulsive asymptote, it can be assumed that due to inertia effects the initial total energy imparted to the system is in the form of kinetic energy only [159]. For the quasi-static loading regime, the load can be assumed to be constant before the maximum deformation is achieved. The derivation of it is as follows:

$$E_{k(t=0)} = \frac{I^2}{2M} \qquad \text{eq (5.48)}$$

$$E_s = \frac{1}{2}Ku_{max}^2 \qquad \text{eq (5.49)}$$

$$E_w = P_0 u_{max} \qquad \text{eq (5.50)}$$

Quasi-static asymptote

$$E_w = E_s, \qquad P_0 u_{max} = \frac{1}{2}Ku_{max}^2 \qquad \therefore \ \frac{P_0}{Ku_{max}} = \frac{1}{2}$$

Impulsive asymptote

$$E_k = E_s, \qquad \frac{I^2}{2M} = \frac{1}{2}Ku_{max}^2 \qquad \therefore \ \frac{I}{\sqrt{KM}x_{max}} = 1$$

Fig. 39 is the pressure-impulse diagram based on the mentioned points. It shows both asymptotes are equal to derivation. The diagram considering load time history with the rebound pressure phase is also shown. Based on the dynamic domain, each curve's position changed. In the domain from impulsive to dynamic, the pressure-impulse curve with only the initial phase has the wider area above the curve, but around the quasi-static area, the opposite effect occurred. It has the same meaning as the response analysis results where the

displacement amplitude is decreased by the inclusion of the rebound phase under the short duration time condition.
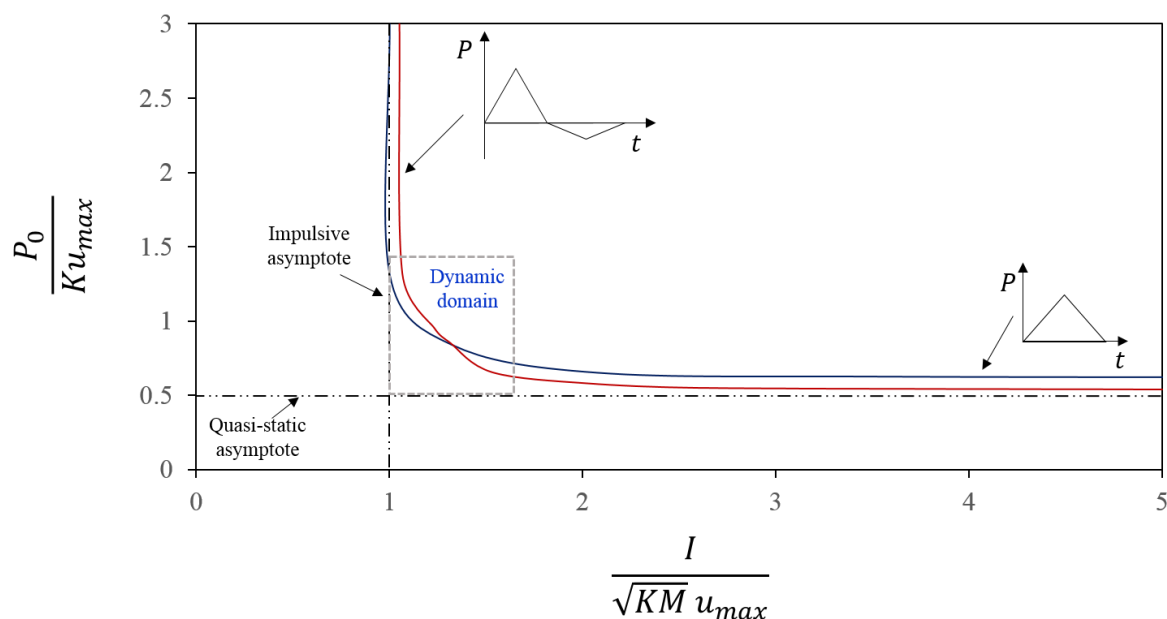
Fig. 39 Pressure-impulse diagram for two types of triangular pressure-time history

5.8 Finite element analysis

5.8.1 Validation of FE model

To further investigate the impulsive response of the beam model, a finite element analysis (FEA) was carried out using the ANSYS Workbench program. FEA normally has three stages: pre-processor, solution and post-processor. In the pre-processor stage, input data should be defined in order to produce the factor that is used for computational analysis in the next phase, such as target model, geometrical shape, material properties, mesh information, loading and boundary conditions. The input data are used to determine the properties of each element and node by computing nodal force and displacement as well as generating element matrices based on the predefined input data set. Both stages are very important. There are many research articles focusing on these stages. For example, User-defined Material (UMAT) is a key issue because it can define the material mechanical behaviour using various material constitutive models even if it is not included in the commercial code of a finite element analysis program [160, 161].

However, the main objective of the present study is not to develop the FEA technique, so commercial code in ANSYS software was used. Fig. 40 shows the main factors covered in the pre-processor stage. I-beam was modelled based on the standard specification for structural steel in ASTM A6/A6M-03 [162]. The dimensions of each part are described in Table 16. Material properties are standards for a steel structure and are summarised in Table 17. For plasticity properties, a bilinear isotropic hardening model was used, and tangent

modulus was calculated based on the recommendation for accidental load cases. In the DNV-RP-C204 document [10], the critical strain and hardening parameters for several steel grades are proposed, and the relationship between the hardening parameter (H) and tangent modulus (Et) is as follows:

$$\text{H} = \frac{E_t}{E} \ , \qquad E_t = H \cdot E \qquad\qquad \text{eq (5.51)}$$

The value of the tangent modulus was obtained by using the above equation. For the loading condition, the triangular-shaped load expressed as time-varying pressure acted upon the external flange of the beam, and the displacement of the mid-span area was measured along with each loading condition. To sum up, the I-beam model composed of structural steel with shell type elements was used to analyse the specific structural response considering explosion wave amplitude, frequencies, and the transition for the pressure phase.

In the post-processor stage, the results data were processed and then shown in graphical form to check or compare each output data.

Table 16. Dimension of I-beam's cross-section
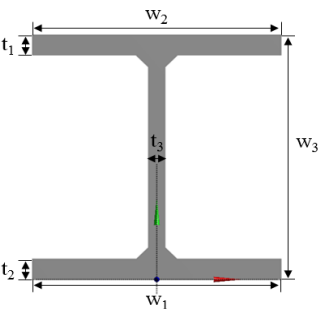
Cross-section (I-section)	Dimension (mm)					
	w1	w2	w3	t1	t2	t3
	103	103	106	8.8	8.8	7.1

Table 17. Material properties of FE-model

Property	Symbol	Value	Unit
Density	ρ	7850	kg/m3
Young's Modulus	E	210000	MPa
Poisson's Ratio	γ	0.3	-
Yield Strength	σ_y	355	MPa
Tangent Modulus	E_t	714	MPa
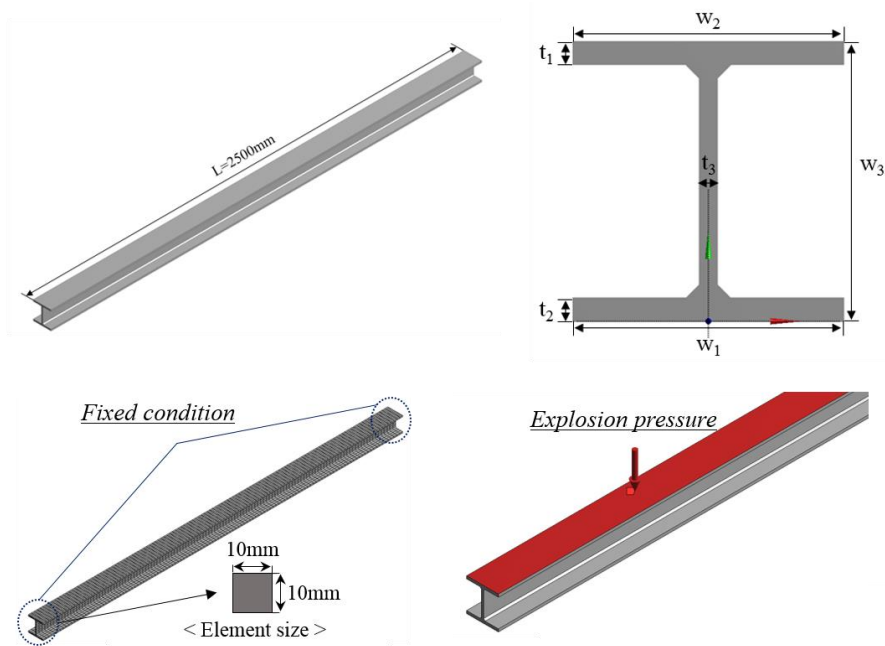
Fig. 40 The detailed configuration for finite element I-beam model

5.8.2 Linear analysis results: contribution of peak pressure and duration time

For the purpose of a number of analyses on the dynamic structural response by explosion pressure, a variety of load amplitudes and frequencies were considered. First, in terms of linear behaviour, the finite element beam model's motions were thoroughly analysed. The typical characteristic of an explosion load is a high amplitude and very short duration time. However, high and short do not mean the absolute value. High amplitude means overpressure relative to the ambient value, and short duration time indicates relative shortness compared to the natural period of the target model. Therefore, in the present study, the loading duration was classified into five cases comparing its length to the beam's Eigen-period as described in Table 18. The response was measured by dividing it into two areas: forced oscillation and free oscillation zone. Therefore, the beam was allowed to freely vibrate for a while even after the end of loading. The peak amplitude level used was in a reasonable range occurring during a gas explosion on an offshore platform [163]. To assess the influence of duration time on structural response, different lengths of duration were used with constant peak pressure (refer to Fig. 41).

The results for these loading conditions are shown in Fig. 42. In the deflection-time curve, all responses showed the dynamic amplification, but its magnitude varied by loading duration times. Except for very short loading case, the maximum deflection values in all cases were much higher than the static solution by the inertial effects and dynamic amplification. To get an overview of the relationship between dynamic amplification and duration time, the Dynamic Amplification Factor (DAF) according to each duration time was plotted in Fig. 43(a). The peak value was measured when the loading duration was equal to the target

model's Eigen-period, and based on this loading condition, if the duration was longer or shorter than it, the DAF decreased. Therefore critical duration time to structural failure varied according to the target's period, and cannot be defined by quantitative aspects. The influence of peak overpressure on structural response, however, shows a perfectly linear relationship. As shown in Fig. 43(b), in all loading conditions, the DAF value increased with the higher overpressure.

Table. 18 The five cases for relative length of explosion pressure

Classification	Relative length (t_d/t_n)	Loading duration (t_d)
Very short	0.1	0.0014s
Slightly short	0.5	0.007s
Eigenperiod	1	0.014s
Long	5	0.07s
Extremely long	10	0.14s
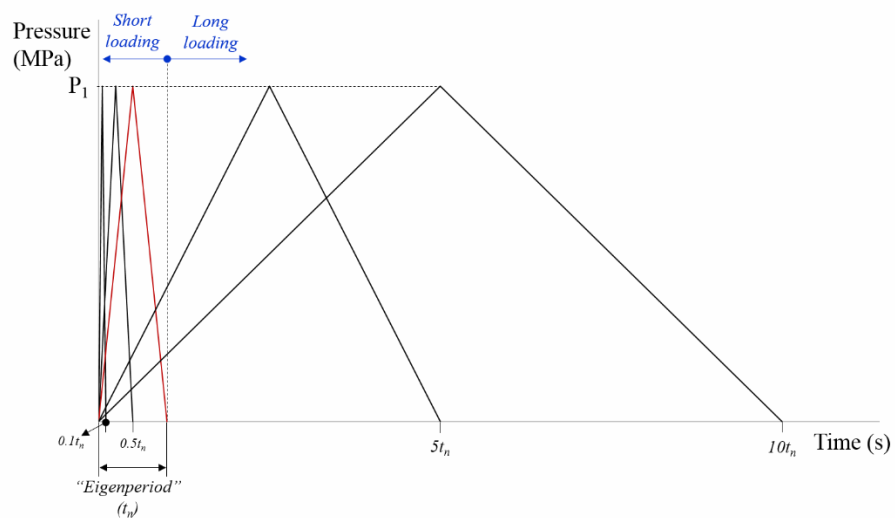
Fig. 41 Applied loading conditions of different duration time with constant peak pressure
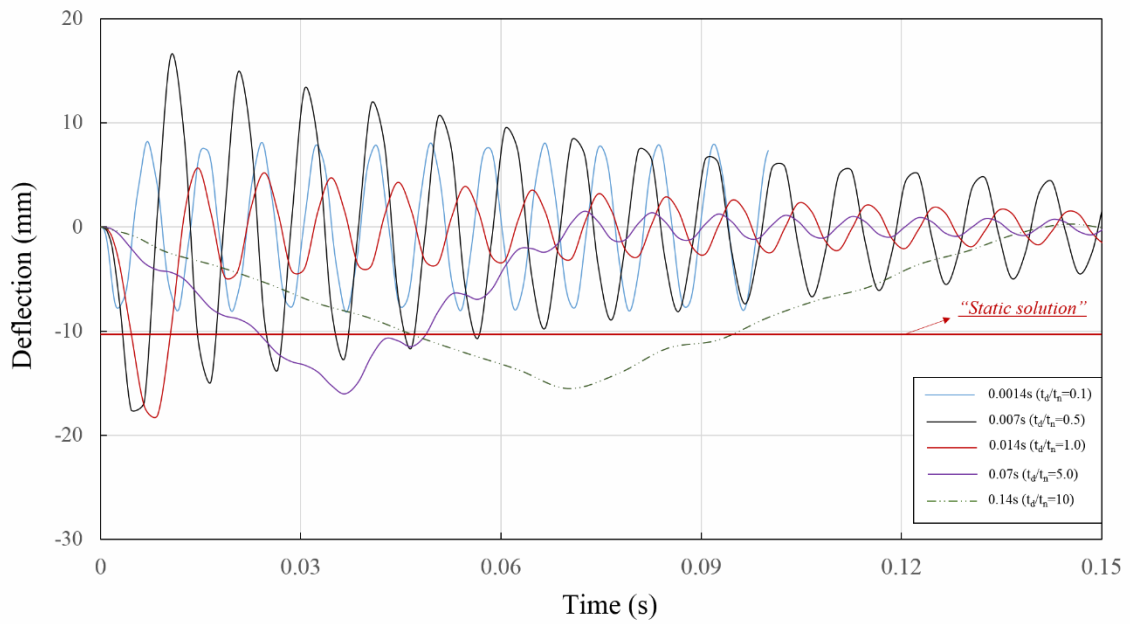
Fig. 42 Results for deflection-time curve
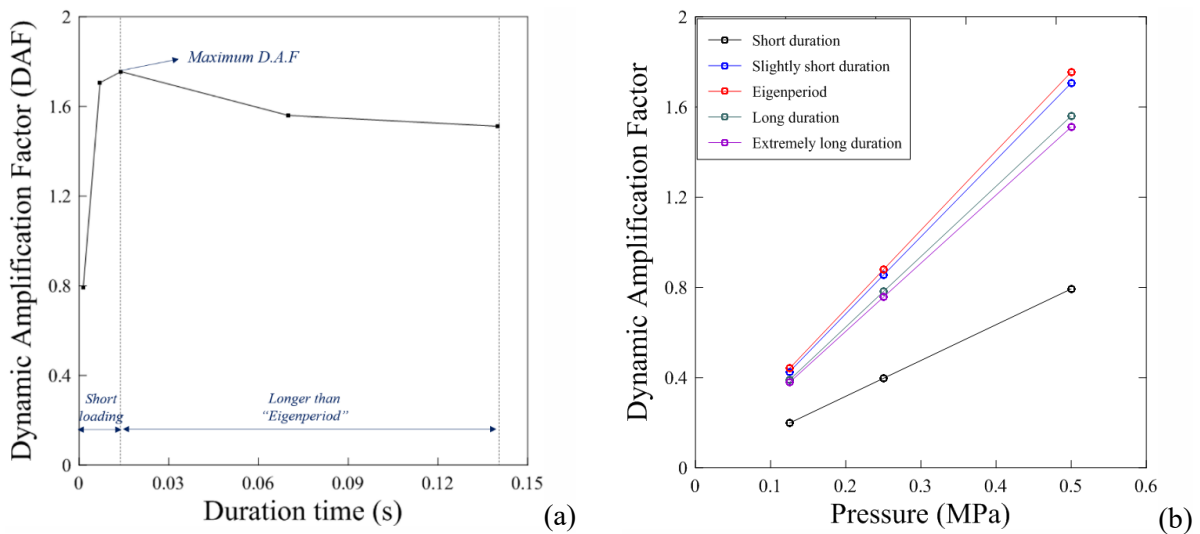
Fig. 43 The variation of dynamic amplification factor according to explosion load properties (a) by duration time, (b) by peak pressure

5.8.3 Linear analysis results: Contribution of the rebound pressure phase

Another issue which needs to be carefully considered in explosion load properties is the influence of the rebound phase on structural behaviour. In the offshore industry and many related studies, the rebound phase is often overlooked in a widely used triangular form of loading condition even though its impulse and frequency considerably influence structural response [164, 165]. The present study investigates the influence of these pressure phase properties on the structural response. By comparing the results for different total

duration time relative to the target's Eigen-period, the physical influence on the structure has been assessed in total length of loading as well as phase transition aspects. Two types of triangular-shaped loads were used. For the assumption method for these load profiles, first total duration was selected considering the target model's period and it was divided into two main categories of shorter than the natural period and longer than the natural period. The reason for this separation is due to the time-dependent response, which means the response would be different based on whether loading duration is shorter or longer than the target's natural period. One was shorter than the Eigen-period, and the other was longer than it. For the relation between each phase duration, reportedly, the rebound phase duration is known to be longer than the initial phase duration [166, 167]. Thus a 1.5 times longer rebound phase duration was selected compared to the initial phase. As a result, a triangular-shaped load was composed of initial and rebound phases. The initial peak pressure is 0.5 MPa and duration time is 0.1s, followed by the rebound phase with less peak amplitude and longer duration compared to the earlier one as indicated in Fig. 44. Each peak pressure was equal, but total duration was different because this is the usual assumption associated with explosion load profiles in the industry or relevant research area [168, 169].

Fig. 45 shows the deflection response for each loading condition. In Fig. 45(a), the loading duration was a quarter of the Eigen-period, so its free oscillation range was between 0.0035s and 0.1s. In addition, Fig. 45(b) indicates the response by the loading of duration 1.25 times longer than the natural period, and free oscillations which occurred between 0.0175s and 0.5s. According to the results, it is clear that a very different deflection pattern was measured. The quick convergence to initial condition after hitting peak point was measured in Fig. 45(b).

For more detailed analysis, the variation of deflection amplitude was investigated. Each amplitude point was measured until arrival at the tenth peak value. A1, A3, A5, A7 and A9 mean peak deflection point in the initial loading direction, and the other values (A2, A4, A6, A8 and A10) indicate the rebound peak deflection points. Under the short loading condition, there is some fluctuation in each amplitude point over the time, but no unexpected results. However, the other case showed noteworthy behaviour, and it is described in Fig. 46. It indicates the normalised deflection value in each amplitude point. A1 and A2 are the maximum values in each zone, and these values gradually decreased over the time.

It is also important to investigate separately the response characteristics based on oscillation stage of forced and free oscillation stages. The stages from A1 to A3 and from A2 to A4 are within the loading duration, that is forced oscillation stage, and all the other sections are included in the free oscillation stage. As described in Fig. 45, the largest decrease occurred in the forced vibration stage, and if the value (P2/P1) was bigger, the decrease was also larger. In other words, rebound pressure has a direct impact on the total response by decreasing the rebound displacement. The bigger the rebound phase's ratio compared to the initial phase, the less rebound displacement occurred. Detailed values for each point are summarised in Table 19.

Pressure (MPa)

* Total Impulse = $I_p + I_n$
* $P_{min.} = 0.25 P_{max.}$
* $D_{neg.} = 1.5 D_{pos.}$

$P_{max.}$

I_p

$D_{neg.}$

$P_{min.}$ $D_{pos.}$ I_n Time (s)
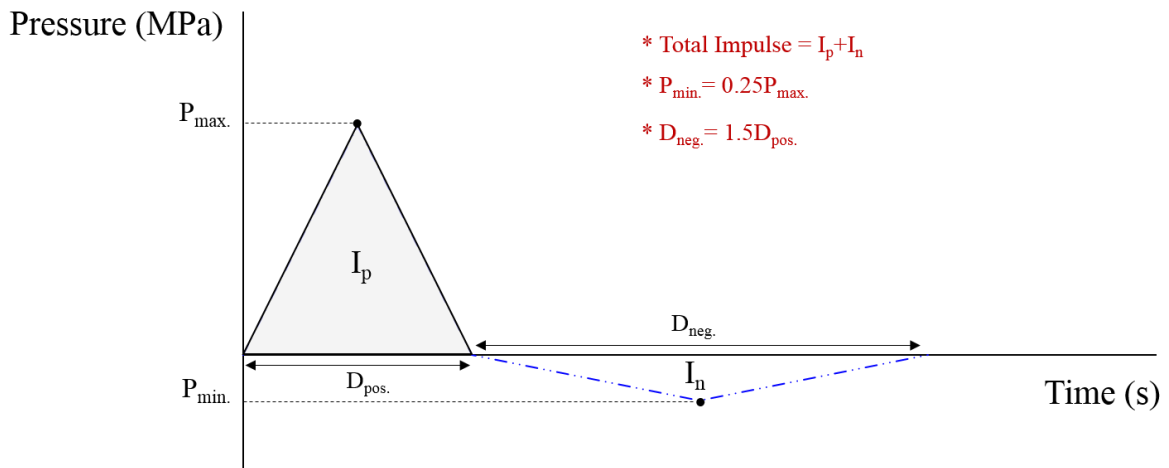
Fig. 44 The loading condition including negative phase (different impulse)

<Initial deflection zone>   <Counter deflection zone>
* $A_1 \rightarrow A_3$: +1.4%   * $A_2 \rightarrow A_4$: -
* $A_3 \rightarrow A_5$: +6.7%   * $A_4 \rightarrow A_6$: -3.9%
* $A_5 \rightarrow A_7$: +2.6%   * $A_6 \rightarrow A_8$: +5.8%
* $A_7 \rightarrow A_9$: +0.3%   * $A_8 \rightarrow A_{10}$: -5.4%
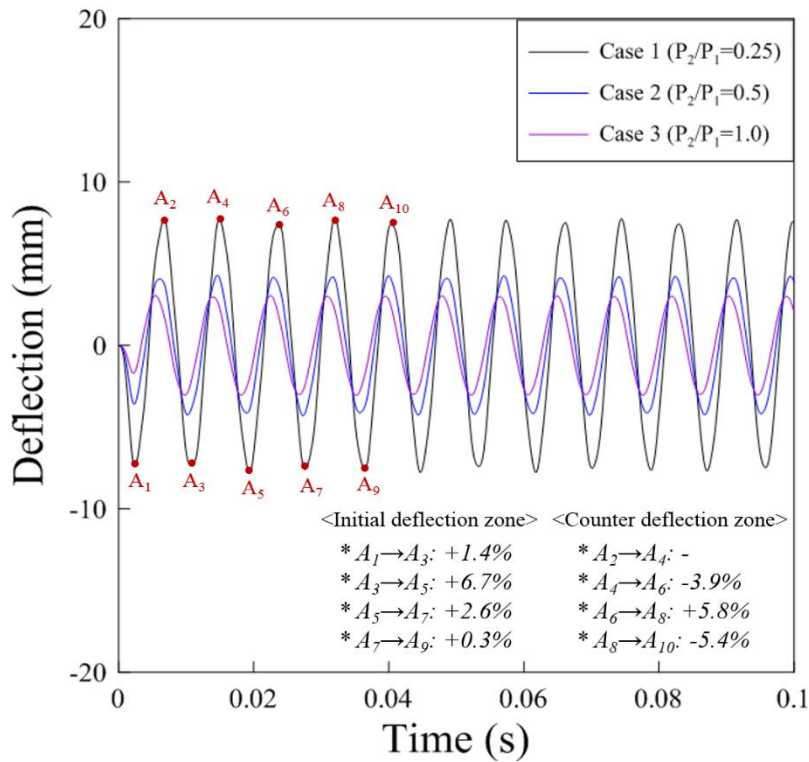
(a)
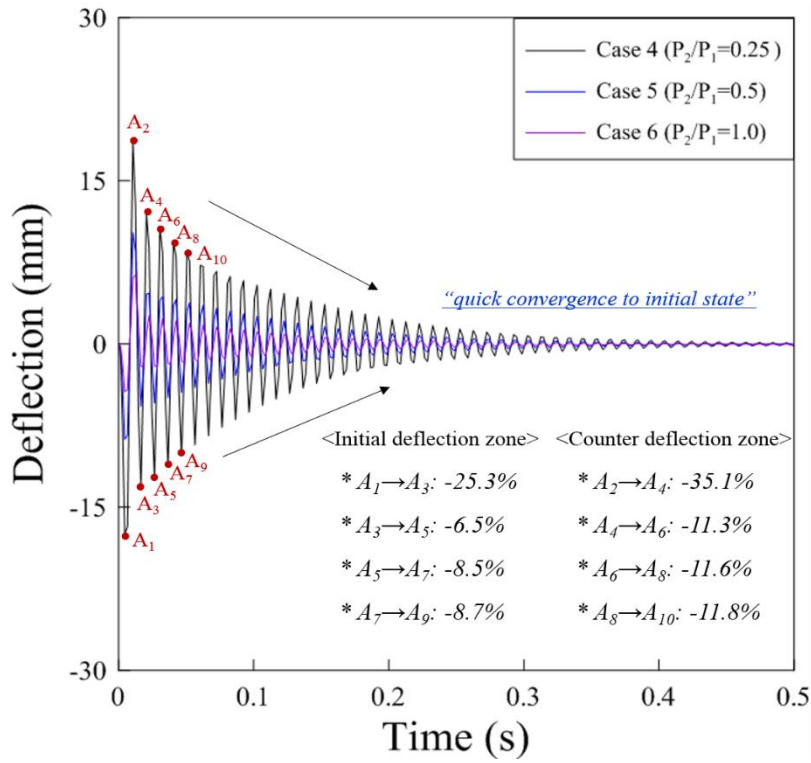
(b)

Fig. 45 Deflection of FE beam model according to different ratio of rebound pressure to positive pressure: (a) shorter than Eigen-period (t_d/t_n=0.25), (b) longer than Eigen-period (t_d/t_n=1.25)

(a)

(b)
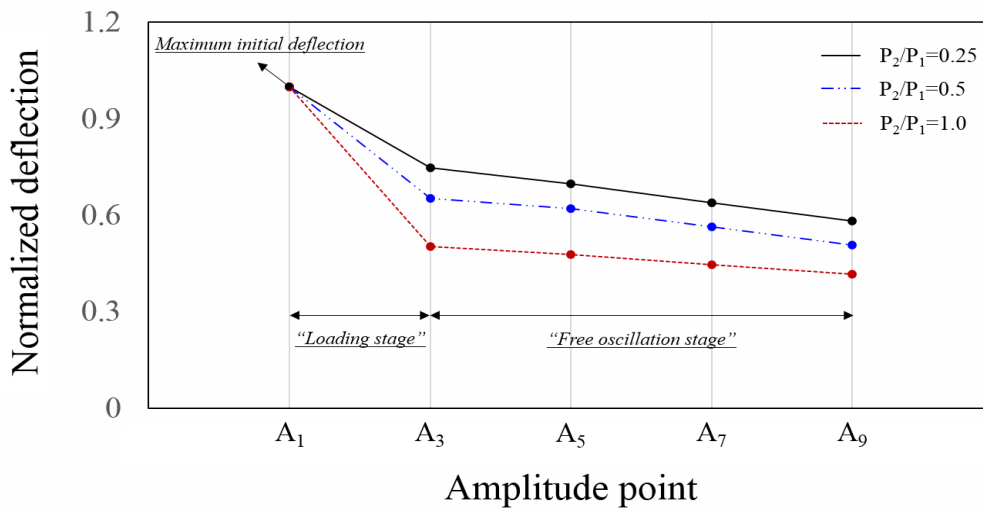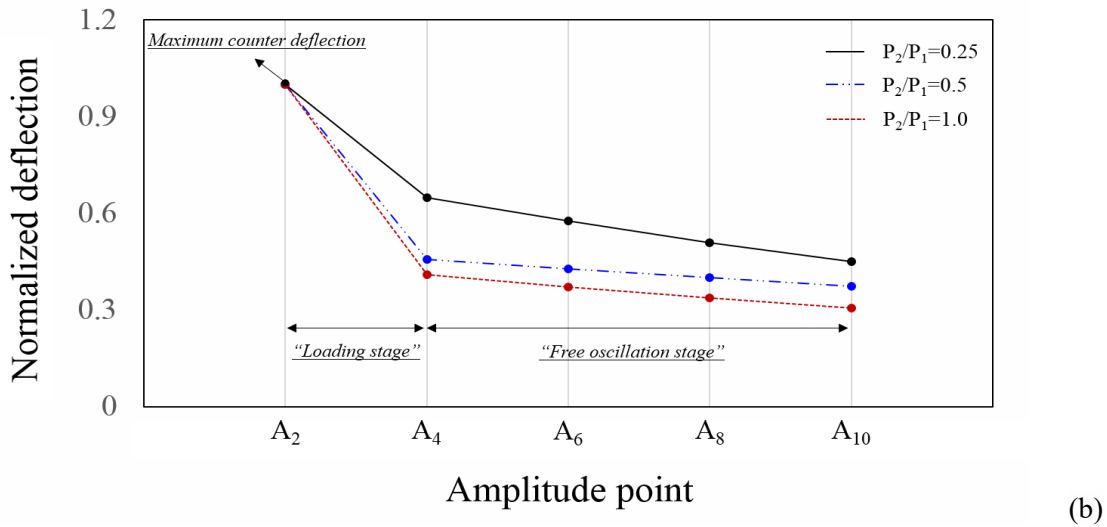
Fig. 46 Normalized deflection of FE beam model according to different ratio of rebound pressure to initial pressure: (a) initial defection zone, (b) rebound deflection zone

Table 19 Summary of peak deflection points

	Initial deflection zone				Rebound deflection zone			
	Variation of deflection (%)				Variation of deflection (%)			
	$A_1{\rightarrow}A_3$	$A_3{\rightarrow}A_5$	$A_5{\rightarrow}A_7$	$A_7{\rightarrow}A_9$	$A_2{\rightarrow}A_4$	$A_4{\rightarrow}A_6$	$A_6{\rightarrow}A_8$	$A_8{\rightarrow}A_{10}$
Case 1	-1.4	+6.7	-2.6	+0.3	-	-3.9	+5.8	-5.4
Case 2	+18.6	-3.0	+4.2	-4.7	+7.6	-3.5	+0.05	+1.9
Case 3	+78.5	-0.4	-1.3	+2.2	-4.5	+3.6	-1.7	+0.6
Case 4	-25.3	-6.5	-8.5	-8.7	-35.1	-11.3	-11.6	-11.8
Case 5	-34.7	-5.1	-9.1	-9.7	-54.3	-6.5	-6.3	-6.8
Case 6	-49.7	-5.1	-6.3	-6.7	-59.1	-9.1	-9.2	-9.2

5.8.4 Nonlinear analysis results

Nonlinear finite element analyses were carried out to examine more specifically the overall structural response of a steel beam model in possible explosion loading conditions. The bilinear isotropic hardening model was used to model the plasticity in the analysis. This section investigates the nonlinear properties such as permanent displacement and plastic strain by core elements in explosion wave loading profiles. For the applied loading condition, first, it was set up as described in Fig. 47. In this analysis, the same impulse but different types of loading were used. While the duration time was a constant value, each peak pressure was

controlled with the same assumption. In all cases, the duration time of the rebound pressure phase was two times longer than the initial phase, but the rebound peak pressure was a fifth of the initial peak pressure.

Based on this assumption, a series of finite element analyses were performed. Fig. 48 shows the result for deflection of the mid-span over the time according to the existence of rebound pressure and the comparison results for the permanent deflections. These figures show that the plastic responses start to oscillate around a permanent deformation in each condition, and the oscillation amplitude was lower along with the higher peak pressure. This means the higher initial peak pressure produces an initial deformation similar to the permanent value. Therefore, it can be said that permanent deformation is more dependent on the level of peak pressure than the duration time length.

Fig. 49 shows the plastic strain contour results according to each loading condition. Under the equal rebound phase, initial peak pressure was divided into two cases of 1.5 times and 3 times higher peak pressure. For the purpose of comparison, only initial phase load cases were also controlled in the same manner. As described in the figure, the most severe plastic deformation occurred at the fixed support-section of the beam, and the higher plastic strain value was measured in the higher initial peak pressure. But, the extent of plastic deformation decreased if the rebound phase was considered. As a result, the explosion loading case involving the rebound pressure phase reduced the permanent displacement and plastic strain value. This is because the rebound phase acted like a superposition effect, rather than applying individually followed by the initial phase, since the total duration of explosion load is extremely short unlike the other impact cases such as seismic or wind loads. Therefore, it can be concluded that the influence of rebound pressure is to somewhat reduce the damage of the initial peak pressure.
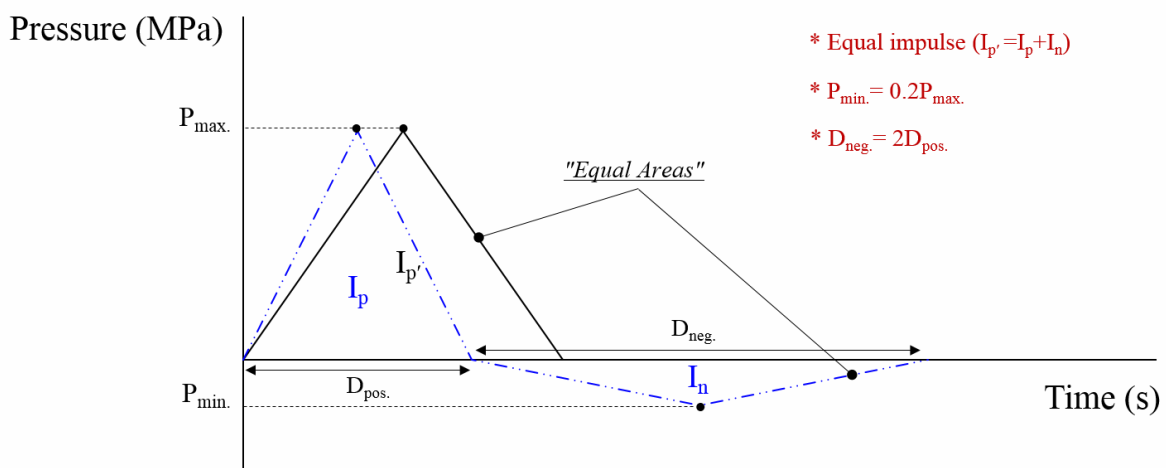

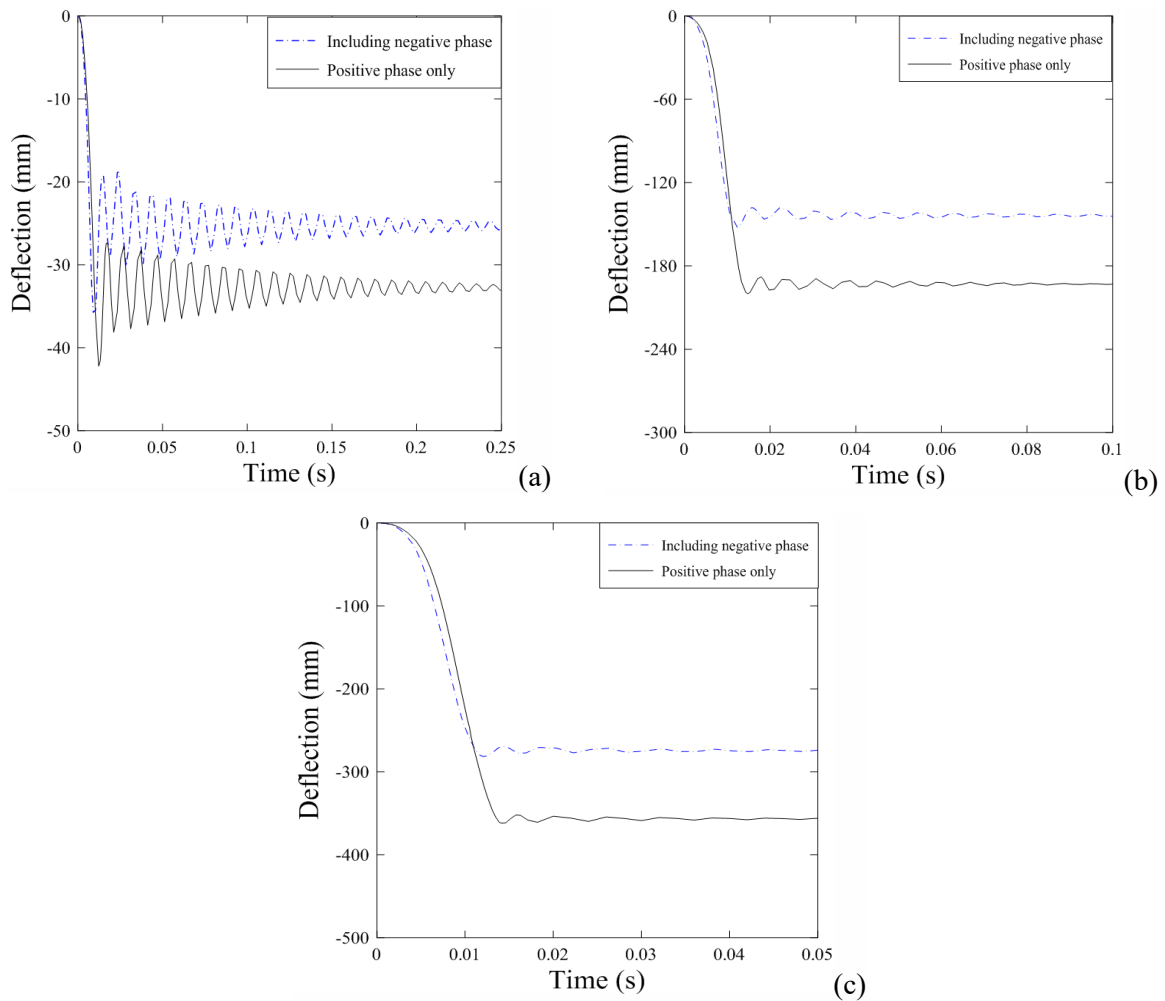Fig. 47 The loading condition with equal impulse

86

Fig. 48 Comparison of permanent deflection under two types of loads
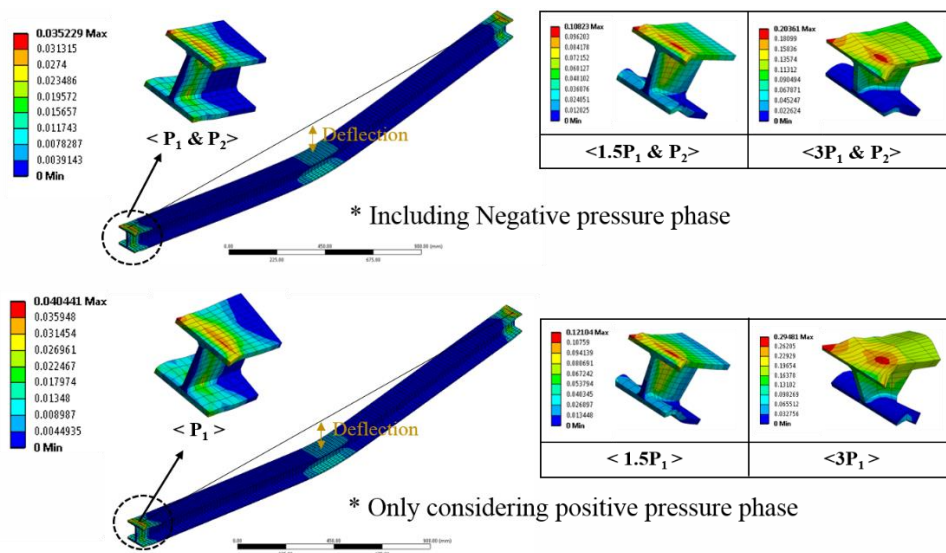

Fig. 49 Comparison of plastic strain contour under two types of loads

5.9 Application

Advanced computational methods provide a many opportunity for the realistic assessment of the structural response subjected to accidental load case that could be induced by unintended events during the operation, installation or decommission tasks. The main purpose of assessment for the accidental loadings is to understand the extent of potential initial damage and to prevent the similar accident in the future. Among these load cases, explosion wave load was key interest in this study. The explosion event begins with accidental release of flammable materials into the environment followed by an ignition source, and then the great amount of energy is given off, so that the structure is ended up in dangerous situation. There are several detrimental factors to structural stability, and explosion wave pressure is normally regarded as the most dominant factor to structural mechanical damage. This study is extensively dealing with gas explosion phenomenon from its numerical implementation to structural response analysis, and research techniques and approaches for explosion analysis using in this study could be practically applied in several sectors as summarized below.

5.9.1 FLACS output monitoring tool

The developed VBA code in this study can be used to classify and investigate the numerical information of explosion wave profiles. The pressure time history files are produced as an output data of FLACS software, and it could be an enormous amount of data according to the user defined variables. The explosion scenarios are usually established considering ignition information, geometry and operation conditions, so that many types of explosion event could be realized in simulation. The VBA code in this study can numerically analyze the simulation results regardless of input properties. Once explosion pressure-time data is acquired through the FLACS, each file can be edited as VBA code input files, and then it brings the numerical information of each file and compares these properties based on scenarios and data types. In addition, real wave shape can be transformed as linear triangular model based on equivalent impulse, so that it also can be used as explosion design load input data in structural analysis. Lastly, the peak pressure and duration time of each data and the graphical characteristic can be monitored using this code. Therefore, it can effectively manage and calculate the design numerical value in relevant future analysis.

5.9.2 Explosion risk criteria

In typical Explosion Risk Assessment (ERA), the risk criteria has been usually established based solely on an overpressure. However, not only overpressure level but also its duration time can influence on the structural dynamic response, so total impulse properties should be used to determine the guideline of tolerance level for explosion potential risk. The explosion impulse could be characterized by a time-varying overpressure and its duration, and the interaction of that impulse and structures is the main cause for partial or global structural failure. The explosion wave is time-dependent load, so its influence on physical behaviour of structures is totally different from static load cases. Therefore, the structures exposed to explosion risk should be designed

to withstand a few possible explosion accidental cases. As described in this study, it was revealed that the widely adopted triangular explosion design load brought more damage about 1.2 times more on the structure compared to the proposed design load considering both initial and rebound pressure phases even though the amount of impulse was exactly same. This is because structural response is very sensitive to the frequency domains and the amplitude of explosion load. Therefore, it is proposed to use a design explosion load representing the non-stationary characteristics of real explosion pressure waves to establish explosion risk criteria through this study.

5.9.3 Gas explosion design load

In typical explosion design, it is a usual approach to disregard the rebound pressure phase. The structural analysis results in this thesis, however, showed the significance of rebound pressure properties on structural damage and deformation. Based on the energy equivalent method, the gas explosion pressure wave profiles could be simplified as a triangular waveform composed of initial and rebound peak pressure (P_{max}, P_{min}), impulses (I_p, I_n) and their duration time (D_p, D_n). The initial pressure phase is the expansion stage, and the burning gas expands and pushes gas outward toward the vent. Excess burnt gas is removed in the combustion process, and the temperature of the remaining burnt gas decreases rapidly and shrinks. That is the reason for the generation of rebound pressure phases, which causes a flow to move in the opposite direction. In addition, the target model response can continuously oscillated between these expansions and shrinkages for some time. However, it was damped quickly, so the initial expansion and shrinkage are more important than the oscillation characteristic. That's why the oscillatory effect of real explosion wave was not considered in this study; only the linear shape of the pressure-time curve was used to analyze the structural dynamic response pattern.

5.9.4 Structural dynamic analysis

The present study proposed a realistic assessment and practical application of the structural analysis technique that enables the explosion pressure wave histories to be defined in the highly congested area bounded by several components without being overly conservative. Moreover, this study found that the rebound pressure phase and frequency domain of an explosion wave are considerably influencing structural damage and deformation even though these properties are normally ignored in a widely used explosion design load form. This study has arranged structural dynamic response pattern very detailed considering the relationship between structure's natural frequency and duration time including total impulse. Therefore, these results can be the guideline for the structural analyses subjected to such an impact load. For example, it is possible to predict roughly damage levels of target structures if the natural frequency of them and expected pulse time are known, and the specific level can be identified based on the pressure-impulse diagram proposed in this thesis.

Chapter 6

Research highlights and discussion

There are many factors causing considerable overestimation in structural response during the typical procedure of probabilistic explosion risk assessment (ERA) in the oil and gas industries. Generally, the typical triangular shaped explosion design load file is using initial peak overpressure and impulse which is widely adopted in TNT explosion responses. However, this research found that gas explosion occurred in very complicated area generates considerable rebound pressure waves unlike TNT explosion. To investigate the effect of this rebound pressure phases, in this study, we performed a series of structural damage analysis considering existing calculation and proposed method, and even compared the risk analysis results. As a result, it was found that overpressure loads only considering initial pressure phase are excessively overestimated in some cases and thus structural damage criteria is also established excessively more than necessary. It is the best to be conservative in design for safety, but it should be reasonably conservative taking economy into consideration. The main findings of this thesis are summarized as follows:

6.1 Findings in gas explosion analysis

The objective of gas explosion analysis was to examine the entire process of explosion computational analysis and investigate the numerical distribution of explosion pressure properties. To conduct the extensive gas explosion pressure data analysis, an exclusive user defined program for an explosion pressure data set acquired from CFD analysis was used. Several analyses revealed which factors can lead to more dangerous situations in explosion waves, and the significance of rebound pressure was confirmed. The following results can be drawn from this chapter.

- The shape of the explosion wave pressure-time curve was dependent on several factors such as explosive source, geometric conditions, structural shapes, obstacle types and congestion level. Most instances of higher pressure were measured near a blast wall.

- Congestion level had a significant impact. Higher initial peak pressure was produced by more congested geometry conditions, so it is important to retain open terrain to prevent higher explosive impact being generated in the design stage or layout procedure.

- From the comparative analysis for initial peak pressure and rebound peak pressure, the initial peak pressure has a relatively larger variation compared to the rebound peak pressure, and in some cases, its level was similar to rebound pressure.

- The features of explosion wave properties in different groups on the blast wall were examined by analysing the CFD results at each position on the blast wall. The intensity of explosion pressure was higher at the bottom of the wall than at the top section because of reflections of pressure waves in the enclosed space.

6.2 Findings in explosion risk analysis

The main purpose of risk analysis for gas explosion events in topside platform was to establish an ERA taking into account potential risk elements with the limit state concept. A number of factors related to uncertainties in explosion risk estimation have been identified. In typical ERA, the main issue is solely the maximum explosion pressure in the initial phase. Hence, each section in the FPSO structure is usually simply determined as a high or low risk facility based on whether the induced initial peak pressure is bigger than the design load. However, the criteria could be different if rebound pressure properties are taken into account. This issue should be checked by investigating the interaction between structural response and these properties as covered in Chapter 5. In summary, chapter 4 categorised the risk assessment for gas explosion using both quantitative and qualitative approaches as well as probabilistic analysis for explosion pressure properties. The primary results are listed as follows.

- Qualitative analysis for explosion risk elements was performed with a risk screening process considering safety function and maintenance doctrine, and the risk level in the consequence severity and likelihood was categorised reflecting the safety function. The congestion level can directly influence the potential explosion risk through the explosion pressure contour analysis.

- In the quantitative risk assessment for an explosion event, the risk acceptance criteria were described based on the application of ALARP.

- The risk screening for the explosion wave data set showed that the risk elements from the explosion wave profile could be divided into peak pressure, impulse and duration. Their properties were thoroughly investigated considering possible explosion circumstances.

- The probability distribution for chosen factors from the explosion wave profile was investigated. It was found that the distribution type of positive and negative phase factors is completely different. The relationship between peak pressure and its impulse was also studied. There is no obvious linear relationship, but positive pressure and impulse are closer to a linear relationship compared to its counterpart.

- The correlation analysis between the explosion wave profile factors found a positive linear relationship among all of the parameters.

- Risk criteria based solely on the positive peak pressure can be inaccurate. For more accurate assessment of explosion risk criteria, other factors should be considered such as peak pressure in each phase with duration time.

6.3 Findings in structural response analysis

This chapter analysed the influence of explosion pressure impact load on structural response and damage. Two different types of structural models were used, and dynamic response features were compared by considering all of the properties and both pressure phases as well as reasonable frequencies related to

explosion load cases. In addition, different pulse shapes based on varied loading rate were used to analyse the influence on the dynamic properties of the structural components. These analyses revealed which factors have a greater influence on structural response. Pressure-impulse diagrams of the analytical model were also used. By indicating the specified damage level based on the combination of explosion pressure and impulse, the pressure-impulse diagrams can assess whether explosion loading damage is in the excess state of allowable limit or not. Lastly, the features of structural response in the presence or absence of the rebound pressure phase were examined based on linear and nonlinear analysis results and the effect of rebound pressure on the structure was described. The primary outcomes of this chapter are summarised.

- Based on the dynamic amplification factor, the influence of explosion loading types on dynamic properties was investigated. As a result, the extent of structural behaviour and damage was more influenced by the initial peak pressure intensity than by the rebound pressure. The higher amplitude of initial peak pressure produced the larger dynamic effect on the structure.

- Maximum displacement was dependent on the rapidity of the loading only if the explosion loading duration time was longer than the target's natural period, and it means that the structural dynamic response does not rely on the shape of loading if its duration is much shorter than the natural period of the target structure.

- The pressure-impulse diagram was drawn depending on whether the rebound pressure phase was involved or not. By comparing the two types of pressure-impulse diagrams, the specific damage level and different dynamic domains were identified.

- The structural dynamic response state was influenced more by the rebound pressure intensity, and rebound pressure played a role in decreasing displacement as well as the plastic deformation extent as it overlapped with the initial pressure phase.

- In structural design procedures for explosion pressure, rebound pressure is normally ignored for a time-effective method and conservative design. Even though it can be a safer approach, it can also lead to over-exaggerated properties in design factors.

- For duration time effect, the relativity of the structural natural period and explosion loading duration is much more important rather than the absolute value. This is because explosion loading has a large number of frequencies and the natural period range can also be wide depending on the component's material properties.

6.4 Future research directions

In spite of many time and effort for this research, there are still several issues need to be studied more. With other properties such as fire, drop object or collision, not only explosion computational simulation but also structural analysis can be more extensive in collecting relevant data set. Further study can be proposed as follows.

First, there are several uncertainties even though explosion scenarios involving many relevant parameters were considered. Although, proper methodologies for explosion risk and structural analysis have been applied to a target model, the findings and results in this study would be partially used if the selected model is newly designed. In addition, this study treated the gas release condition in offshore facility with idealized assumption. More practical conditions of actual hydrocarbon release are required. Thus further research will cover the establishment of a detailed confidence level category according to real conditions for gas release risk assessment to provide a more reliable and effective methodology.

Second, the analyses for structural response subjected to explosion loadings in this thesis were carried out using commercial code in ANSYS software, so simplified nonlinear material properties were used in finite element analysis. For more accurate verification, user defined material model which can describe plastic behavior more detailed could be developed, and this knowledge would also be extended to investigate other materials nonlinearity. Since this study only considered explosion pressure loading, other loading types such as thermal load by fire, impact by drop object, etc. could be used to analyze potential risk in offshore facilities.

Third, explosion risk analysis requires high level accuracy and practical experience. An explosion event in offshore facilities is very complicated and a lot of parameters are related to the consequence of an explosion. Although CFD method is very useful in this field, it is not fully developed. Thus experimental verification is required in such an analysis. Large scale explosion test is almost impossible due to many safety issues, but the development of lab scale tests or experimental apparatus are needed for reasonable application of the results and more practical explosion risk analysis.

Reference

[1] Y. Zhu, X. M. Qian, Z.Y. Liu, P. Huang and M.Q. Yuan, Analysis and assessment of the Qingdao crude oil vapour explosion accident: Lessons learnt. Journal of Loss Prevention in the Process Industries, 2015. 33:p. 289-303.

[2] HSE. Accident statistics for floating offshore units on the UK continental shelf (1980–2003). HMSO RR 353. London: Health and Safety Executive; 2005.

[3] FABIG Technical Note 8 Protection of piping systems subject to fires and explosions. The steel construction Institute.

[4] NORSOK Z-013, 2010. Risk and Emergency Preparedness Assessment. Norsok standard, Available from: Standard Norge, Postboks 242,N-1326 Lysaker, Norway.

[5] ISO 19901-3, 2010. In: Petroleum and Natural Gas Industries e Specific Requirements of Offshore Structures Part 3: Topside Structure, International Organization for Standardization.

[6] J.T. Berg, J. R. Bakke, F. Fearnley, 2000. A CFD layout sensitivity study to identify optimum safe design of a FPSO. In: Offshore Technology Conference OTC- 12159-MS.

[7] C. Chan, I. O. Moen, and J. H. S Lee, Influence of confinement on flame acceleration due to repeated obstacles. Combust. Flame, 1983. 49 (1):p. 27-39.

[8] Scandpower, 2007. Ignition Modeling in Risk Analysis. Report 89.390.008/R1.

[9] Gilsanz, R, Hamburger, R., Barker, D., Smith, J. L. and Rahimian, A. 2015. Design of Blast Resistant Structures, American Institute of Steel Construction.

[10] DNV-RP-C204, 2010. Design against accidental loads, Det Norske Veritas (DNV).

[11] M. Yang and S. Ahmari, Investigation of effect of negative phase of blast loading on cable net curtain walls through the linearized stiffness matrix method, Int. J. Impact Eng. 61 (2013) 36–47.

[12] T. Krauthammer and A. Altenberg, Negative phase blast effects on glass panels, Int. J. Impact Eng. 24 (2000) 1–17.

[13] M. Teich and N. Gebbeken, The influence of the underpressure phase on the dynamic response of structures subjected to blast loads, Int. J. Protective Struct. 1 (2010) 219–233.

[14] Cullen, W., 1990. The Public Inquiry into the Piper Alpha Disaster. Stationery Office Books, London, England.

[15] J. M. Sohn, S. J. Kim, B. H. Kim and J. K. Paik, Nonlinear structural consequence analysis of FPSO topside blast walls. Ocean Engineering, 2013. 60:p. 149-162.

[16] Pate-Cornell, M. E. (1993). Risk analysis and risk management for offshore platforms: lessons from the Piper Alpha accident. Journal of Offshore Mechanics and Arctic Engineering, 115(3), 179-190.

[17] Drysdale, D. D., & Sylvester-Evans, R. (1998). The explosion and fire on the Piper Alpha platform, 6 July 1988. A case study. Philosophical Transactions of the Royal Society of London. Series A: Mathematical, Physical and Engineering Sciences, 356(1748), 2929-2951.

[18] Flin, R. (2001). Decision making in crises: The Piper Alpha disaster. Managing crises: Threats, dilemmas, opportunities, 103-118.

[19] Paté-Cornell, M. E. (1993). Learning from the piper alpha accident: A postmortem analysis of technical and organizational factors. Risk Analysis, 13(2), 215-232.

[20] Alexander, D. A. (1993). The Piper Alpha oil rig disaster. In International handbook of traumatic stress syndromes (pp. 461-470). Springer, Boston, MA.

[21] White, H. K., Hsing, P. Y., Cho, W., Shank, T. M., Cordes, E. E., Quattrini, A. M., ... & Brooks, J. M. (2012). Impact of the Deepwater Horizon oil spill on a deep-water coral community in the Gulf of Mexico. Proceedings of the National Academy of Sciences, 109(50), 20303-20308.

[22] Kujawinski, E. B., Kido Soule, M. C., Valentine, D. L., Boysen, A. K., Longnecker, K., & Redmond, M. C. (2011). Fate of dispersants associated with the Deepwater Horizon oil spill. Environmental science & technology, 45(4), 1298-1306.

[23] Camilli, R., Reddy, C. M., Yoerger, D. R., Van Mooy, B. A., Jakuba, M. V., Kinsey, J. C., ... & Maloney, J. V. (2010). Tracking hydrocarbon plume transport and biodegradation at Deepwater Horizon. Science, 330(6001), 201-204.

[24] Skogdalen, J. E., & Vinnem, J. E. (2012). Quantitative risk analysis of oil and gas drilling, using Deepwater Horizon as case study. Reliability Engineering & System Safety, 100, 58-66.

[25] Eckle, P., Burgherr, P., & Michaux, E. (2012). Risk of large oil spills: a statistical analysis in the aftermath of Deepwater Horizon. Environmental science & technology, 46(23), 13002-13008.

[26] Reader, T. W., & O'Connor, P. (2014). The Deepwater Horizon explosion: non-technical skills, safety culture, and system complexity. Journal of Risk Research, 17(3), 405-424.

[27] Dan, S., Lee, C. J., Park, J., Shin, D., & Yoon, E. S. (2014). Quantitative risk analysis of fire and explosion on the top-side LNG-liquefaction process of LNG-FPSO. Process Safety and Environmental Protection, 92(5), 430-441.

[28] Brighton, P. W. M., Fearnley, P. J., & Brearley, I. G. (1995). HSE assessment of explosion risk analysis in offshore safety cases.

[29] Hansen, O. R., Kjellander, M. T., Martini, R., & Pappas, J. A. (2016). Estimation of explosion loading on small and medium sized equipment from CFD simulations. Journal of Loss Prevention in the Process Industries, 41, 382-398.

[30] Jin, Y., & Jang, B. S. (2018). Probabilistic explosion risk analysis for offshore topside process area. Part II: Development of gas cloud multivariate frequency distribution (MVFD). Journal of Loss Prevention in the Process Industries, 51, 159-168.

[31] Sohn, J. M., Kim, S. J., Kim, B. H., & Paik, J. K. (2013). Nonlinear structural consequence analysis of FPSO topside blastwalls. Ocean engineering, 60, 149-162.

[32] Syed, Z. I., Mohamed, O. A., & Rahman, S. A. (2016). Non-linear finite element analysis of offshore

stainless steel blast wall under high impulsive pressure loads. Procedia Engineering, 145, 1275-1282.

[33] Ming, F. R., Zhang, A. M., Xue, Y. Z., & Wang, S. P. (2016). Damage characteristics of ship structures subjected to shockwaves of underwater contact explosions. Ocean Engineering, 117, 359-382.

[34] Moriyama, K., & Park, H. S. (2015). Probability distribution of ex-vessel steam explosion loads considering influences of water level and trigger timing. Nuclear Engineering and Design, 293, 292-303.

[35] Li, J., & Hao, H. (2018). Far-field pressure prediction of a vented gas explosion from storage tanks by using new CFD simulation guidance. Process Safety and Environmental Protection, 119, 360-378.

[36] Rigby, S. E., Tyas, A., & Bennett, T. (2014). Elastic–plastic response of plates subjected to cleared blast loads. International Journal of Impact Engineering, 66, 37-47.

[37] Parlin, N. J., Davids, W. G., Nagy, E., & Cummins, T. (2014). Dynamic response of lightweight wood-based flexible wall panels to blast and impulse loading. Construction and Building Materials, 50, 237-245.

[38] Geng, J., Mander, T., & Baker, Q. (2015). Blast wave clearing behavior for positive and negative phases. Journal of Loss Prevention in the Process Industries, 37, 143-151.

[39] Wang, G., & Zhang, S. (2014). Damage prediction of concrete gravity dams subjected to underwater explosion shock loading. Engineering failure analysis, 39, 72-91.

[40] Larcher, M. (2008). Pressure-time functions for the description of air blast waves. JRC technical note, 46829.

[41] Bjerketvedt, D., Bakke, J.R., Wingerden, K.V., 1997. Gas explosion handbook. J. Hazard. Mater. 52, 1–150. British Standards Institution.,2005a,

[42] Koshiba, Y., Hasegawa, T., & Ohtani, H. (2018). Numerical and experimental study of the explosion pressures and flammability limits of lower alkenes in nitrous oxide atmosphere. *Process Safety and Environmental Protection*, *118*, 59-67.

[43] Li, J., & Hao, H. (2018). Far-field pressure prediction of a vented gas explosion from storage tanks by using new CFD simulation guidance. *Process Safety and Environmental Protection*, *119*, 360-378.

[44] Mitu, M., & Brandes, E. (2017). Influence of pressure, temperature and vessel volume on explosion characteristics of ethanol/air mixtures in closed spherical vessels. *Fuel*, *203*, 460-468.

[45] Askar, E., Schröder, V., Schmid, T., & Schwarze, M. (2018). Explosion characteristics of mildly flammable refrigerants ignited with high-energy ignition sources in closed systems. *International Journal of Refrigeration*, *90*, 249-256.

[46] Cao, Y., Guo, J., Hu, K., Xie, L., & Li, B. (2017). Effect of ignition location on external explosion in hydrogen–air explosion venting. *International Journal of Hydrogen Energy*, *42*(15), 10547-10554.

[47] Mittal, M. (2017). Explosion pressure measurement of methane-air mixtures in different sizes of confinement. *Journal of Loss Prevention in the Process Industries*, *46*, 200-208.

[48] Edelia, E. M., Winkler, R., Sengupta, D., El-Halwagi, M. M., & Mannan, M. S. (2018). A computational fluid dynamics evaluation of unconfined hydrogen explosions in high pressure applications. *International*

Journal of Hydrogen Energy, *43*(33), 16411-16420.

[49] Li, H., Guo, J., Yang, F., Wang, C., Zhang, J., & Lu, S. (2018). Explosion venting of hydrogen-air mixtures from a duct to a vented vessel. *International Journal of Hydrogen Energy*, *43*(24), 11307-11313.

[50] Zhang, Q., Wang, Y., & Lian, Z. (2017). Explosion hazards of LPG-air mixtures in vented enclosure with obstacles. *Journal of hazardous materials*, *334*, 59-67.

[51] Zhang, K., Wang, Z., Ni, L., Cui, Y., Zhen, Y., & Cui, Y. (2017). Effect of one obstacle on methane–air explosion in linked vessels. *Process Safety and Environmental Protection*, *105*, 217-223.

[52] Na'Inna, A. M., Phylaktou, H. N., & Andrews, G. E. (2017). Explosion flame acceleration over obstacles: effects of separation distance for a range of scales. *Process Safety and Environmental Protection*, *107*, 309-316.

[53] Guo, Y., He, L., Wang, D., & Liu, S. (2016). Numerical investigation of surface conduit parallel gas pipeline explosive based on the TNT equivalent weight method. Journal of Loss Prevention in the Process Industries, 44, 360-368.

[54] Alonso, F. D., Ferradas, E. G., Minarro, M. D., Aznar, A. M., Gimeno, J. R., & Pérez, J. F. S. (2008). Consequence analysis by means of characteristic curves to determine the damage to buildings from the detonation of explosive substances as a function of TNT equivalence. Journal of Loss Prevention in the Process Industries, 21(1), 74-81.

[55] Short, M., & Jackson, S. I. (2015). Dynamics of high sound-speed metal confiners driven by non-ideal high-explosive detonation. Combustion and Flame, 162(5), 1857-1867.

[56] Ning, H., Yude, L., Hongpeng, Z., & Chunpeng, L. (2012). Research on the TNT equivalence of aluminized explosive. Procedia Engineering, 43, 449-452.

[57] Edri, I. E., Grisaro, H. Y., & Yankelevsky, D. Z. (2019). TNT equivalency in an internal explosion event. Journal of hazardous materials, 374, 248-257.

[58] W. C. Brasie and D. W. Simpson, 1968. Guidelines for estimating damage from explosion, Chemical Engineering Progress Loss Prevention, 2: 91.

[59] R. J. Harris, M. J. Wickens, Understanding vapour cloud explosion – An experimental study, 55th Autumn meeting of the institution of gas engineers (1989).

[60] Berg, A. C. van den, 1985. The multi-energy method- A framework for vapour cloud explosion blast prediction. Journal Hazardous Materials, 12:1-10.

[61] W. P. M. Mercx, A. C. van den Berg, C. J. Hayhurst, N. J. Robertson and K. C. Moran, Developments in vapour cloud explosion blast modelling, Journal of Hazardous Materials, 2000, 71:301-319.

[62] K. G. Kinsella, A rapid assessment methodology for the prediction of vapour cloud explosion overpressure, International Conference of Safety and Loss Prevention, Singapore, 1992.

[63] Qiao, A., Zang, S., 2010. Advanced CFD modelling on vapour dispersion and vapour cloud explosion. Journal of Loss Prevention in the Process Industries. 23, 843-848.

[64] Hansen, O. R., Gavelli, F., Ichard, M. and Davis, S. G. 2010. Validation of FLACS against experimental data sets from the model evaluation database for LNG vapor dispersion. Journal of Loss Prevention in the Process Industries, 23(6), 857-877.

[65] Middha, P., Hansen, O.R., Grune, J. and Kotchourko, A. 2010. CFD calculations of gas leak dispersion and subsequent gas explosions: Validation against ignited impinging hydrogen jet experiments. Journal of Hazardous Materials. 179, 84–94.

[66] Hjertager, B. H. and Solberg, T. 1999. A review of computational fluid dynamics modelling of gas explosion. In Prevention of Hazardous Fires and Explosions, 77-91.

[67] Wang, D., Qian, X., Yuan, M., Ji, T., Xu, W. and Liu, S. 2017. Numerical simulation analysis of explosion process and destructive effect by gas explosion accident in buildings. Journal of Loss Prevention in the Process Industries, 49, 215-227.

[68] Li, J., Ma, G., and Abdel-jawad, M. 2016. Gas dispersion risk analysis of safety gap effect on the innovation FLNG vessel with a cylindrical platform. Journal of Loss Prevention in the Process Industries, 40, 304-316.

[69] Hansen, O. R., Kjellander, M. T. and Pappas, J. A. 2016. Explosion loading on equipment from CFD simulations. Journal of Loss Prevention in the Process Industries, 44, 601-613.

[70] Dadashzadeh, M., Abbassi, R., Khan, F. and Hawboldt, K. 2013. Explosion modelling and analysis of BP Deepwater Horizon accident, 57, 150-160.

[71] Das, B. and Weinberg, M. 2012. Improving flammable mass estimation for vapor cloud explosion modelling in an offshore QRA. Safety Science, 50, 1218-1227.

[72] Gieras, M., Klements, R., Rarata, G. and Wolanski, P. 2006. Determination of explosion parameters of methane-air mixtures in the chamber of 40dm3 at normal and elevated temperature. Journal of Loss Prevention in the Process Industries. 19, 263-270.

[73] Jingde, L., Hong, H., Yanchao, S., Qin, F., Zhan, L. and Li, C. 2018. Experimental and computational fluid dynamics study of separation gap effect on gas explosion mitigation for methane storage tanks. Journal of Loss Prevention in the Process Industries. 55, 359-380.

[74] Bhosale, V. A., Patil, K. I. and Dehankar, P. B. 2015. Study of accidental releases heavy gas dispersion comparing slab models and screen-3 model. International Journal of Engineering Sciences & Research Technology, 4(1), 765-769.

[75] Yang, D., Chen, G., Shi, J. and Li, X. 2019. Effect of gas composition on dispersion characteristics of blowout gas on offshore platform. International Journal of Naval Architecture and Ocean Engineering, 11, 914-922.

[76] Kashi, E., Mirzaei, F. and Mirzaei, F. 2015. Analysis of gas dispersion and ventilation within a comprehensive CAD model of an offshore platform via computational fluid dynamics. Journal of Loss Prevention in the Process Industries, 36, 125-133.

[77] Mc-Quaid, J. 1989. Chapter 11. Dispersal of Chemicals in Methods for assessing and reducing injury from chemical accidents, Edited by Philippe Bourdeau and Gareth Green, Published by John Wiley & Sons Ltd. 162-165.

[78] Li, X. Chen, G. Zhu, H. and Xu, C. 2018. Gas dispersion and deflagration above sea from subsea release and its impact on offshore platform. Ocean Engineering, 163, 157-168.

[79] Ahmed, I., Bengherbia, T., Zhvansky, R., Ferrara, G., Wen, J. X., & Stocks, N. G. (2016). Validation of geometry modelling approaches for offshore gas dispersion simulations. Journal of Loss Prevention in the Process Industries, 44, 594-600.

[80] Li, Y., Chen, D., Cheng, S., Xu, T., Huang, Q., Guo, X., ... & Liu, X. (2015). An improved model for heavy gas dispersion using time-varying wind data: Mathematical basis, physical assumptions, and case studies. Journal of Loss Prevention in the Process Industries, 36, 20-29.

[81] Dadashzadeh, M., Ahmad, A., & Khan, F. (2016). Dispersion modelling and analysis of hydrogen fuel gas released in an enclosed area: A CFD-based approach. Fuel, 184, 192-201.

[82] Harby, K., Chiva, S., & Muñoz-Cobo, J. L. (2017). Modelling and experimental investigation of horizontal buoyant gas jets injected into stagnant uniform ambient liquid. International Journal of Multiphase Flow, 93, 33-47.

[83] Prasad, K., Pitts, W. M., Fernandez, M., & Yang, J. C. (2012). Natural and forced ventilation of buoyant gas released in a full-scale garage: Comparison of model predictions and experimental data. International journal of hydrogen energy, 37(22), 17436-17445.

[84] Hu, L. H., Chen, L. F., & Tang, W. (2014). A global model on temperature profile of buoyant ceiling gas flow in a channel with combining mass and heat loss due to ceiling extraction and longitudinal forced air flow. International Journal of Heat and Mass Transfer, 79, 885-892.

[85] Chen, Y. L., & Hsiao, S. C. (2018). Numerical modeling of a buoyant round jet under regular waves. Ocean Engineering, 161, 154-167.

[86] Pasquill, F. 1961. The Estimation of the Dispersion of Windborne Material. Meteorological Magazin, 90, 33-49.

[87] Mack, A., & Spruijt, M. P. N. (2013). Validation of OpenFoam for heavy gas dispersion applications. *Journal of hazardous materials*, *262*, 504-516.

[88] Busini, V., & Rota, R. (2014). Influence of the shape of mitigation barriers on heavy gas dispersion. *Journal of Loss Prevention in the Process Industries*, *29*, 13-21.

[89] Bjerketbedt, D., Bakke, J. R., Wingerden, K. V. 1997. Gas explosion handbook. Journal of Hazardous Materials. 52, 1-150.

[90] Health & Safety Executive (HSE). 2005. Protection of piping systems subject to fires and explosions. Research Report 285, 35-64.

[91] Lee, D. H., Kim, S. J., Lee, M. S., & Paik, J. K. (2019). Ultimate limit state based design versus allowable working stress based design for box girder crane structures. Thin-Walled Structures, 134, 491-507.

[92] Paik, J. K. and Thayamballi, A. K. 2003. Ultimate Limit State Design of Steel-Plated Structures, John Wiley & Sons Ltd, 1-20

[93] NOPSEMA Guidance note. 2017. Hazard identification and risk assessment, N-04600-GN1613, 5-15.

[94] Vinnem, J. E. (2014). Offshore Risk Assessment, Vol 2.: Principles, Modelling and Applications of QRA Studies. Springer.

[95] Cioca, I. L., & Moraru, R. I. (2012). Explosion and/or fire risk assessment methodology: a common approach, structured for underground coalmine environments/Metoda szacowania ryzyka wybuchu i pożarów: podejście ogólne, dostosowane do środowiska kopalni podziemnej. Archives of Mining Sciences, 57(1), 53-60.

[96] Rausand, M. (2013). Risk assessment: theory, methods, and applications (Vol. 115). John Wiley & Sons.

[97] Rovins, J.E., Wilson, T.M., Hayes, J., Jensen, S. J., Dohaney, J., Mitchell, J., Johnston, D.M. and Davies, A. 2015. Risk Assessment Handbook. GNS Science Miscellaneous Series, 84, 71p.

[98] Cameron, I. T. and Raman, R. 2005. Process systems risk management. ELSEVIER Academic press, 37-154.

[99] Hazardous Industry Planning Advisory. 2011. HAZOP Guidelines, NSW Government Planning, 3-15.

[100] Hong, E. S., Lee, I. M., Shin, H. S., Nam, S. W., & Kong, J. S. (2009). Quantitative risk evaluation based on event tree analysis technique: application to the design of shield TBM. Tunnelling and Underground Space Technology, 24(3), 269-277.

[101] Ericson, C. A. (2015). Hazard analysis techniques for system safety. John Wiley & Sons.

[102] Azzi, C., Rogstadkjernet, L., van Wingerden, K., Choi, J., & Ryu, Y. (2016). Influence of scenario choices when performing CFD simulations for explosion risk analyses: Focus on dispersion. Journal of Loss Prevention in the Process Industries, 41, 87-96.

[103] Dan, S., Kim, H., Shin, D., & Yoon, E. S. (2012). Quantitative Risk Analysis of New Energy Stations by CFD-Based Explosion Simulation. In *Computer Aided Chemical Engineering* (Vol. 31, pp. 305-309). Elsevier.

[104] Arzamendi, G., & Gandıa, L. M. (2013). Hydrogen Hazards and Risks Analysis through CFD Simulations. Renewable Hydrogen Technologies: Production, Purification, Storage, Applications and Safety, 437.

[105] Ye, Q., Jia, Z. Z., Liu, W., Wu, T. R., & Lu, Y. (2018). Numerical Simulation on Destruction Process of Ventilation Door by Gas Explosion. Procedia engineering, *211*, 934-944.

[106] Hansen, O.R., Gavelli, F., Davis, S.G., Middha, P., 2013. Equivalent cloud methods used for explosion risk and consequence studies. Journal of Loss Prevention in the Process Industries. 26, 511–527.

[107] Qiao, A., & Zhang, S. (2010). Advanced CFD modeling on vapor dispersion and vapor cloud explosion. Journal of loss prevention in the process industries, 23(6), 843-848.

[108] Middha, P., Hansen, O.R. and Storvik, I.E. 2009. Validation of CFD-model for hydrogen dispersion. Journal of Loss Prevention in the Process Industries, 22, 1034–1038.

[109] Kang, K. Y., Heo, Y., Rogstadkjernet, L., Choi, K. H., & Lee, J. M. (2017). Structural response of blast wall to gas explosion on semi-confined offshore plant topside. International Journal of Structural Stability and Dynamics, 17(02), 1750021.

[110] Kang, K. Y., & Wang, X. (2018). A Stepwise Risk Assessment for Explosion Events considering Probability Distribution of Explosion Load Parameters. Complexity, 2018.

[111] Dasgotra, A., Teja, G. V., Sharma, A., & Mishra, K. B. (2018). CFD modeling of large-scale flammable cloud dispersion using FLACS. Journal of Loss Prevention in the Process Industries, 56, 531-536.

[112] Hansen, O. R., & Johnson, D. M. (2015). Improved far-field blast predictions from fast deflagrations, DDTs and detonations of vapour clouds using FLACS CFD. Journal of Loss Prevention in the Process Industries, 35, 293-306.

[113] Vyazmina, E., & Jallais, S. (2016). Validation and recommendations for FLACS CFD and engineering approaches to model hydrogen vented explosions: effects of concentration, obstruction vent area and ignition position. international journal of hydrogen energy, 41(33), 15101-15109.

[114] Chille, F., Bakke, J. R., & Wingerden, K. V. (2008). Use of CFD tools for prediction of explosion loads. Proceedings of the Handling Exceptions in Structural Engineering.

[115] European Committee for Standardization. (2002). EN ISO 19900: Petroleum and Natural Gas Industries: General Requirements for Offshore Structures. CEN.

[116] Moan, T., Amdahl, J., & Ersdal, G. (2019). Assessment of ship impact risk to offshore structures-New NORSOK N-003 guidelines. Marine Structures, 63, 480-494.

[117] Amdahl, J., Watan, R., Hu, Z., & Holmås, T. (2012, July). Broad side ship collision with jacket legs: examination of NORSOK N-004 analysis procedure. In ASME 2012 31st International Conference on Ocean, Offshore and Arctic Engineering (pp. 745-751). American Society of Mechanical Engineers.

[118] Kindracki, J., Kobiera, A., Rarata, G., & Wolanski, P. 2007. Influence of ignition position and obstacles on explosion development in methane–air mixture in closed vessels. Journal of Loss Prevention in the Process Industries, 20(4-6), 551-561.

[119] ISO. (2007). Glass in building—Explosion-resistant security glazing—Test and classification for arena air-blast loading. ISO 16933

[120] UKOOA, H. (2003). Fire and explosion guidance, part 1: avoidance and mitigation of explosions. Issue 1.

[121] Paik, J. K., & Thayamballi, A. K. 2007. Ship-shaped offshore installations: design, building, and operation. Cambridge University Press.

[122] Cheng, J. C., Tan, Y., Song, Y., Liu, X., & Wang, X. (2017). A semi-automated approach to generate 4D/5D BIM models for evaluating different offshore oil and gas platform decommissioning options. Visualization in Engineering, 5(1), 12.

[123] Ma, G., & Sun, L. (2012). The design and implement of FPSO assets management system. Procedia Environmental Sciences, 12, 484-490.

[124] Song, Y., Wang, X., Tan, Y., Wu, P., Sutrisna, M., Cheng, J., & Hampson, K. (2017). Trends and opportunities of BIM-GIS integration in the architecture, engineering and construction industry: A review from a spatio-temporal statistical perspective. ISPRS International Journal of Geo-Information, 6(12), 397.

[125] Singh, V., Gu, N., & Wang, X. (2011). A theoretical framework of a BIM-based multi-disciplinary collaboration platform. Automation in construction, 20(2), 134-144.

[126] Chai, J., Chi, H. L., Wang, X., Wu, C., Jung, K. H., & Lee, J. M. (2016). Automatic as-built modeling for concurrent progress tracking of plant construction based on laser scanning. Concurrent Engineering, 24(4), 369-380.

[127] Li, X., Wu, P., Shen, G. Q., Wang, X., & Teng, Y. (2017). Mapping the knowledge domains of Building Information Modeling (BIM): A bibliometric approach. Automation in Construction, 84, 195-206.

[128] Hamburger, R., & Whittaker, A. (2004). Design of steel structures for blast-related progressive collapse resistance. Modern steel construction, 44(3), 45-51.

[129] Goel, M. D., & Matsagar, V. A. (2013). Blast-resistant design of structures. Practice Periodical on Structural Design and Construction, 19(2), 04014007.

[130] Ngo, T., Mendis, P., Gupta, A., & Ramsay, J. (2007). Blast loading and blast effects on structures–an overview. Electronic Journal of Structural Engineering, 7(S1), 76-91.

[131] Markowski, A. S., Mannan, M. S., Kotynia, A., & Pawlak, H. (2011). Application of fuzzy logic to explosion risk assessment. Journal of Loss Prevention in the Process Industries, 24(6), 780-790.

[132] Han, Z. Y., & Weng, W. G. (2011). Comparison study on qualitative and quantitative risk assessment methods for urban natural gas pipeline network. Journal of hazardous materials, 189(1-2), 509-518.

[133] Tan, Y., Song, Y., Liu, X., Wang, X., & Cheng, J. C. (2017). A BIM-based framework for lift planning in topsides disassembly of offshore oil and gas platforms. Automation in construction, 79, 19-30.

[134] Zhou, X. Q., Yu, J., Ye, J. B., Liu, S. Y., Liao, R. G., & Li, X. W. (2018). Complex modeling of the effects of blasting on the stability of surrounding rocks and embankment in water-conveyance tunnels. Complexity, 2018.

[135] Kang, K. Y., Choi, K. H., Choi, J., Ryu, Y., & Lee, J. M. (2016). Dynamic response of structural models according to characteristics of gas explosion on topside platform. Ocean Engineering, 113, 174-190.

[136] Huang, Y., Ma, G., & Li, J. (2017). Multi-level explosion risk analysis (MLERA) for accidental gas explosion events in super-large FLNG facilities. Journal of Loss Prevention in the Process Industries, 45, 242-254.

[137] API, R. 2FB, Recommended Practice for the Design of Offshore Facilities against Fire and Blast Loading. 2006. Washington, DC: API.

[138] Melchers, R. E. (2001). On the ALARP approach to risk management. Reliability Engineering & System Safety, 71(2), 201-208.

[139] Jones-Lee, M., & Aven, T. (2011). ALARP—What does it really mean?. Reliability Engineering & System Safety, 96(8), 877-882.

[140] Schofield, S. (1998). Offshore QRA and the ALARP principle. Reliability engineering & system safety, 61(1-2), 31-37.

[141] Bowles, D. S. (2004). ALARP evaluation: Using cost effectiveness and disproportionality to justify risk reduction. Ancold Bulletin, 89-104.

[142] Kolios, A., & Brennan, F. (2009, July). Reliability based design for novel offshore structures. In 3rd International Conference on Integrity, Chengdu, China.

[143] Stahl, B. (1975, January). Probabilistic methods for offshore platforms. In Annual Meeting Papers, Division of Production. American Petroleum Institute.

[144] Sundararajan, C. R. (2012). Probabilistic structural mechanics handbook: theory and industrial applications. Springer Science & Business Media.

[145] Paik, J. K., Czujko, J., Kim, B. J., Seo, J. K., Ryu, H. S., Ha, Y. C., ... & Musial, B. (2011). Quantitative assessment of hydrocarbon explosion and fire risks in offshore installations. Marine Structures, 24(2), 73-96.

[146] Devore, J. L., & Berk, K. N. (2012). Modern mathematical statistics with applications (p. 350). New York: Springer.

[147] Zhang, F., Wu, C., Zhao, X. L., & Li, Z. X. (2017). Numerical derivation of pressure-impulse diagrams for square UHPCFDST columns. Thin-Walled Structures, 115, 188-195.

[148] Zhang, H., Chen, D., Wu, C., Wang, X., Lee, J. M., & Jung, K. H. (2017). Dynamic modeling and dynamical analysis of pump-turbines in S-shaped regions during runaway operation. Energy Conversion and Management, 138, 375-382.

[149] Zhang, H., Chen, D., Wu, C., & Wang, X. (2018). Dynamics analysis of the fast-slow hydro-turbine governing system with different time-scale coupling. Communications in Nonlinear Science and Numerical Simulation, 54, 136-147.

[150] Baker, W. E., Cox, P. A., Kulesz, J. J., Strehlow, R. A., & Westine, P. S. (2012). Explosion hazards and evaluation (Vol. 5). Elsevier.

[151] Chandrasekaran, S. (2016). Offshore structural engineering: reliability and risk assessment. CRC Press.

[152] Chopra, A. K. (2001). Dynamics of structures: theory and applications to earthquake engineering. Prentice-Hall.

[153] Li, Q. M., & Meng, H. (2002). Pulse loading shape effects on pressure–impulse diagram of an elastic–plastic, single-degree-of-freedom structural model. International journal of mechanical sciences, 44(9), 1985-1998.

[154] Morison, C. M. (2006). Dynamic response of walls and slabs by single-degree-of-freedom analysis—a critical review and revision. International Journal of Impact Engineering, 32(8), 1214-1247.

[155] Ikago, K., Saito, K., & Inoue, N. (2012). Seismic control of single-degree-of-freedom structure using tuned viscous mass damper. Earthquake Engineering & Structural Dynamics, 41(3), 453-474.

[156] Paz, M. (1985). Structural dynamics (pp. 23-64). New York: Van Nostrand Reinhold.

[157] Nassif, H., & Nowak, A. S. (1995). Dynamic load spectra for girder bridges. Transportation Research Record, (1476).

[158] Soh, T. B. (2004). Load-impulse diagrams of reinforced concrete beams subjected to concentrated transient loading(Doctoral dissertation, Pennsylvania State University).

[159] Sharmila, C., Anandavalli, N. Arunachalam, N. and Prakash, A. (2014). Pressure-Impulse diagram for damage assessment of structural elements subjected to blast loads: A state-of-art review. International Journal of Civil Engineering and Technology, 5(3), 275-284.

[160] Zhang, J., Zhu, C., Li, X., Pei, J., & Chen, J. (2017). Characterizing the three-stage rutting behavior of asphalt pavement with semi-rigid base by using UMAT in ABAQUS. Construction and Building Materials, 140, 496-507.

[161] Shiyekar, S. M., & Lavate, P. (2015). Flexure of power law governed functionally graded plates using ABAQUS UMAT. Aerospace Science and Technology, 46, 51-59.

[162] ASTM, A. (2011). Standard specification for general requirements for rolled structural steel bars, plates, shapes, and sheet piling.

[163] Li, J., Ma, G., Hao, H., & Huang, Y. (2016). Gas explosion analysis of safety gap effect on the innovating FLNG vessel with a cylindrical platform. Journal of Loss Prevention in the Process Industries, 44, 263-274.

[164] Sohn, J. M., & Kim, S. J. (2017). Numerical Investigation of Structural Response of Corrugated Blast Wall Depending on Blast Load Pulse Shapes. Latin American Journal of Solids and Structures, 14(9), 1710-1722.

[165] Bounds, W. L. (Ed.). (2010). Design of blast-resistant buildings in petrochemical facilities. ASCE Publications.

[166] Geng, J., Mander, T., & Baker, Q. (2015). Blast wave clearing behavior for positive and negative phases. Journal of Loss Prevention in the Process Industries, 37, 143-151.

[167] Heo, Y. (2013). Structural response of offshore plants to risk-based blast load. Architectural research, 15(3), 151-158.

[168] Netherton, M. D., & Stewart, M. G. (2016). Risk-based blast-load modelling: Techniques, models and benefits. International Journal of Protective Structures, 7(3), 430-451.

[169] Hidallana-Gamage, H. D., Thambiratnam, D. P., & Perera, N. J. (2017). Influence of the negative phase and support flexibility on the blast response of laminated glass panels. Construction and Building Materials, 154, 462-481.